



**UNIVERSIDADE FEDERAL DO CEARÁ**  
**CENTRO DE TECNOLOGIA**  
**DEPARTAMENTO DE ENGENHARIA QUÍMICA**  
**PROGRAMA DE PÓS-GRADUAÇÃO EM ENGENHARIA QUÍMICA**

**KÍMBERLE PAIVA DOS SANTOS AMORIM**

**PRODUCTION OF MULTI-ACTIVE BIOCATALYSTS THROUGH LIPASE AND  
LACCASE LAYER-BY-LAYER CO-IMMOBILIZATION USING DIFFERENT  
SUPPORTS**

**FORTALEZA**

**2022**

KÍMBERLE PAIVA DOS SANTOS AMORIM

PRODUCTION OF MULTI-ACTIVE BIOCATALYSTS THROUGH LIPASE AND  
LACCASE LAYER-BY-LAYER CO-IMMOBILIZATION USING DIFFERENT  
SUPPORTS

Tese apresentada ao Programa de Pós-Graduação em Engenharia Química da Universidade Federal do Ceará, como parte dos requisitos para obtenção do título de Doutora em Engenharia Química. Área de concentração: Processos Químicos e Bioquímicos.

Orientador: Prof.<sup>a</sup> Dra. Luciana Rocha Barros Gonçalves.

FORTALEZA

2022

Dados Internacionais de Catalogação na Publicação  
Universidade Federal do Ceará  
Biblioteca Universitária

Gerada automaticamente pelo módulo Catalog, mediante os dados fornecidos pelo(a) autor(a)

---

A543p Amorim, Kímberle Paiva dos Santos.

Production of multi-active biocatalysts through lipase and laccase layer-by-layer co-immobilization using different supports / Kímberle Paiva dos Santos Amorim. – 2022.

136 f. : il. color.

Tese (doutorado) – Universidade Federal do Ceará, Centro de Tecnologia, Programa de Pós-Graduação em Engenharia Química, Fortaleza, 2022.

Orientação: Profa. Dra. Luciana Rocha Barros Gonçalves.

1. lipase. 2. lacase. 3. co-imobilização. 4. agarose. 5. celulose nanocristalina. I. Título.

CDD 660

---

KÍMBERLE PAIVA DOS SANTOS AMORIM

PRODUCTION OF MULTI-ACTIVE BIOCATALYSTS THROUGH LIPASE AND  
LACCASE LAYER-BY-LAYER CO-IMMOBILIZATION USING DIFFERENT  
SUPPORTS

Tese apresentada ao Programa de Pós-Graduação em Engenharia Química da Universidade Federal do Ceará, como parte dos requisitos para obtenção do título de Doutora em Engenharia Química. Área de concentração: Processos Químicos e Bioquímicos.

Aprovada em 08/07/2022.

BANCA EXAMINADORA

---

Prof.<sup>a</sup> Dra. Luciana Rocha Barros Gonçalves (Orientadora)  
Universidade Federal do Ceará (UFC)

---

Prof. Dr. José Cleiton Sousa dos Santos  
Universidade Federal do Ceará (UFC)

---

Prof. Dr. Cleverton Diniz Teixeira de Freitas  
Universidade Federal do Ceará (UFC)

---

Prof.<sup>a</sup> Dra. Nathália Saraiva Rios  
Universidade Federal do Rio Grande do Norte (UFRN)

---

Prof.<sup>a</sup> Dra. Camilla Salviano Bezerra Aragão  
Instituto Federal do Sertão Pernambucano (IFSertãoPE)

To God.

To my husband, Júnior,

And to my family, Jeter, Érica,

Mikaelle, Marcelo and Melissa.

## ACKNOWLEDGEMENTS

I am very grateful to my God, for created me and for always showing me that His path is much better than what I plan. I am also grateful for His grace in my life and for the constant demonstration of His love. Everything I have comes from Him.

I thank my beloved husband for his daily care and love. His leadership over our home brings me peace and security and his encouragement always pushes me beyond what I think I am capable of. God really knew I would need you to accomplish this mission and so many others to come.

To my parents, Jeter and Érica, my eternal gratitude, honor and love. Like an arrow in your hands, I have been prepared along most of my life to be launched in the direction that God intended, and I want you to reap the fruits of that promise with me.

To my dear parents-in-laws, Eugênia and Amorim, who have always shown so much love and encouragement. You are an example of care for me.

To my sister, Mikaelle, my brother-in-law, Marcelo, and my sweet niece Melissa. How good it is to share our difficulties and joys with you daily. Thank you for all the encouragement, you were essential.

I also thank my beloved grandmothers, Luzenir and Zequinha, for your example and care through your teachings and prayers that make me keep going where I should go. I am also grateful to my uncles, especially to my aunt Quézia, a true friend and a professional example.

I am grateful for so many friends who make my life happy, especially Priscilla, Andre, Kézia, Werbeth, Ívila, Rennan, Elano and Paulinha. Even without knowing it, you helped me in many moments, you are true gifts from God.

I also thank all my church friends, especially my leaders Filho and Rafa, for so much care, love and teachings that made me grow personally and professionally.

To my dear Professor Luciana, who for almost 12 years has guided me, taught me and helped me directly to grow professionally and personally. Her orientation was essential. Also, her example of ethics, strength and care for the students will always be with me wherever I go.

To my friends Bruna, Nathalia, Ravena, Paulinha, Ju, Eddie, Carlos and Layanne. You made my working days much lighter and special. To professors Cleiton and Cris for all the help and inspiration during these years. I also thank everyone who is part of GPBio who always do their best to make the research group an example in everything. I thank also Karolina, for

teaching me and helping me, even if for a short time in person, but that continues in a virtual way.

I thank Ana Iraidy and Maira for the support with the preparation of some materials.

I thank Mr. Luís for his daily care and help. I also thank Valdelice for always helping us with laboratory demands.

I thank also Embrapa for all the support with some material preparations.

I am grateful to Funcap, for the support and financial support, as well as to CAPES and CNPq.

“God has hidden all the treasures of wisdom  
and knowledge in Christ.” (Colossians 2:3,  
Holly Bible)



## RESUMO

O uso conjunto de diferentes enzimas é comumente necessário para realizar um processo completo, como em sínteses de compostos e em degradação de poluentes de efluentes industriais, por exemplo. Lipases e lacases podem colaborar juntas para a síntese de fármacos, polímeros e compostos enantiomericamente enriquecidos, por exemplo, e em bioremediação. A imobilização de enzimas ajuda a superar algumas das suas limitações, como instabilidade e dificuldade de reuso. Neste trabalho, dois materiais (agarose e celulose) foram testados como suportes para co-imobilização de lipase e lacase usando estratégia multicamada, com polietilenoimina como cola entre as camadas de enzima. Lipase de *Pseudomonas fluorescenes* (usada para ambos os suportes), lacase de *Aspergillus sp.* (para suportes à base de agarose) e lacase de *Trametes versicolor* (para suportes à base de celulose) foram escolhidas para esse estudo devido às suas reconhecidas performances catalíticas. Primeiramente, materiais porosos à base de agarose — DEAE e octil agarose (OA) — foram testados como suportes para co-imobilização. OA mostrou-se o mais adequado, proporcionando um biocatalisador multiativo de alta estabilidade (100% da atividade da lipase foi mantida após 48h à 50 °C, pH 7). Estudos de transferência de massa demonstraram que foi possível obter biocatalisadores heterogêneos com atividade de  $88,59 \pm 1,0$  U/g para lipase e  $51,14 \pm 1,31$  U/g para lacase sem limitações difusionais internas. Em segundo lugar, suportes à base de celulose nanocristalina (CNC) foram usados para a mesma estratégia multicamada previamente estudada. Ensaios de FTIR e MEV demonstraram modificações químicas e morfológicas causadas pelas funcionalizações realizadas nesse suporte. Então, a primeira camada de enzima (lipase) foi imobilizada utilizando CNC e CNC funcionalizada com aldeído, que produziu biocatalisadores com características distintas (atividade e estabilidade). CNC oxidada com periodato (CNCox) usado como suporte resultou no biocatalisador com maior atividade ( $16,01 \pm 1,05$  U/g quando se utilizou 1,7 mg/g de carga proteica para imobilização) e estabilidade ( $t_{1/2} = 9,86 \pm 1,94$ , à 60 °C). Assim, CNCox foi utilizado como suporte para a co-imobilização, que produziu um biocatalisador multiativo com estabilidade térmica melhorada, com a lipase co-imobilizada mantendo mais de 90% de sua atividade ao longo de 48 h de incubação à 50 °C. Além disso, ele pôde ser aplicado em ciclos reacionais usando substratos padrões de ambas enzimas. Os biocatalisadores multiativos produzidos neste trabalho usando diferentes suportes apresentam grande potencial para serem aplicados em sistemas multienzimáticos de interesse industrial.

**Palavras-chave:** lipase; lacase; co-imobilização; agarose; celulose nanocristalina.

## ABSTRACT

The tandem use of different enzymes is commonly necessary to accomplish a whole process, such as for compounds synthesis and for degradation of pollutants from industrial effluents, for example. Lipases and laccases can co-collaborate to the synthesis of pharmaceuticals, some polymers and enantiomerically enriched compounds, for example, and in bioremediation. Immobilization of enzyme helps to overcome some limitations related to their instability and difficult to reuse. In this work, two materials (agarose and cellulose) were tested as support for lipase and laccase co-immobilization through a layer-by-layer strategy, using polyethyleneimine as a glue between enzyme layers. Lipase from *Pseudomonas fluorescenes* (used for both materials), laccase from *Aspergillus sp.* (for agarose based support), and laccase from *Trametes versicolor* (for cellulose based supports) were chosen for this study due to their well-recognized catalytic performances. Firstly, porous materials based on agarose — DEAE and octyl agarose (OA) — were tested as supports for the co-immobilization. OA showed to be the most appropriate, providing a multi-active and highly thermally stable biocatalyst (keeping 100% of lipase activity after 48h at 50 °C, pH 7). Mass transfer studies showed that it was possible to obtain heterogeneous biocatalysts with activity of  $88.59 \pm 1.0$  U/g for lipase and  $51.14 \pm 1.31$  U/g for laccase without internal diffusional limitations. Secondly, supports based on cellulose nanocrystalline (CNC) were tested for the same layer-by-layer strategy previously studied. FTIR and SEM assays demonstrated the chemical and morphological changes caused by the functionalizations performed on this support. Then, the first layer of enzyme (lipase) was immobilized using CNC and CNC functionalized with aldehyde, which produced biocatalysts with distinct characteristics (activity and stability). Functionalized CNC obtained through periodate oxidation (CNCox) showed to be the support providing a biocatalyst with higher activity ( $16.01 \pm 1.05$  U/g when 1.7 mg/g of protein load was used for immobilization) and stability ( $t_{1/2} = 9.86 \pm 1.94$ , at 60 °C). Thus, CNCox was used as support for the co-immobilization, which produced a multi-active biocatalyst with improved thermal stability, with co-immobilized lipase keeping more than 90% of its activity along 48 h of incubation at 50 °C. Besides, it could be applied in recycles of reactions using standard substrates of both enzymes. The multi-active biocatalysts produced in this work using different supports present a great potential to be applied in multi-enzymatic systems of industrial interest.

**Key-words:** lipase; laccase; co-immobilization; agarose; cellulose nanocrystalline.

## LIST OF ILLUSTRATIONS

Figure 1.1	- Representation of the three multi-active biocatalyst obtained through the co-immobilization of lipase and laccase. Lipase in blue, laccase in pink, polythyleneimine (PEI) in red, glutaraldehyde in green and representation of covalent attachment allowed by the functionalization of CNC in orange.....	23
Figure 2.1	- Schematic representation of lipase from <i>Pseudomonas fluorescens</i> (PFL) crystal structure (PDB lipase code: 2Z8X) with the active site (catalytic triad) in red and the lid in green. The following structure was taken from Protein Data Bank (PDB) by using PyMol Educational.....	34
Figure 2.2	- Schematic representation of Laccase from <i>Myceliophthora thermophila</i> expressed in <i>Aspergillus oryzae</i> crystal structure (PDB code: 6F5K). TNC (two type 3 coopers and the type 2 cooper/ spheres) site in red, T <sub>1</sub> copper (sphere) and His508 (T <sub>1</sub> copper ligand) in orange, Glu235 in blue and two Ca <sup>+</sup> in yellow. The following structure was taken from Protein Data Bank (PDB) by using PyMol Educational.....	36
Figure 2.3	- Schematic representation of Laccase from <i>Trametes versicolor</i> crystal structure (PDB code: 1GYC). TNC (two type 3 coopers and the type 2 cooper/ spheres) site in red, T <sub>1</sub> copper (sphere) and His458 (T <sub>1</sub> copper ligand) in orange, tripeptide His452-Cys453-His454 in green and tripeptide Leu459-Glu460-Ala461 in blue. The following structure was taken from Protein Data Bank (PDB) by using PyMol Educational.....	38
Figure 2.4	- Representation of the surface chemical structure of Sepharose-DEAE (diethylaminoethyl).....	44
Figure 2.5	- Representation of the surface chemical structure of Octyl-Agarose....	45

Figure 2.6	- Representation of the chemical structure of cellulose with the hydroxyl groups (that can be chemically modified) in red. ....	47
Figure 2.7	- Silylation (silane grafting) of CNC to generate an amino-functionalized CNC support followed by glutaraldehyde activation...	48
Figure 2.8	- Oxidation of CNC using sodium periodate (NaIO <sub>4</sub> ) to form a dialdehyde cellulose.....	49
Figure 3.1	- Schematic representation of the layer-by-layer strategy used for the co-immobilization of the enzymes and a hypothetical application of the multi-active biocatalyst in a cascade reaction.....	64
Figure 3.2	- The two reversed layer-by-layer strategies followed for the co-immobilization of lipase (PFL) and laccase (Lac) proposed in the current study. (A) Protocol I: DEAE-Sepharose-laccase-PEI-lipase (DEAE-Lac-PEI-PFL); (B) Protocol II: Octyl-Agarose-lipase-PEI-laccase-GA (OA-PFL-PEI-Lac-GA). PEI: polyethyleneimine; GA: glutaraldehyde; DEAE: diethylaminoethyl.....	67
Figure 3.3	- SDS-page of the soluble enzymes and the biocatalysts in each stage of the 4-step co-immobilization process using Octyl-agarose as support. Lanes: (1) Molecular weight marker; (2) Soluble PFL, molecular weight around 33 kDa; (3) Soluble Laccase, molecular weight around 85 kDa; (4) OA-PFL; (5) OA-PFL-PEI; (6) OA-PFL-PEI-Lac; (7) OA-PFL-PEI-Lac-GA.....	76
Figure 3.4	- Temperature dependence of PFL (A) and Laccase (B) activity profiles. Hollow shapes and dashed lines: soluble enzyme; Solid shapes and solid lines: heterogeneous biocatalyst (2 mg <sub>protein</sub> /g <sub>support</sub> of each enzyme).....	78
Figure 3.5	- Plot of ln (V <sub>max</sub> ) versus 1/T for calculating the activation energy via the Arrhenius equation for PFL (A) and Laccase (B). Hollow shapes and dashed lines: soluble enzyme; Solid shapes and lines: heterogeneous biocatalyst containing 2 mg <sub>protein</sub> /g <sub>support</sub> of each enzyme.....	79

Figure 3.6	- Michaelis-Menten fit of PFL (A) and laccase (B) data. Open circle: Soluble enzyme; Solid circle: heterogeneous biocatalysts; Dashed line: fitting for the soluble enzyme; Solid line: fitting for the heterogeneous biocatalysts.....	80
Figure 3.7	- The activity of the heterogeneous biocatalysts. PFL activity (A) and Laccase activity (B) as a function of enzyme load on the support.....	83
Figure S3.1	- Stirred tank reactor used for monitoring initial rates (enzyme activity assay) catalyzed by the soluble and immobilized enzymes.....	91
Figure S3.2	- Inactivation profiles of soluble (dashed lines) and co-immobilized (solid lines) PFL (black) and laccase (blue) incubated at 50 °C (pH7) during 48 hours.....	91
Figure 4.1	- Aldehyde functionalization of CNC using two different chemical modifications. In red, cellulose oxidation by sodium periodate leads to the glucopyranoside ring's cleavage and the introduction of two aldehyde groups, forming a “dialdehyde cellulose” (CNCox). In green, the preparation of an aminated cellulose through the silane grafting of cellulose using 3-aminopropyltriethoxysilane (APTES) is followed by the glutaraldehyde activation of the aminated cellulose. Elaborated by the author.....	97
Figure 4.2	- Immobilization course of PFL onto CNC conducted at pH 7. A solution containing soluble PFL at the pH of immobilization (7) was used as reference (dashed lines); solid lines represent the supernatant of PFL immobilization onto CNC at different conditions: using only a 5mM sodium phosphate buffer (■), with the addition of NaCl 200mM (●) or with the addition of 1% Triton-X (▲).....	105
Figure 4.3	- Stability at 60 °C and pH 7 (50mM Tris-HCl buffer) of soluble PFL (○) and PFL immobilized onto unmodified CNC (■). Heterogeneous biocatalysts were obtained after 2 hours of immobilization (solid black line) and 7 hours of immobilization (dashed black line).....	106

Figure 4.4	- Influence of the initial NaIO <sub>4</sub> concentration on the aldehyde content in the oxidized CNC, expressed in μmol of CHO per gram of CNC. Tested concentrations: 250 (■), 500 (▲), and 1000(●) μmol NaIO <sub>4</sub> /g of CNC at pH 3 (solid lines) and pH 5 (dashed lines).....	108
Figure 4.5	- SEM images and EDS spectra of MCC (A), CNC (B), CNCox-250 (obtained at pH 5) (C), CNCox-1000 (obtained at pH 5) (D) and CNC-GA (E).....	110
Figure 4.6	- FTIR spectra of CNC, CNCox-250, CNCox-1000, and CNC-GA.....	111
Figure 4.7	- Immobilization course of PFL onto CNC and modified CNCs at pH 7. A solution containing soluble PFL at the pH of immobilization (7) was used as reference (□); Solid lines represent the supernatant of PFL immobilization using the following supports: CNC (●), CNCox-250 (▲), CNCox-1000 (▼), and CNC-GA (◀).....	112
Figure 4.8	- Stability at 60 °C and pH 7 (50mM Tris-HCl buffer) of soluble PFL (●) and PFL immobilized onto different activated supports — CNCox (A) and CNC-GA (B). Supports: CNCox-250 (■), CNCox-1000 (■), and CNC-GA (■). The heterogeneous biocatalysts were obtained after different immobilization times: 2 hours for CNCox and 5 hours for CNC-GA (solid lines); 7 hours for CNCox and 24 hours for CNC-GA (dashed lines).....	116
Figure 4.9	- Theoretical activity (textured columns) and actual (measured) activity (solid columns) of the heterogeneous biocatalysts from immobilization of PFL onto CNCox- 250 (■) or CNC-GA (■) for 24 hours, at pH 7 (5mM sodium phosphate buffer) and 25 °C, using different protein loads at the beginning of immobilization.....	119
Figure 4.10	- Thermal stability at 50 °C and pH 7 (50mM Tris-HCl buffer) of soluble (dashed lines) and co-immobilized (solid lines) PFL (black) and laccase (blue) using CNCox-250 as support.....	123

Figure 4.11 - Operational stability of co-immobilized PFL and laccase. CNCox-250-PFL-PEI-Lac-GA was used as biocatalyst in the recycles of pNPB hydrolysis (black line) and ABTS oxidation (blue line) for PFL and laccase analysis, respectively.....

## LIST OF TABLES

Table 3.1	- Catalytic activity for both enzymes in each stage of the 3-step immobilization process using DEAE as support.....	74
Table 3.2	- Catalytic activities for both enzymes in each stage of the 4-steps co-immobilization process using octyl-agarose as support.....	75
Table 3.3	- Kinetic parameters from the Michaelis-Menten model adjustment using the values obtained from the reactions for both enzymes performed at different substrate concentrations.....	80
Table 3.4	- Diffusivity parameters for PFL and Laccase using pNPB and ABTS as substrates, respectively. $D_{AB}$ ( $\text{cm}^2/\text{s}$ ) is the diffusion coefficient of solute A in solvent B. $D_{AB e}$ ( $\text{cm}^2/\text{s}$ ) is the effective diffusivity, considering the specificities of the agarose-based support. $\Phi$ (dimensionless) is Weisz's modulus calculated at the maximum tested substrate concentration.....	82
Table 3.5	- Weisz's modulus ( $\Phi$ , dimensionless) was calculated for reactions using heterogeneous biocatalysts obtained from immobilization with different initial protein loads.....	84
Table 4.1	- Activities of the heterogeneous biocatalysts before ( $t = 0$ ) and after 2 h of desorption in the presence of 5mM sodium phosphate buffer, NaCl 1M or Triton-X 1% (the last two prepared in 5 mM sodium phosphate buffer), performed at pH 7 and 25 °C. Each biocatalyst was obtained from PFL immobilization during 24 hours, using 5mM sodium phosphate buffer and 1.7 mg/g of protein load.....	113
Table 4.2	- Values of half-life and initial activity ( $t = 0$ ) obtained from the deactivation assays at 60 °C and pH 7 (50mM Tris-HCl buffer) of soluble PFL and PFL immobilized onto CNC and modified CNC during different immobilization times. All the half-life values were obtained from Sadana & Henley equation, except for CNCox-250 2	117



hours and CNC-GA 24 hours.....

Table 4.3 - Catalytic activity for immobilized lipase and laccase after each stage of the 4-steps co-immobilization process using CNCox-250 as support. Immobilizations were performed using two initial protein loading: 1.7 mg<sub>protein</sub>/g<sub>support</sub> for each enzyme and 10 mg<sub>protein</sub>/g<sub>support</sub> for each one.....

## LIST OF ABBREVIATIONS AND ACRONYMS

PFL	Lipase from <i>Pseudomonas fluorescenes</i>
Lac	Laccase
DEAE	Diethylaminoethyl
OA	Octyl-Agarose
CNC	Cellulose nanocrystalline
PEI	Polyethylenimine
<i>p</i> NPB	<i>p</i> - nitrophenyl butyrate
ABTS	2,2'-Azino-bis (3-ethylbenzothiazoline-6-sulfonic acid) diammonium salt
DEAE-Lac	Lac immobilized on DEAE-Sepharose
DEAE-Lac-PEI	DEAE-Lac coated with PEI
DEAE-Lac-PEI-PFL	PFL immobilized on DEAE-Lac-PEI
OA-PFL	PFL immobilized on OA
OA-PFL-PEI	OA-PFL coated with PEI
OA-PFL-PEI-Lac	Lac immobilized on OA-PFL-PEI
OA-PFL-PEI-Lac-GA	OA-PFL-PEI-Lac crosslinked with glutaraldehyde
BSA	Bovine serum albumin
CHO	Aldehyde groups
CMC	Cellulose microcrystalline
APTES	3- aminopropyltriethoxysilane
CNCox	CNC oxidized using NaIO <sub>4</sub>
CNCox-250	CNC oxidized using 250 μmol NaIO <sub>4</sub> /g of CNC
CNCox-1000	CNC oxidized using 1000 μmol NaIO <sub>4</sub> /g of CNC
CNC-GA	CNC activated with gluyaraldehyde
CNCox-250-PFL	PFL immobilized on CNCox-250
CNCox-250-PFL-PEI	CNCox-250-PFL coated with PEI
CNCox-250-PFL-PEI-Lac	Lac immobilized on CNCox-250-PFL-PEI
CNCox-250-PFL-PEI-Lac-GA	CNCox-250-PFL-PEI-Lac crosslinked with glutaraldehyde

## SUMMARY

<b>1</b>	<b>INTRODUCTION AND OBJECTIVES</b>	<b>20</b>
<b>1.1</b>	<b>Introduction</b>	<b>21</b>
<b>1.2</b>	<b>Objectives</b>	<b>24</b>
<i>1.2.1</i>	<i>General objectives</i>	<i>24</i>
<i>1.2.2</i>	<i>Specifics Objectives</i>	<i>24</i>
<b>1.3</b>	<b>References</b>	<b>25</b>
<b>2</b>	<b>LITERATURE REVIEW</b>	<b>28</b>
<b>2.1</b>	<b>Enzyme immobilization</b>	<b>29</b>
<i>2.1.1</i>	<i>Immobilization by adsorption</i>	<i>30</i>
<i>2.1.2</i>	<i>Immobilization by covalent attachment</i>	<i>31</i>
<i>2.1.3</i>	<i>Use of crosslinker in enzyme immobilizations</i>	<i>31</i>
<b>2.2</b>	<b>Lipases</b>	<b>32</b>
<i>2.2.1</i>	<i>Lipase from <i>Pseudomonas fluorescens</i></i>	<i>33</i>
<b>2.3</b>	<b>Laccases</b>	<b>34</b>
<i>2.3.1</i>	<i>Novozymes 51003</i>	<i>35</i>
<i>2.3.2</i>	<i>Laccase from <i>Trametes versicolor</i></i>	<i>37</i>
<b>2.4</b>	<b>Multi-enzymes system</b>	<b>38</b>
<i>2.4.1</i>	<i>One pot system/Cascade reactions</i>	<i>39</i>
<i>2.4.2</i>	<i>Lipases and laccases</i>	<i>39</i>
<b>2.5</b>	<b>Co-immobilization of enzymes</b>	<b>40</b>
<i>2.5.1</i>	<i>Layer-by-layer strategy</i>	<i>41</i>
<b>2.6</b>	<b>Supports for enzyme immobilization</b>	<b>42</b>
<i>2.6.1</i>	<i>Agarose based supports</i>	<i>43</i>
<i>2.6.1.1</i>	<i>DEAE-Sepharose</i>	<i>43</i>
<i>2.6.1.2</i>	<i>Octyl- Agarose</i>	<i>44</i>
<i>2.6.3</i>	<i>Cellulose nanocrystalline</i>	<i>45</i>
<i>2.6.3.1</i>	<i>Cellulose activation</i>	<i>46</i>
<b>2.7</b>	<b>References</b>	<b>49</b>
<b>3</b>	<b>CO-IMMOBILIZATION OF LIPASE AND LACCASE ON AGAROSE-BASED SUPPORTS VIA LAYER-BY-LAYER STRATEGY: EFFECT OF DIFFUSIONAL LIMITATIONS</b>	<b>60</b>

<b>3.1</b>	<b>Abstract</b>	61
<b>3.2</b>	<b>Introduction</b>	62
<b>3.3</b>	<b>Materials and methods</b>	66
3.3.1	<i>Materials</i>	66
3.3.2	<i>Methods</i>	66
3.3.2.1	<i>Co-immobilization of laccase and lipase</i>	66
3.3.2.2	<i>Soluble enzyme and heterogeneous biocatalysts activity</i>	69
3.3.2.3	<i>Protein concentration</i>	70
3.3.2.4	<i>SDS-PAGE analysis</i>	70
3.3.2.5	<i>Thermal stability</i>	70
3.3.2.6	<i>Temperature dependence of the heterogeneous biocatalysts' activity</i>	71
3.3.2.7	<i>Diffusivity analysis</i>	71
<b>3.4</b>	<b>Results and discussion</b>	72
3.4.1	<i>Production and characterization of heterogeneous biocatalyst containing lipase and laccase</i>	72
3.4.1.1	<i>Co-immobilization of lipase and laccase onto agarose-based supports</i>	72
3.4.1.2	<i>Thermal stability at 50 °C</i>	76
3.4.1.3	<i>Temperature-dependent activity profiles of soluble and immobilized enzymes</i>	77
3.4.2	<i>Reaction and Diffusion analysis</i>	79
3.4.3	<i>Influence of internal mass transfer at high enzyme loadings</i>	82
<b>3.5</b>	<b>Conclusions</b>	84
<b>3.6</b>	<b>Acknowledgments</b>	85
<b>3.7</b>	<b>References</b>	85
<b>3.8</b>	<b>Supplementary Material</b>	91
<b>4</b>	<b>CHEMICAL MODIFICATIONS IN CELLULOSE NANOCRYSTALLINE FOR ITS APPLICATION AS SUPPORT FOR LIPASE AND LACCASE LAYER-BY-LAYER CO-IMMOBILIZATION</b>	92
<b>4.1</b>	<b>Abstract</b>	93
<b>4.2</b>	<b>Introduction</b>	94
<b>4.3</b>	<b>Experimental</b>	98
4.3.1	<i>Materials</i>	98

4.3.2	<i>CNC preparation</i>	98
4.3.3	<i>CNC oxidation and quantification of aldehyde groups</i>	99
4.3.4	<i>CNC activation with glutaraldehyde</i>	100
4.3.5	<i>CNC and functionalized CNC characterization</i>	100
4.3.6	<i>Determination of enzyme activity, protein concentration and some immobilization parameters</i>	101
4.3.7	<i>PFL and laccase co-immobilization</i>	102
4.3.8	<i>Desorption</i>	103
4.3.9	<i>Thermal Stability</i>	103
4.3.10	<i>Operational stability of the co-immobilized enzymes</i>	104
4.3.11	<i>Statistical analysis</i>	104
4.4	<b>Results and Discussion</b>	104
4.4.1	<i>PFL immobilization onto unmodified CNC</i>	105
4.4.2	<i>CNC functionalization with aldehyde groups and characterization</i>	107
4.4.3	<i>Immobilization of PFL using different activated CNCs</i>	112
4.4.4	<i>Thermal stability of PFL immobilized onto CNC-based supports</i>	115
4.4.5	<i>Effect of enzyme loading on PFL immobilization</i>	118
4.4.6	<i>Co-immobilization of lipase and laccase onto CNCox-250 support</i>	120
4.4.7	<i>Thermal stability of enzymes co-immobilized onto CNCox-250</i>	122
4.4.8	<i>Reuse of co-immobilized enzymes</i>	124
4.5	<b>Conclusions</b>	125
4.6	<b>Acknowledgements</b>	126
4.7	<b>References</b>	126
5	<b>FINAL CONSIDERATIONS</b>	132

# Chapter 1

**Introduction and Objectives**

## 1.1 Introduction

Multienzymatic systems are commonly necessary to accomplish multi-reactional processes, both with cascade and parallel reactions. When some of those steps can be integrated and this processes sequence accomplished in a single vessel, it can be named an “one-pot” approach, which may minimize hazardous side products as well as reduction of isolation and purification steps (Hayashi, 2016; Scheibel e Gitsov, 2019; Sulman, Matveeva e Bronstein, 2019; Villegas *et al.*, 2019). Besides decreasing by-products and pollutants release, some advantages of using multi-enzymes are related to reducing substrate diffusion, which minimizes the time of reaction and intermediates loss (Ren *et al.*, 2019). A relevant increase in the areas of application of multienzymatic systems have been observed, both in research and industry, especially for biomedical engineering, biosensors production and biotransformation (Hwang e Lee, 2019).

In this work, a multi-enzyme biocatalyst was produced by co-immobilizing lipase and laccase onto different supports. Lipases have found applicability in several industrial areas, then they are among the most popular enzymes in bioprocess, both in research and industrial levels (Rios, Mendez-Sanchez, *et al.*, 2019; Sarmah *et al.*, 2018; Soni *et al.*, 2018). Laccases, in turn, have attracted more and more attention and focus of researches on the development of biocatalysts with oxidative activity and are broadly used in different industrial processes for compounds synthesis or other necessary biotransformations as well (Mate e Alcalde, 2017; Moreno *et al.*, 2020). Laccase and lipase enzymes can work together to accomplish several kinds of processes by co-catalyzing different reactions. Some examples are the synthesis of pharmaceuticals (Zhang *et al.*, 2019) and enantiomerically enriched dimeric phenols (Gavezzotti *et al.*, 2011), the production of structured copolymers (Scheibel e Gitsov, 2019) and the degradation of several compounds in different effluents (Balaji, Arulazhagan e Ebenezer, 2014; Kadri *et al.*, 2017).

The immobilization of different enzymes has been studied as a very important matter to increase the applicability of such biocatalysts in industrial processes by reducing the cost related to the production of new enzymes (Drozd *et al.*, 2019). The primary objective of developing a technology for the immobilization of a given enzyme is the physical confinement of its catalytic activity aiming its easy reutilization by facilitating the biocatalyst filtration or even its application in a continuous way (Mohamad *et al.*, 2015). Other valuable advantages sought by a well-developed immobilization technology are related to the enhancement of important features such as activity, selectivity and, the most commonly searched, stability

(Santos, dos *et al.*, 2017). With co-immobilized enzymes, the catalytic efficiency of these multi-active biocatalysts can be improved if a well-ordered immobilization strategy, such as layer-by-layer approach, is applied (Arana-Peña, Rios, *et al.*, 2020; Peng *et al.*, 2020). Besides, using a multilayer approach to perform the co-immobilization of different enzymes, the loading capacity can be increased, since one enzyme is immobilized over a previously immobilized enzyme layer (Arana-Peña *et al.*, 2021). In this work, lipase and laccase were co-immobilized through a 4-steps procedure. Firstly, the first enzyme was immobilized onto the support. Then, polyethyleneimine (PEI) was used to cover this first enzyme layer and allows the immobilization of the second enzyme, working as a glue (Arana-Peña, Rios, *et al.*, 2020). So, the second enzyme was co-immobilized over the PEI layer. Finally, a crosslinking with glutaraldehyde was performed to avoid enzyme release (Arana-Peña, Carballares, *et al.*, 2020; Arana-Peña, Rios, *et al.*, 2020; Rios, Arana-Peña, *et al.*, 2019).

The different interactions that the first enzyme layer and the support could establish were also investigated. Several immobilization techniques have been explored by the researchers for years, which one presenting advantages and disadvantages for different enzymes and applications. For example, adsorption is one of the simplest and fast methods and includes physical interactions such as electrostatics or hydrophobic. However, they are sometimes insufficient to maintain the enzyme attached onto the support under different reaction environments (Tran e Balkus Jr, 2018). Immobilization by covalent attachment, in turn, is established by covalent bond formation between active groups on the support and amino acid residues of the enzyme, which may provide an interesting increase on the stability. Nevertheless, one of the greatest challenges related to this immobilization method is to not compromise the residues of amino acids present in the active site to those covalent attachments established with the support (Romero-Fernández e Paradisi, 2019). Thereby, sometimes is most advantageous to combine different immobilization strategies to overcome such constraints and achieve the suitable biocatalyst (Tran e Balkus Jr, 2018).

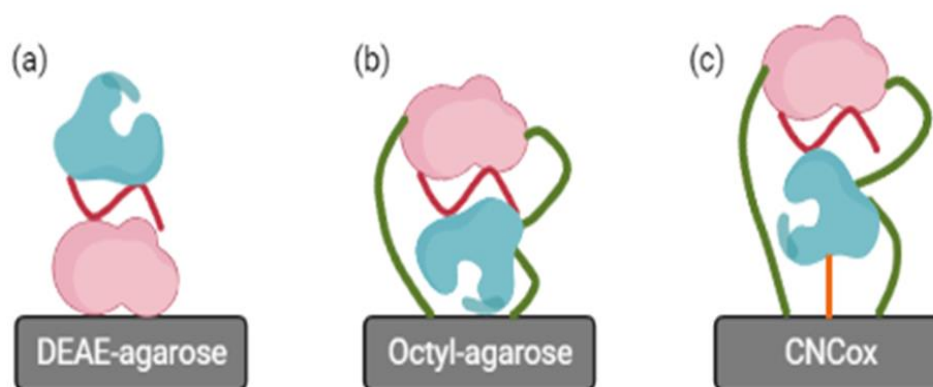
Another crucial point in the development of an appropriate immobilization technique for a desired enzyme is a proper choice of the support, which should be based on some crucial points for it will directly affect the final properties of the produced insoluble biocatalyst (Zdarta *et al.*, 2018). First of all, the cost related to the obtainment of the material, its functionalization (if it is needed) and the toxicity of the support must be taken into account. Regarding to the application of the final biocatalyst (reactor, mixing device, flow's speed in continuous processes, etc), mechanical properties are crucial for the success of the catalyst process (Zucca, Fernandez-Lafuente e Sanjust, 2016). Other support specific features have



great importance for the final reaction rate and stability of the immobilized enzyme, such as surface area, pore length and diameter, particle size, internal morphology and active groups (Santos *et al.*, 2015).

In the face of so many challenges, the objective of this work was to study and develop a multi-active biocatalyst by the co-immobilization of two different enzymes — Lipase and Laccase — using distinct supports. Aiming the obtainment of a high loaded biocatalyst, it was chosen supports with elevated surface area. The study was divided in two sections. The first part of this work (Chapter 3, a published paper) studied the co-immobilization of those two enzymes onto DEAE-agarose (Fig. 1.1 a) and Octyl-agarose (Fig. 1.1 b), materials very used for enzymes immobilization and well known by its porosity. With these supports, two different orders of co-immobilization were applied. The second part of the study (Chapter 4) analyzed the use of a nanosized support, derived from cellulose nanocrystalline (CNC), for the co-immobilization of lipase and laccase. Firstly, the interactions between the lipase (first enzyme layer) and the support were investigated. Since aldehyde-activated supports are well recognized for their results in application for lipase immobilization and stabilization, different aldehyde-functionalizations of the support were performed and the heterogeneous biocatalyst produced were analyzed (Cai *et al.*, 2018; Orrego *et al.*, 2018; Poppe *et al.*, 2013). Then, it was chosen an oxidized CNC (CNCox) as carrier to proceed with the co-immobilization process. In each section of this work, different aspects were studied according to the particularities of each enzymes-support system produced.

Figure 1.1 – Representation of the three multi-active biocatalyst obtained through the co-immobilization of lipase and laccase. Lipase in blue, laccase in pink, polythyleneimine (PEI) in red, glutaraldehyde in green and representation of covalent attachment allowed by the functionalization of CNC in orange.



## 1.2 Objectives

### 1.2.1 General objectives

Production of multi-active and stable biocatalysts by the co-immobilization of lipase and laccase onto supports based on agarose and nanocellulose.

### 1.2.2 Specifics Objectives

- Apply strategies based on layer-by-layer approach for co-immobilization of lipase and laccase onto agarose based support, having polyethylenimine (PEI) as intermediate between the two enzymes layer;
- Characterize the obtained biocatalyst with respect to activity and thermal stability;
- Study the influences of external and internal mass transfer limitations on the biocatalyst activity;
- Produce biocatalyst highly loaded for posterior application in target process of multi-reactions;
- Apply the most successful strategy detected for the co-immobilization on agarose based supports with the support based on CNC;
- Study the immobilization of lipase from *Pseudomonas fluorescens* (PFL) onto CNC and the interactions between enzyme and support;
- Functionalize CNC with aldehyde support by using different chemical agents and protocols and characterize them;
- Immobilize PFL onto functionalized CNCs and characterize them with respect to activity and thermal stability;
- Increase the PFL load for immobilization using the supports which presented better results in characterization;
- Apply the support which presented best results with PFL for the co-immobilization of this enzyme and laccase;
- Characterize the biocatalyst produced with respect to activity and stability;
- Apply the insoluble biocatalyst in recycles of catalysis using standard substrates of both enzymes;

### 1.3 References

ARANA-PEÑA, S.; RIOS, N. S.; *et al.* Coimmobilization of different lipases: Simple layer by layer enzyme spatial ordering. **International Journal of Biological Macromolecules**, v. 145, p. 856–864, 2020.

ARANA-PEÑA, S.; CARBALLARES, D.; *et al.* One pot use of combilipases for full modification of oils and fats: Multifunctional and heterogeneous substrates. **Catalysts**, v. 10, n. 6, p. 605, 2020.

ARANA-PEÑA, S. *et al.* Enzyme co-immobilization: Always the biocatalyst designers' choice...or not? **Biotechnology Advances**, v. 51, n. March 2020, 2021.

BALAJI, V.; ARULAZHAGAN, P.; EBENEZER, P. Enzymatic bioremediation of polyaromatic hydrocarbons by fungal consortia enriched from petroleum contaminated soil and oil seeds. **Journal of Environmental Biology**, v. 35, n. 3, p. 521–529, 2014.

CAI, Q. *et al.* Enhanced activity and stability of industrial lipases immobilized onto spherelike bacterial cellulose. **International Journal of Biological Macromolecules**, v. 109, p. 1174–1181, 2018.

DROZD, R. *et al.* Functionalized Magnetic Bacterial Cellulose Beads as Carrier for Lecitase® Ultra Immobilization. **Applied Biochemistry and Biotechnology**, v. 187, n. 1, p. 176–193, 2019.

GAVEZZOTTI, P. *et al.* Synthesis of enantiomerically enriched dimers of vinylphenols by tandem action of laccases and lipases. **Advanced Synthesis and Catalysis**, v. 353, n. 13, p. 2421–2430, 2011.

HAYASHI, Y. Pot economy and one-pot synthesis. **Chemical Science**, v. 7, p. 866–880, 2016.

HWANG, E. T.; LEE, S. Multienzymatic Cascade Reactions via Enzyme Complex by Immobilization. **ACS Catalysis**, v. 9, n. 5, p. 4402–4425, 2019.

KADRI, T. *et al.* Biodegradation of polycyclic aromatic hydrocarbons (PAHs) by fungal enzymes: A review. **Journal of Environmental Sciences (China)**, v. 51, p. 52–74, 2017.

MATE, D. M.; ALCALDE, M. Minireview Laccase : a multi-purpose biocatalyst at the forefront of biotechnology. **Microbial Biotechnology**, v. 10, n. 6, p. 1457–1467, 2017.

MOHAMAD, N. R. *et al.* An overview of technologies for immobilization of enzymes and surface analysis techniques for immobilized enzymes. **Biotechnology and Biotechnological Equipment**, v. 29, n. 2, p. 205–220, 2015.

MORENO, A. D. *et al.* Laccases as versatile enzymes: from industrial uses to novel applications. **Journal of Chemical Technology and Biotechnology**, v. 95, n. 3, p. 481–494, 2020.

ORREGO, A. H. *et al.* Stabilization of immobilized lipases by intense intramolecular cross-linking of their surfaces by using aldehyde-dextran polymers. **International Journal of Molecular Sciences**, v. 19, n. 2, p. 1–16, 2018.

PENG, F. *et al.* Co-immobilization of multiple enzymes by self-assembly and chemical crosslinking for cofactor regeneration and robust biocatalysis. **International Journal of Biological Macromolecules**, v. 162, p. 445–453, 2020.

- POPPE, J. K. *et al.* Enzymatic Multipoint covalent immobilization of lipases on aldehyde-activated support : Characterization and application in transesterification reaction. **Journal of Molecular Catalysis B: Enzymatic**, v. 94, p. 57–62, 2013.
- REN, S. *et al.* Recent progress in multienzymes co-immobilization and multienzyme system applications. **Chemical Engineering Journal**, v. 373, n. February, p. 1254–1278, 2019.
- RIOS, N. S.; ARANA-PENÑA, S.; *et al.* Increasing the enzyme loading capacity of porous supports by a layer-by-layer immobilization strategy using PEI as glue. **Catalysts**, v. 9, n. 7, p. 576, 2019.
- RIOS, N. S.; MENDEZ-SANCHEZ, C.; *et al.* Immobilization of lipase from *Pseudomonas fluorescens* on glyoxyl-octyl-agarose beads: Improved stability and reusability. **Biochimica et Biophysica Acta (BBA) - Proteins and Proteomics**, v. 1867, n. 9, p. 741–747, set. 2019.
- ROMERO-FERNÁNDEZ, M.; PARADISI, F. General overview on immobilization techniques of enzymes for biocatalysis. **Catalyst Immobilization: Methods and Applications**, p. 409–435, 2019.
- SANTOS, J. C. S. DOS *et al.* Importance of the support properties for immobilization or purification of enzymes. **CHEM CAT CHEM**, v. 7, n. 16, p. 2413–2432, 2015.
- SANTOS, J. C. S. DOS *et al.* Immobilization of CALB on activated chitosan: Application to enzymatic synthesis in supercritical and near-critical carbon dioxide. **Biotechnology Reports**, v. 14, p. 16–26, 2017.
- SARMAH, N. *et al.* Recent advances on sources and industrial applications of lipases. **Biotechnology Progress**, v. 34, n. 1, p. 5–28, jan. 2018.
- SCHEIBEL, D. M.; GITSOV, I. Unprecedented Enzymatic Synthesis of Perfectly Structured Alternating Copolymers via “green” Reaction Cocatalyzed by Laccase and Lipase Compartmentalized within Supramolecular Complexes. **Biomacromolecules**, v. 20, n. 2, p. 927–936, 2019.
- SONI, S. *et al.* Exploration of the expeditious potential of *Pseudomonas fluorescens* lipase in the kinetic resolution of racemic intermediates and its validation through molecular docking. **CHIRALITY**, v. 30, p. 85–94, 2018.
- SULMAN, E. M.; MATVEEVA, V. G.; BRONSTEIN, L. M. Design of biocatalysts for efficient catalytic processes. **Current Opinion in Chemical Engineering**, v. 26, p. 1–8, 2019.
- TRAN, D. N.; BALKUS JR, K. J. Perspective of Recent Progress in Immobilization of Enzymes. **ACS Catalysis**, v. 7, n. 1, p. 41–57, 2018.
- VILLEGAS, M. *et al.* The Journal of Supercritical Fluids Development of an integrated one-pot process for the production and impregnation of starch aerogels in supercritical carbon dioxide. **The Journal of Supercritical Fluids**, v. 154, p. 104592, 2019.
- ZDARTA, J. *et al.* A general overview of support materials for enzyme immobilization: Characteristics, properties, practical utility. **Catalysts**, v. 8, n. 2, 2018.
- ZHANG, Y. *et al.* A one-pot process for synthesis of mitomycin analogs catalyzed by laccase/lipase optimized by response surface methodology. **Engineering in Life Sciences**, v. 19, n. 11, p. 805–814, 2019.
- ZUCCA, P.; FERNANDEZ-LAFUENTE, R.; SANJUST, E. Agarose and its derivatives as

supports for enzyme immobilization. **Molecules**, v. 21, n. 11, p. 1577, 2016.

# Chapter 2

Literature review

## 2 LITERATURE REVIEW

In this chapter, the following topics used for the development of this thesis will be discussed: enzyme immobilization, lipases, laccases, multi-enzymes system, co-immobilization of enzymes and supports for enzyme immobilization.

### 2.1 Enzyme immobilization

Enzymes present several advantages that make them so attractive for using as catalysts in a wide range of reactions. They are biodegradable catalysts that can work under mild reaction conditions (temperature, pH and pressure) and in aqueous solvents. Also a lower energy requirement, chemo, regio and enantioselectivity are among their advantageous characteristics (Castillo, Del *et al.*, 2019; Sulman, Matveeva e Bronstein, 2019; Zhu *et al.*, 2019). These biocatalysts have a high cost and need to be recovered to make their industrial use indeed viable (Sulman, Matveeva e Bronstein, 2019). Industrially, enzymes can be recovered by ultrafiltration technique with use of membranes to be reused, however it would make the process much more complex (Han, Zhou e You, 2020).

Immobilization is defined as to physically confine an enzyme in a defined region of space, retaining its catalytic activity (Inagaki e Ueda, 1987). Then, immobilization facilitates the separation of the enzyme from the medium after a catalytic cycle, lowering the cost of obtaining new enzymes, and allows their application in continuous processes. In addition, immobilization aims to overcome some intrinsic problems related to the low stability of such molecules under some harsh conditions used in industry and may allow also the increase of working conditions (temperature and pH) range (Caparco *et al.*, 2020; Rai, Kumar e Yadav, 2021; Ren *et al.*, 2020; Sulman, Matveeva e Bronstein, 2019; Xie, Zhang e Simpson, 2022). Immobilization may change other characteristics as selectivity and specificity of the enzyme, improve solvent tolerance and can prevent inhibition phenomena (Arana-peña, Rios, Carballares, *et al.*, 2020; Boudrant, Woodley e Fernandez-Lafuente, 2020; Castillo, Del *et al.*, 2019). Besides, the use of immobilized enzymes allows a better control of the reaction and prevents the contamination of the product by the enzyme (Nguyen *et al.*, 2019).

The immobilization of an enzyme can be accomplished by two ways regarding to the utilization of insoluble supports — carrier-bound and carrier-free (Rai, Kumar e Yadav, 2021). Enzymes can be immobilized through four general methods — encapsulation, crosslinked aggregation (CLEA), via non-covalent (adsorption) or covalent adsorption

attachment—whose choice should be made depending on the final application (Caparco *et al.*, 2020; Vera, 2020).

Depending on the chosen method, some structural changes may occur during immobilization processes, resulting in a decrease of enzyme activity (Silva-Torres *et al.*, 2019). The methods of immobilization are governed by the characteristics of the different amino acids residues which can interact or react with the insoluble support by different ways (Andrades, de *et al.*, 2019).

### **2.1.1 Immobilization by adsorption**

Adsorption is one of the most applied methods for enzyme immobilization (Cristóvão *et al.*, 2011). Its great potential is due to the low cost of the process and no need of chemical agents to change the support to make it able to immobilize the enzyme. Besides, adsorption methods are quite simple and do not decrease the enzyme activity (Andrades, de *et al.*, 2019; Mohamad *et al.*, 2015). The adsorption of an enzyme onto a support can be made by different physical interactions, such as hydrophobic, ionic exchanges, hydrogen bonding and van der Waals forces (Jesionowski, Zdarta e Krajewska, 2014).

Immobilization by adsorption can be reversible, which is an attractive point when using some kinds of material as support (Caparco *et al.*, 2020). However, the fact that the enzymes are immobilized by weak forces and that can result in an easy release of them from the support is one of the main drawbacks of this method of enzyme immobilization (Mohamad *et al.*, 2015). Then, some activity loss can be observed during the operation of the catalytic process as a result of the enzyme release (Cristóvão *et al.*, 2011).

The immobilization by ionic exchange interactions strongly depending on the pH of the medium and the isoelectric point of the enzyme (Mohamad *et al.*, 2015). In some cases, a mixed adsorption may occur (with both hydrophobic and ionic exchange interactions), which helps to prevent the enzyme release. However, this does not necessarily imply an increase in stability (Rueda *et al.*, 2016). During the immobilization, adsorption of a second layer can occur on the top of the first enzyme layer, resulting in a multilayer construction (Cristóvão *et al.*, 2011; Li *et al.*, 2018).



### **2.1.2 Immobilization by covalent attachment**

Immobilization by covalent attachment is one of the most studied methodologies because of the stability provided for the immobilized enzyme and the irreversibility of the binding, which prevents the release of the biocatalyst. Generally, covalent methods are complexes, with more steps, and need longer times of contact between enzyme and support to have the immobilization accomplished (Andrades, de *et al.*, 2019; dos Santos *et al.*, 2020). The amino acids residues present in enzyme chain are used for the covalent attachment between enzyme and support (Caparco *et al.*, 2020).

Commonly the material used for enzyme immobilization should be chemically modified to allow the formation of covalent bonds between the amino acid residues of the enzyme molecules and the selected supports. This chemical modification, also known as activation or functionalization of the support, can be performed with the use of various agents such as glutaraldehyde, divinylsulfone, glyoxyl, epichlorohydrin and formaldehyde (Abreu *et al.*, 2014; Cao *et al.*, 2014; Liu, Li e Yan, 2017; Oliveira *et al.*, 2017; Rios *et al.*, 2016; Santos, J. C. S. Dos *et al.*, 2015; Santos, dos *et al.*, 2017). Normally, a first adsorption occurs before the establishment of covalente bonds (Silva *et al.*, 2012).

Occasionally, the reactive residues in enzymes able to be covalently attached to the support can be present in the reactive site, which can decrease its activity when immobilized (Caparco *et al.*, 2020). Also, if a great amount of covalent bonds is established, the tridimensional structure of the enzyme may be affected, leading to the decay of its activity as well. However, the strong rigidification acquired by this formation of multipoint covalent attachment is very related to advantageous high enzyme stability achievement (Manzo *et al.*, 2015; Souza *et al.*, 2017).

### **2.1.3 Use of crosslinker in enzyme immobilizations**

An strategy that could allows the obtainment of immobilized enzymes with great activity and stability is the crosslinking of previously adsorbed enzymes. Crosslinking of immobilized enzymes can be performed by physical interactions, which is the case when some ionic polymers, as dextran sulfate or polyethyleneimine (PEI), are used as crosslinker (Rodrigues *et al.*, 2019). Crosslinking by chemical reaction can be achieved by a covalent binding between some groups ( $-OH$  and  $-NH_3$ , for example) and the reagent used as crosslinker agent (Mak, 2019). Chemical crosslinking consists of a 3D network formation

reaction between enzyme, support and chemical agent, which is called as crosslinker agent (Alamsyah; *et al.*, 2017; Noreen *et al.*, 2016). Then, crosslinkers can be used to decrease enzyme release from the support (Orrego *et al.*, 2018).

Several chemicals can be used as crosslinker, such as aldehyde-dextran, genipin, formaldehyde, carbodiimides (Cavello, Contreras-Esquivel e Cavalitto, 2014; Deb *et al.*, 2015; Marszałł e Siódmiak, 2012; Orrego *et al.*, 2018). When a bifunctional agent is used as crosslinker, a higher rigidification of the immobilized enzyme can be reached (Siar *et al.*, 2018). Several enzymes previously adsorbed on a support have been treated using glutaraldehyde as chemical crosslinker agent (Ait Braham *et al.*, 2019; Siar *et al.*, 2018). Glutaraldehyde has several advantages that make it one of the most used crosslinker: high reactivity (can quickly react with amino groups at pH 7), low cost, availability and efficiency in stabilization. Besides, it can react with other groups than amine, as phenol, thiol and imidazole present in enzyme chain (Migneault *et al.*, 2004).

## 2.2 Lipases

Lipases are class of hydrolytic enzymes widely used in several processes covering a wide range of industrial areas, such as food, energy, fine chemicals, pharmaceuticals, detergent, among others, and in the development of biosensors as well (Abreu *et al.*, 2014; Arana-Peña, Carballares, Corberan, *et al.*, 2020; Arana-peña, Rios, Mendez-sanchez, *et al.*, 2020; Siqueira *et al.*, 2015). They are classified (IUPAC) as triacylglycerol acyl hydrolases (E.C. 3.1.1.3) (Monteiro *et al.*, 2019). Lipases can be obtained from several kinds of microorganisms, animals and plants, which results in enzymes with different characteristics and properties. Commercial lipases are mainly obtained from fungi, yeast and bacteria. Due to their higher thermostability and tolerance to solvents, bacterial lipases have broad industrial applications and present an important role in academic researches (Liu, Li e Yan, 2017; Matte *et al.*, 2014).

These enzymes are reported to present an extensive specificity and a great chemo-, stereo- and regio-specificity (Brem *et al.*, 2012; Cai *et al.*, 2018). Originally, lipases catalyze the hydrolysis of triglycerides generating free fatty acids and glycerol (Rodrigues *et al.*, 2019). In addition to hydrolysis, these enzymes can perform the catalysis of several kinds of reactions, as esterification, transesterification, epoxidation, alcoholysis, etc (Monteiro *et al.*, 2019). Besides, they can perform the synthesis of enantiomerically enriched monomers and catalyze chiral resolutions (Wang *et al.*, 2015). They present a moderate stability and no need of cofactor

to perform the catalysis. Besides, lipases are known for their promiscuity, being able to catalyze a wide range of substrates, even several non-natural ones (Arana-Peña, Carballares, Berenguer-Murcia, *et al.*, 2020; Arana-peña, Rios, Carballares, *et al.*, 2020; Lokha *et al.*, 2020).

The reaction conditions have a great influence on the lipase characteristics and even not great changes can result in important modifications in their conformation altering their activity, selectivity or specificity (Lokha *et al.*, 2020). Originally, lipases perform their function by the phenomena known as interfacial activation, where the lid that covers their catalytic center interacts with the interface of the triglyceride (natural substrates) drops to expose this center to the reaction medium (Arana-peña, Rios, Carballares, *et al.*, 2020). This lid can interact also with other hydrophobic surfaces, such as an hydrophobic support, another lipase (open form) or an hydrophobic protein (Rios, Mendez-Sanchez, *et al.*, 2019). Then, there is an equilibrium between the two forms in solution: open and closed conformation (Arana-Peña, Carballares, Corberan, *et al.*, 2020).

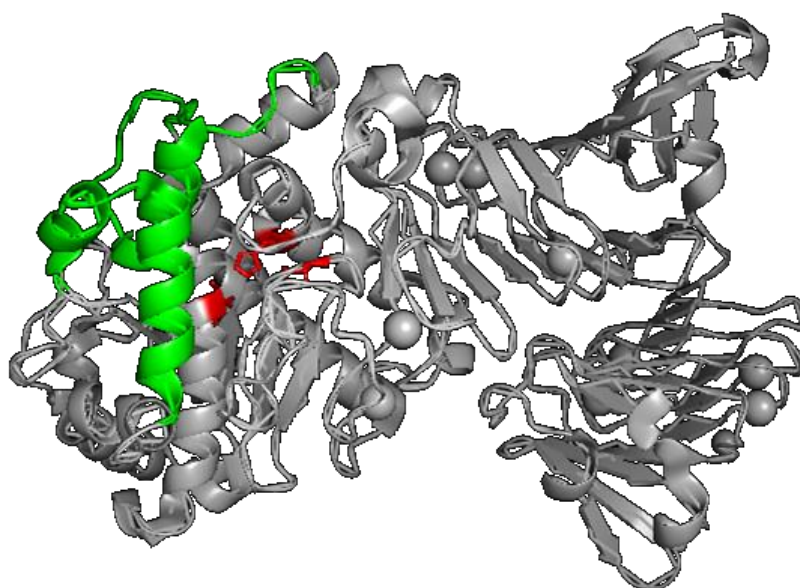
### **2.2.1 Lipase from *Pseudomonas fluorescens***

Among the various lipases of bacterial origin, those of the genus *Pseudomonas* are among the most commonly used in the field of biotechnological applications (Brem *et al.*, 2012; Christopher, Kumar e Zambare, 2014; Guldhe *et al.*, 2015; Liu, Li e Yan, 2017). Lipase from *Pseudomonas fluorescens* (PFL) is an enzyme very reported in literature (Arana-peña, Rios, Carballares, *et al.*, 2020; Han *et al.*, 2016; Nunes *et al.*, 2013; Rios, Mendez-Sanchez, *et al.*, 2019). This lipase has an expressive importance in this groups of enzyme, for it catalyze reaction of transesterification, aromatic compounds synthesis, acylation of alcohols and synthesis of fatty acid methyl ester, among others (Dwivedee *et al.*, 2017). In addition, this enzyme has been shown to be efficient in kinetic resolutions of racemic alcohols, acids and esters, as well as in the synthesis of enantiopure intermediates of drugs such as the  $\beta$ -blockers propranolol, atenolol and pindolol (Lima *et al.*, 2017; Soni *et al.*, 2018).

The lid present in PFL is related to be large (Arana-peña, Rios, Carballares, *et al.*, 2020). This enzyme has a molecular volume of  $3 \times 4 \times 5 \text{ nm}^3$  and an average molecular diameter of around 5 nm (50 Å) (Lima *et al.*, 2015). Literature reports the molecular weight of PFL from different strains varying from 33 to 55 kDa, different optimum pH (the most of them around 8 – 9) and an isoelectric point at pH 4 (Rios *et al.*, 2018). Besides, it presents activity from pH 5 to pH 10 and up to 100 °C (Liu, Li e Yan, 2017). Its primary structure is formed by 449 amino acids and its catalytic triad is composed by residues Ser-206, Asp-254 and His-312 (Soni

*et al.*, 2017). Fig. 2.1 shows a schematic representation of PFL (the PDB code is related to the lipase from *Pseudomonas* sp. MIS38, which is reported as a great template for PFL, with an identical catalytic triad) with its lid covering the catalytic site (Angkawidjaja *et al.*, 2007; Soni *et al.*, 2017, 2018). It is reported that PFL can form aggregates (dimers), and the presence of detergent can undo these aggregates and increase greatly its activity (Rios *et al.*, 2018).

Figure 2.1 - Schematic representation of lipase from *Pseudomonas fluorescens* PFL crystal structure (PDB lipase code: 2Z8X) with the active site (catalytic triad) in red and the lid in green. The following structure was taken from Protein Data Bank (PDB) by using PyMol Educational.



Source: Elaborated by the author

### 2.3 Laccases

Laccases (EC 1.10.3.2) are extracellular enzymes part of the oxidases group and can be obtained from several sources, such as bacteria, lichens, fungi, prokaryotes and insects and are reported to be multicopper enzymes. Among the several sources of these enzymes, wood-rotting fungi (such as *Trametes versicolor*, *Trametes hirsuta* etc) are the main producers (Bebić, Banjanac, Ćorović, *et al.*, 2020). As a multicopper enzyme, laccase present three kinds of copper atoms: T<sub>1</sub>, T<sub>2</sub> and T<sub>3</sub>. The type 1 copper is responsible for the blue color of the enzyme and is reported to participate of the reaction with the substrates and can be replaced by mercury or cobalt. The type 2 copper forms a triangle with the two type 3 coopers and work together in the reduction of O<sub>2</sub> and are responsible to stock the electrons donated by the reducing substrates. The two type 3 coopers and the type 2 cooper form what is called as a trinuclear copper cluster

(TNC) (Cristóvão *et al.*, 2011; Ernst *et al.*, 2018; Kadri *et al.*, 2017; Morozova *et al.*, 2007; Vera, 2020; Zhu *et al.*, 2019).

They are able to perform the oxidation of a broad set of aromatic substrates by reducing the oxygen (air) into water. It can work with aromatic hydroxyl, polyphenols and also methoxy substituted monophenols, for example. Besides, their functional activities can be expanded to work with other groups, as phenyl-aryl ethers, if laccases are in the presence of radical mediators. Laccases are very applied in processes of bioremediation, degrading several pollutants (in soil or water), such as bisphenol A, chlorophenols, nonylphenol and other chemicals as well. Besides, their application covers process of wine clarification, baking, detergent production, beverage processing, pharmaceuticals synthesis, paper industry, development of biosensors, among others (Bebić, Banjanac, Rusmirović, *et al.*, 2020; Crestini, Melone e Saladino, 2011; Guerberoff e Camusso, 2019; Pramanik *et al.*, 2019; Ren *et al.*, 2019; Sankar *et al.*, 2020). Laccases can perform one-electron oxidation. Then, when the catalysis of some substrates that can donate two electrons are carried out by these enzymes, radicals may be generated and a non-enzymatic reaction occurs subsequently (Kadri *et al.*, 2017).

Laccases from fungal sources generally present an molecular weight of 60 – 70 kDa and an isoelectric point in the range of pH 3 – pH 7, mostly near to pH 4 (Bebić, Banjanac, Rusmirović, *et al.*, 2020). Restrictions such as low stability, elevated sensibility and high production cost limits their wide application in industry (Vera, 2020). Most of the isolated laccase present low activity, however the addition of some heavy metal ions, such as cobalt, zinc, calcium and cooper, is related in literature to increase laccase activity (Sankar *et al.*, 2020). Laccases have presented greater affinity for organic supports than inorganic ones (Bebić, Banjanac, Rusmirović, *et al.*, 2020).

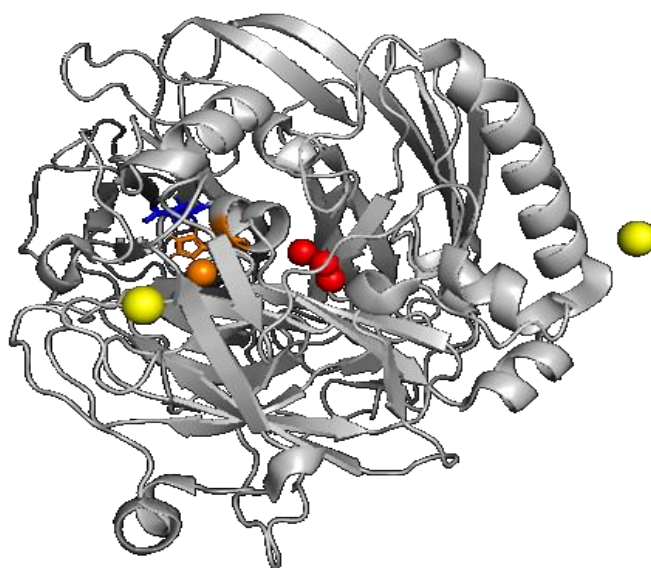
### **2.3.1 *Novozymes 51003***

Laccase from *Myceliophthora thermophila* expressed in *Aspergillus oryzae* is commercially know as Novozym® 51003 (Bebić, Banjanac, Rusmirović, *et al.*, 2020). Then, this enzyme is obtained by submerged fermentation and is considered is a stable and robust laccase. Its molecular weight is reported as 56 kDa (Wellington *et al.*, 2013). However, literature reports results of SDS-PAGE showing an apparent molecular weight of 83 kDa. This augmented mass could be related with the glycosylation of this enzyme, since laccases are normally reported to present a high degree of N-glycosylation (Ernst *et al.*, 2018). Its isoelectric point is found to be around pH 4 (Bebić, Banjanac, Rusmirović, *et al.*, 2020). Several

applications are reported in literature for Novozymes 51003, such as degradation of pesticide lindane, pulp delignification, sulfamethoxazole (antibiotic) removal, among others (Bebić, Banjanac, Ćorović, *et al.*, 2020; Bebić, Banjanac, Rusmirović, *et al.*, 2020; Haugland *et al.*, 2019; Jia *et al.*, 2013). Also, this enzyme is reported to work in the synthesis of several pharmaceuticals compounds (Romero-Guido, Baez e Torres, 2018; Wellington *et al.*, 2013).

The crystal structure of laccase produced by a recombinant *Myceliophthora thermophila* overexpressed in *Aspergillus oryzae* is reported in literature in its schematic representation is showed in Fig. 2.2. It is constituted by 559 residues of amino-acids. Besides the 4 coppers founded in laccases, two  $\text{Ca}^+$  were identified and are reported to be originated from the crystallization conditions. For the oxidation of phenolic substrates, the catalytic cycle starts with the electron transfer to the  $\text{T}_1$  cooper, for it is reported to be the primary electron acceptor. Then, the electrons are transferred to the TNC site (formed by the two type 3 coopers and the type 2 cooper) for the reduction of molecular oxygen to occur. With the help of a bridging water molecule, Glu235 along with His508 ( $\text{T}_1$  copper ligand) constitutes a polar site for the recognition of phenol groups. Besides, the residue Glu235 (negatively charged) is greatly involved in the catalytic cycle, for it facilitated the abstraction of protons from the  $-\text{OH}$  group of substrate (Ernst *et al.*, 2018; Kallio *et al.*, 2009).

Figure 2.2 - Schematic representation of Laccase from *Myceliophthora thermophila* expressed in *Aspergillus oryzae* crystal structure (PDB code: 6F5K). TNC (two type 3 coopers and the type 2 cooper/ spheres) site in red,  $\text{T}_1$  copper (sphere) and His508 ( $\text{T}_1$  copper ligand) in orange, Glu235 in blue and two  $\text{Ca}^+$  in yellow. The following structure was taken from Protein Data Bank (PDB) by using PyMol Educational.



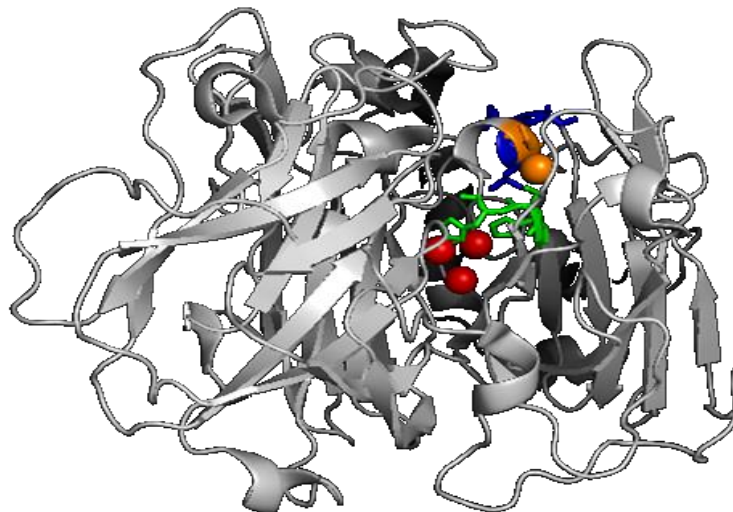
Source: Elaborated by the author

### 2.3.2 Laccase from *Trametes versicolor*

Laccase from *Trametes versicolor* is one of the most prominent laccases in study (Addorisio *et al.*, 2013; Kołodziejczak-Radzimska *et al.*, 2020). It is reported to be part of the high-potential (redox) laccases group (Morozova *et al.*, 2007). Its isoelectric point is reported to be around pH 4 and the optimum temperature as 50 °C (Xia *et al.*, 2016). It's a monomeric enzyme with a molecular weight around 60 – 70 kDa (Addorisio *et al.*, 2013; Zhang *et al.*, 2019). Literature reports several applications for laccase from *Trametes versicolor*, such as micropollutants removal and detection, synthesis of dimeric phenols, antioxidant compounds and intermediates (pharmaceuticals), lignin bioprocessing, elimination of pharmaceuticals presents in wastewater, synthesis of naphthoquinone (pharmaceuticals), among others (Crestini, Melone e Saladino, 2011; Gavezzotti *et al.*, 2011; Jia *et al.*, 2013; Romero-Guido, Baez e Torres, 2018; Touahar *et al.*, 2014; Zhang *et al.*, 2019).

A laccase from *Trametes versicolor* was produced and its crystal structure was reported in literature. The schematic representation of this enzyme is showed in Fig. 2.3. Its structure is formed by 449 amino acids residues and has approximate dimensions of 65 x 55 x 45 Å<sup>3</sup>. It was identified a small negatively charged cavity close to T<sub>1</sub> copper (primary electron acceptor) where the substrate binds and is also important to stabilize the generated radical cation during the catalysis. A tripeptide (His452-Cys453-His454) is connecting T<sub>1</sub> site and the other 3 coppers. T<sub>2</sub> copper and the two T<sub>3</sub> coppers forms the TNC site responsible for the oxygen reduction. Then, the molecular oxygen access this last site and water is released to the medium. The presence of the tripeptide Leu459-Glu460-Ala461 in the crystal structure of this laccase from *Trametes versicolor* is reported to be characteristic of laccases with high redox potential (Piontek, Antorini e Choinowski, 2002).

Figure 2.3 - Schematic representation of Laccase from *Trametes versicolor* crystal structure (PDB code: 1GYC). TNC (two type 3 coopers and the type 2 cooper/ spheres) site in red, T<sub>1</sub> copper (sphere) and His458 (T<sub>1</sub> copper ligand) in orange, tripeptide His452-Cys453-His454 in green and tripeptide Leu459-Glu460-Ala461 in blue. The following structure was taken from Protein Data Bank (PDB) by using PyMol Educational.



Source: Elaborated by the author

## 2.4 Multi-enzymes system

A large part of the developed scientific research is focused on the elaboration of more efficient and cleaner processes. One great example in biocatalysis field of such efficient process is the integration of different reactions catalyzed by two or more enzymes in a called multi-enzymes system (Ricca, Brucher e Schrittwieser, 2011). Then, the use of such kind of system allows the accomplishment of highly complex processes. In Nature, several enzymes present in living organisms normally co-work in cascade or multi-step reactions to perform different processes. Indeed, the use of multi-enzymatic systems for complexes catalysis has been exploited long ago with the use of native microorganisms (*in vivo* approach) for the production of vinegar, for example (Lopez-Gallego e Schmidt-Dannert, 2010; Zhao *et al.*, 2014).

The use of multi-enzymes systems for the industrial production of different compounds has attracted increasing attention due to several advantages mainly related to the minimization of down-stream steps and a consequent more profitable exploitation of resources. Multi-enzymes systems can be useful to perform several kinds of multi-reactions: cascade, parallel or in a network configuration. The use of different enzymes in the accomplishment of



a whole process can be carried out in a modular or in a one-pot approach (Ardao e Zeng, 2013; Brenna *et al.*, 2017).

#### **2.4.1 One pot system/Cascade reactions**

Multi-steps or cascade reactions generally need more than one single enzyme to accomplish the whole process (Vera, 2020; Yu *et al.*, 2021). For that, cascade reactions performed by multi-enzymes systems has gained more and more space for industrial production of several compounds (Ren *et al.*, 2019, 2020). When a multi-enzymatic system is used to perform the catalysis of a cascade reaction, the product of one enzyme (intermediate) should diffuse from its active site to another in order to continues the reaction. A very common way to perform a whole process using multi-enzymes system is placing them in a single reactor, which is called as one-pot process. Performing this whole transformation in a single decrease the time of substrate/product (intermediate) transportations and their waste or losses as well (Ardao e Zeng, 2013; Ren *et al.*, 2019; Yu *et al.*, 2021). Similar to all industrial biocatalysis using soluble enzymes, application of multi-enzymes systems in large-scale present some challenges related to the difficulty of recovering and low stability of enzymes in soluble form (Long *et al.*, 2020).

#### **2.4.2 Lipases and laccases**

Several multi-enzymes systems using the tandem effect of lipase and laccase are reported in literature. A cascade system was prepared using lipase immobilized onto diatomites and laccase immobilized onto glass beads for the synthesis of a mitomycins analog (antibiotic). The co-catalysis consisted in a first formation of quinone (phenol oxidation catalyzed by the laccase), followed by a lipase-catalyzed reaction between the amine and the formed quinone (C-N coupling) (Zhang *et al.*, 2020). Literature reports also another successfully tandem use of lipase (commercial/immobilized on acrylic resin) and laccase (immobilized onto a nanoparticle metal-organic framework). These enzymes were applied for the synthesis of 2,5-Furandicarboxylic acid (FDCA), a biorenewable chemical used for several applications (plastics, drugs, polyamides, etc), from 5-hydroxymethylfurfural (HMF) (Chang *et al.*, 2019).

Lipase and laccase (co-immobilized in polymer complexes) co-worked to catalyze the synthesis of a perfectly structured alternating fluorescent copolymer in a one-pot system. The process could be performed only by laccase action, however the addition of lipase enzyme improved the product yield up to 30.7%. The process consisted in a first catechol oxidation

catalyzed by laccase generating o-quinone, followed by diamines addition (Michael addition) catalyzed by lipase (copolymerization process) (Scheibel e Gitsov, 2019). Another tandem use of lipase and laccase for the synthesis of polymers are related in literature. These two enzymes (laccase in soluble form, and some commercial lipases in both soluble and immobilized forms) were applied for the production of enantiomerically enriched dimers of vinylphenols. Firstly, laccase catalyzed the oxidation of isoeugenol and vinylguaiacol, which generated racemic compounds. Then, lipase catalyzed the alcoholysis reaction for product the enantiomerically enriched compounds (Gavezzotti *et al.*, 2011). These enzymes can co-work also in bioremediation processes, degrading different pollutants, such those ones present in olive mill wastewater and polyaromatic hydrocarbons (Balaji, Arulazhagan e Ebenezer, 2014; Zerva *et al.*, 2017).

## 2.5 Co-immobilization of enzymes

Cascade reactions performed by co-immobilized enzymes are inspired by Nature, in which several enzymes that are close to each other are co-working to accomplish a process (Sulman, Matveeva e Bronstein, 2019). Co-immobilize a multi-enzymes system leads to an easier process of recovering them after a catalytic cycle (Ren *et al.*, 2019). Besides, it helps to overcome some problems of the application of multi-enzymes in a one-pot system related to the stability of these biocatalysts (Yu *et al.*, 2021).

Working with co-immobilized enzymes rather than single-immobilized enzymes present an important advantage related to the local concentration of intermediated produced, since it will not need to diffuse to other particle to meet another catalytic site (Vera, 2020). Then, the product generated by the first enzyme act as substrate to the following enzyme and it improves the catalysis general performance (Long *et al.*, 2020). Also, by decreasing the reaction time, inhibition phenomena or some inactivation process can be minimized (Torres e Batista-Viera, 2019). Besides improving the conversion, the use of co-immobilized enzymes facilitates downstream process as well (Ren *et al.*, 2019).

This technique could bring advantages even in the case of co-immobilizing several enzymes of the same class. For example, the use if co-immobilized lipases in hydrolysis of oils, in which an important change of pH occurs, allows the hydrolytic activity to work longer because of the differences in the optimal pH of each on of these enzymes (Arana-Peña, Rios, *et al.*, 2020) . Literature related also the co-immobilization of three different laccases in order to

expand the range of optimum pH of the biocatalyst by taking advantage of the difference in the characteristics of each enzyme (Vera, 2020).

The co-immobilization of different class of enzymes has been the subject of research in the field of biocatalysis. For example, literature reports the use of glycosyltransferase (C-glycosyltransferase from rice and sucrose synthase from soybean) co-immobilized onto an anionic support to the cascade process of nothofagin synthesis with an efficient reuse of the biocatalysts (Liu, Tegl e Nidetzky, 2021). A one-pot conversion of gluconic acid from corn straw cellulose was performed using cellulose, glucose oxidase and catalase co-immobilized onto Eudragit L-100 (Yu *et al.*, 2021). The use of co-immobilized  $\beta$ -galactosidase, D-arabinose isomerase and D-xylose isomerase in the biotransformation of lactose from whey showed to minimize the inhibition of lactose hydrolysis product when compared to single-immobilized enzymes (Torres e Batista-Viera, 2019).

One strategy used to co-immobilize different enzymes is through the simultaneously mixing of the enzymes, using previously determined amount of each on, with the support in order to attach them by covalent interactions or adsorption, for example (Ozyilmaz e Tukel, 2007; Torres e Batista-Viera, 2019; Vera, 2020). Different enzymes can be co-immobilized also through carrier-free methods, as crosslinked aggregates enzymes, generating what is called as combi-CLEAs (Talekar *et al.*, 2013; Touahar *et al.*, 2014). Co-immobilizing different enzymes has great challenges, for one should choice a support, co-immobilization strategy and conditions that allow the interaction between enzyme with distinct characteristics and the support resulting in an active and stable biocatalyst (Peng *et al.*, 2020).

### ***2.5.1 Layer-by-layer strategy***

Co-immobilization of multi-enzymes through a random way can result in a biocatalyst with low catalytic efficiency (Peng *et al.*, 2020). On the other side, a layer-by-layer strategy could overcome a problem related to co-immobilization techniques: enzyme activities decrease as a result of the reduction of enzyme loading on the support (Arana-Peña, Rios, *et al.*, 2020). Besides, well-ordered co-immobilization may enhance the catalytic efficiency of the produced biocatalyst (Peng *et al.*, 2020).

PEI (polyethyleneimine) is reported in literature as an useful reagent to work as a glue between two enzyme layers. This cationic polymer — with primary, secondary and tertiary amino groups — is able to interact through ionic exchanges with several proteins (Arana-Peña, Rios, *et al.*, 2020). It is useful also to produce immobilized biocatalysts with higher activity by

placing on a support several layers of the same enzyme using PEI as a linker between the layers. (Arana-peña, Rios, Mendez-sanchez, *et al.*, 2020). Literature reports the use of PEI in process of immobilization of different enzymes, such as laccase, lipase, D-aminoacid oxidase and  $\beta$ -galactosidase, with successful results (Arana-Peña, Rios, *et al.*, 2020; Khoobi *et al.*, 2015; Pessela *et al.*, 2005; Xia *et al.*, 2016).

In order to avoid the release of the enzymes (linked by PEI) from the support, it is necessary to form some covalent bonds between them. For that, glutaraldehyde can be used as a crosslinker agent and have already showed great results together with the use of PEI in enzyme immobilization procedures (Arana-Peña, Rios, *et al.*, 2020; Arana-peña, Rios, Mendez-sanchez, *et al.*, 2020; Rios, Arana-Peña, *et al.*, 2019). Then, different enzymes can be immobilized using a layer-by-layer approach, having PEI as a glue between the enzyme layers and glutaraldehyde as a final layer for the crosslinking of the biocatalyst.

## 2.6 Supports for enzyme immobilization

Among all the known methods for enzyme immobilization, those one using carriers are the most used due to the amount and diversity of materials available (or that can be produced) to be used as support for certain industrial applications (Manzo *et al.*, 2015; Santos, J. C. S. *et al.*, 2015). The choice of the appropriate material to be used as support is a key point for a successful enzyme immobilization (Xie, Zhang e Simpson, 2022). Supports for immobilization can be organic or inorganic, natural or synthesized. Organic supports are the most used, with the natural ones being the least expensive and the easiest to degrade (Albuquerque *et al.*, 2016; Bezerra *et al.*, 2015; Chen *et al.*, 2014; Dhake *et al.*, 2012; Matte *et al.*, 2014). In organic polymers, the groups most frequently used to form bonds, after activation, are the hydroxyl and/or amino groups, present in materials such as agarose, chitosan and cellulose (Demirkan, Avci e Aykut, 2018; Rueda *et al.*, 2016; Santos, dos *et al.*, 2017).

Surface area, affinity for the enzyme, presence of groups able to attach the protein (or able to be activated), mechanical resistance, insolubility and inertia to the reaction medium are the main characteristics to be observed for the support choice (Bebić, Banjanac, Rusmirović, *et al.*, 2020). Another important characteristic of the support which should be taken into account is the loading capacity, that represents the maximum amount of enzyme that this support is able to retain (per gram of support) (Arana-peña, Rios, Mendez-sanchez, *et al.*, 2020). The use of nanomaterials as support for enzyme immobilization enables high amount of enzymes attached per gram of carrier (Romero-Guido, Baez e Torres, 2018). Besides, several micro or nano-sized

particles presenting different porosity have been studied for the use as enzyme immobilization support (Bebić, Banjanac, Rusmirović, *et al.*, 2020). Porous supports are very attractive because they allow high enzyme loading and protect the protein from the environment (Bebić, Banjanac, Rusmirović, *et al.*, 2020; Inagaki e Ueda, 1987).

Lipase has been successfully immobilized onto several supports, such as magnetic nanoparticles, bacterial cellulose, layered double hydroxides, anion-exchange resin, agarose, Immobead, etc. (Alamsyah; *et al.*, 2017; Drozd *et al.*, 2019; Matte *et al.*, 2014; Monteiro *et al.*, 2019; Rueda *et al.*, 2016; Silva Dias *et al.*, 2019). Laccase immobilization has been successfully achieved by using different supports, such as silica nanoparticle, mesoporous alumina (Al<sub>2</sub>O<sub>3</sub>), magnetic chitosan, green coconut fiber, cellulose-based Granocel, SBA-15, among others (Bautista, Morales e Sanz, 2015; Bebić, Banjanac, Ćorović, *et al.*, 2020; Cristóvão *et al.*, 2011; Kołodziejczak-Radzimska *et al.*, 2020; Pramanik *et al.*, 2019; Rekuć *et al.*, 2008).

### **2.6.1 Agarose based supports**

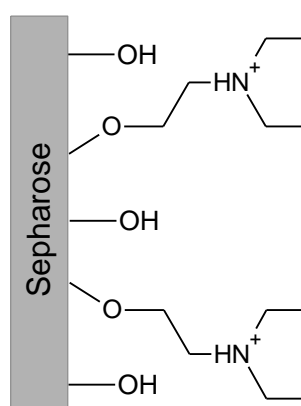
Several porous materials have been applied as support for different enzyme immobilizations, for they allow the improvement of biocatalyst activity by increasing the loading capacity. Besides, when the material present large pores (> 25 nm), the enzyme denaturation during immobilization is reduced as well (Sulman, Matveeva e Bronstein, 2019). Sepharose (Agarose) is a commercial porous material that can be found with different pore size. It is an inert matrix that has been chemically modified by different functionalization methods, resulting in a wide range of agarose-based materials (Lokha *et al.*, 2020). Agarose or agarose based supports are among the most used supports for different enzyme immobilization and stabilization (Arana-peña, Rios, Carballares, *et al.*, 2020; Gonçalves *et al.*, 2008; Lokha *et al.*, 2020; Rueda; *et al.*, 2015; Siar *et al.*, 2018; Tardioli *et al.*, 2003).

#### **2.6.1.1 DEAE-Sepharose**

DEAE-Sepharose (known also as DEAE-Agarose) is a commercial aminated support and, since it is derived from Agarose, it brings all the advantages of such porous carrier (Mateo *et al.*, 2000). The schematic representation of its chemical surface is showed in Fig. 2.4 (Jesionowski, Zdarta e Krajewska, 2014; Zhu *et al.*, 2017). It is formed by a polysaccharide sepharose with the ionic group diethylaminoethyl (DEAE) covalently linked to it. DEAE-Agarose is an anion-exchange resin and has been widely applied to interact with proteins, either

for separation and purification processes or for immobilization procedures. This positively charged material can immobilize enzymes with negative charges. To allow the ionic exchange between enzyme and support, such immobilization should be performed using conditions of pH above the isoelectric point of the target enzyme (Mateo *et al.*, 2000; Morais Júnior, de *et al.*, 2018; Souza *et al.*, 2017; Zhu *et al.*, 2017). Literature reports the immobilization of different enzymes onto DEAE-Agarose, such as lipase, peptidase and laccase (Britos *et al.*, 2018; Britos e Trelles, 2016; Oliveira *et al.*, 2022; Pereira *et al.*, 2015; Rosa-Garzon, da *et al.*, 2020; Souza *et al.*, 2017).

Figure 2.4 – Representation of the surface chemical structure of Sepharose-DEAE (diethylaminoethyl).



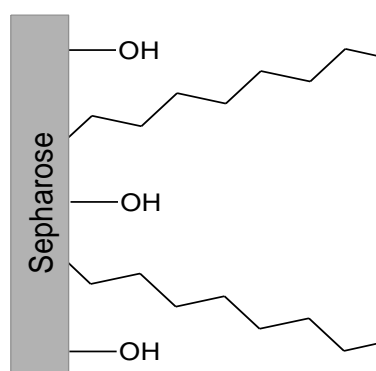
Source: Elaborated by the author

### 2.6.1.2 Octyl- Agarose

Octyl-Agarose is a hydrophobic support derived from a functionalization of agarose and its surface chemical structure is schematized in Fig. 2.5 (Lokha *et al.*, 2020; Rueda *et al.*, 2015). Different lipases have been immobilized using octyl-agarose as carrier (Arana-peña, Rios, Carballares, *et al.*, 2020; Arana-peña, Rios, Mendez-sanchez, *et al.*, 2020; Manoel *et al.*, 2015; Peirce *et al.*, 2016; Rios, Arana-Peña, *et al.*, 2019). The physicochemical characteristics of these enzymes make their immobilization by adsorption using hydrophobic material as support a simple and efficient method to insolubilize them (Yousefi, Mohammadi e Habibi, 2014). These immobilizations may be performed under a wide range of pHs and the protocols are in general very simple (Rodrigues *et al.*, 2019). Lipase immobilization by

hydrophobic interactions can be relatively strong, for its involves several points of the enzyme, although it could be reversible in the presence of substrates or products behaving as detergent (Arana-peña, Rios, Carballares, *et al.*, 2020). Also, when in contact with hydrophobic supports, lipases can interact to open its lid displacing the equilibrium to the open conformation (similar to interfacial activation) (Sánchez-Otero *et al.*, 2022). Then, besides resulting on the insolubilization of the enzyme, the immobilization using such kind of supports allows also the hyperactivation and stabilization of these biocatalysts (Arana-peña, Rios, Mendez-sanchez, *et al.*, 2020). Using octyl-agarose as support, lipase immobilization can be reached very fast (Arana-peña, Rios, Carballares, *et al.*, 2020). Particularly, immobilization of lipase from *Pseudomonas fluorescens* by adsorption onto octyl-agarose can allows more stabilization than using a multipoint covalent method (Albuquerque *et al.*, 2016; Arana-peña, Rios, Carballares, *et al.*, 2020).

Figure 2.5 – Representation of the surface chemical structure of Octyl-Agarose.



Source: Elaborated by the author

### 2.6.3 Cellulose nanocrystalline

Natural polymers have greatly attracted attention for their friendly-environment aspect (Drozd *et al.*, 2019). Cellulose is the most abundant polymer on Earth and can be synthesized by plants, animals or bacteria. It constitutes an immeasurable source of raw material, since it combines low cost and biocompatibility for several applications (Islam *et al.*, 2018). Literature reports several studies involving the immobilization of different enzymes in cellulose or in cellulose-based materials — such as cellulose nanofiber and crystalline cellulose (Cao *et al.*, 2016; Kim *et al.*, 2015; Rekuć *et al.*, 2008; Sampaio *et al.*, 2016; Uth *et al.*, 2014).

They have shown attractive properties and may replace some of the synthetic materials used as support for protein immobilization (Sathishkumar *et al.*, 2014; Uth *et al.*, 2014). Nanosized material has attracted increasing attention for using as support (Nguyen *et al.*, 2019). Nanocellulose refers to a nanostructured cellulosic material and can be identified by three different configurations: cellulose nanocrystal (CNC), cellulose nanofibers (CNF) and bacterial cellulose (BC). These nano-sized materials present a lighter weight and higher volumetric surface area, which may extend their application for industrial aims (Sharma *et al.*, 2019). The cellulose nanocrystalline (CNC) can be obtained by a treatment of cellulose fibers through the cleavage of its amorphous region for the crystalline portions release (Yang, Chen e Ven, van de, 2015).

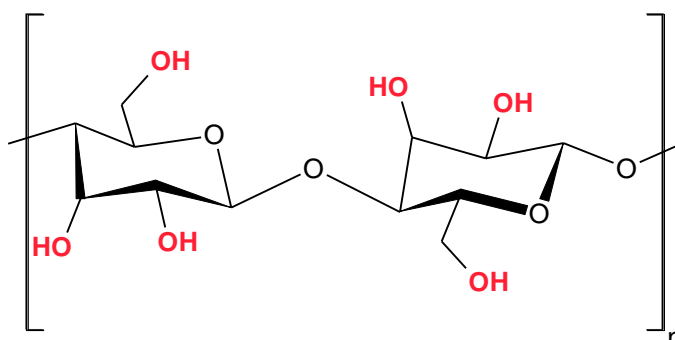
High stiffness, large surface area, high aspect ratio and good hardness and strength are some of the properties that made CNC attractive for using as nanomaterial in several areas, such as drug delivery and protein immobilization (Cao *et al.*, 2014; Incani e Danumah, 2013). Some characteristics of CNC depends on the crude material and process of extraction but remained in typical ranges, as the width (less than tens of nm, generally), length (20 to thousands of nm) and surface area ( $150\text{-}250\text{ m}^2\text{g}^{-1}$ ) (Cao *et al.*, 2014; Islam *et al.*, 2018). CNC can be obtained from cellulose by some mechanical processes, such as high pressure homogenization, microfluidization and ultrasonication (Wang, 2019).

#### 2.6.3.1 Cellulose activation

The cellulose chain is composed by units of cellobiose (anhydro-D-glucopyranose) linked by  $\beta$ -1,4 glycosidic bonds (Islam *et al.*, 2018). Three hydroxyl groups can be found in each monomer unit (Fig. 2.6), which contributes for the crystalline packing through the formation of ordered hydrogen bonds. The hydroxyl groups can be used also to interact with enzymes, or even be modified or functionalized in order to establish stronger interactions with these biomacromolecules (Sulaiman *et al.*, 2014).



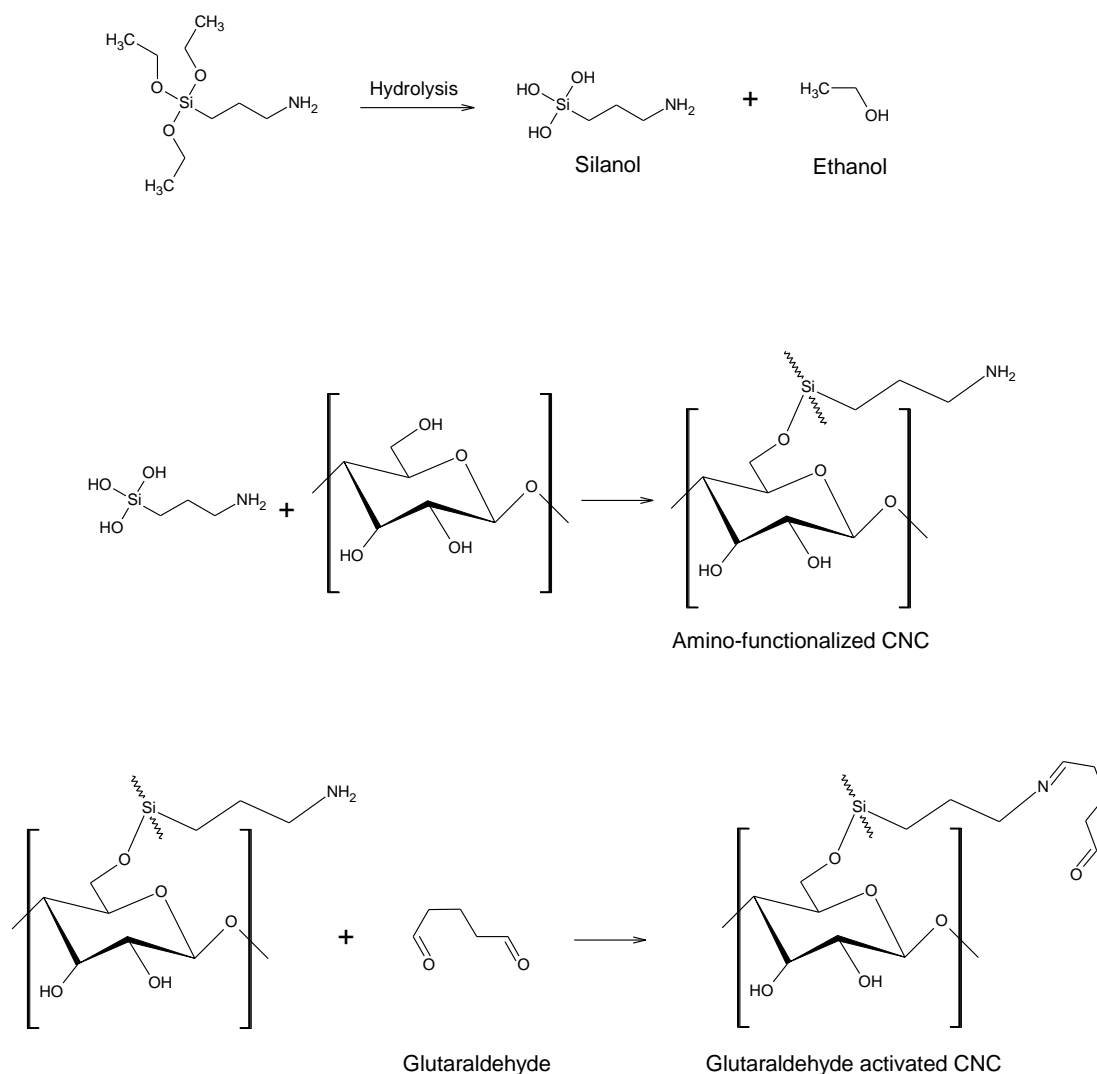
Figure 2.6 – Representation of the chemical structure of cellulose with the hydroxyl groups (that can be chemically modified) in red.



Source: Elaborated by the author

Supports having primary amino groups can be activated with glutaraldehyde, one of the most used reagents in enzyme immobilization methodologies. A glutaraldehyde-activated support is considered heterofunctional, for the enzyme can be firstly immobilized by ionic exchange followed by the covalent attachment with the primary amino groups present in the enzyme residues (Ait Braham *et al.*, 2019; Andrades, de *et al.*, 2019). Amino-functionalized CNC can be obtained through silylation (silane grafting) of this material. 3-aminopropyltriethoxysilane (APTES) is reported in literature as a very useful silane that can be used to modify CNC. In general, silylation using APTES has three steps (Fig. 2.7). The first one is the generation of silanol by the hydrolysis of the alkoxy groups. Then, this silanol is adsorbed onto the CNC surface (hydroxyl groups in CNC and silanol forms hydrogen bonds). Finally, chemical reaction occurs leading to the formation of Si-O-C bonds (Gennari *et al.*, 2020; Khanjanzadeh *et al.*, 2018). After silylation, CNC can be activated using glutaraldehyde according to the methodologies broadly described in literature to generate an aldehyde-functionalized CNC. Fig. 2.7 shows a schematic representation of the activation using glutaraldehyde. It is important to note that it is an hypothetical reaction with one single molecule of glutaraldehyde, since it can be found also at dimeric or cyclic form (Barbosa *et al.*, 2013, 2014).

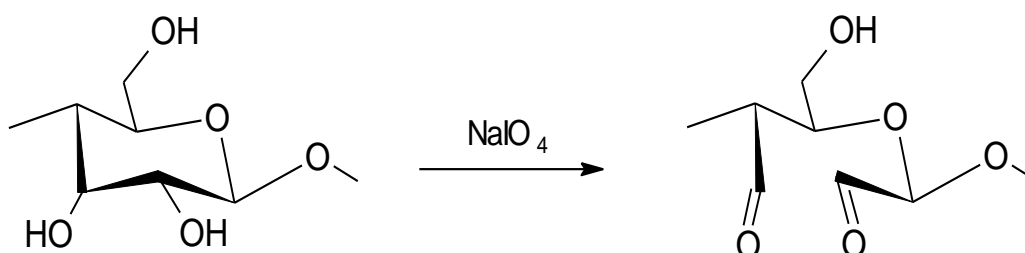
Figure 2.7 – Silylation (silane grafting) of CNC to generate an amino-functionalized CNC support followed by glutaraldehyde activation.



Source: Elaborated by the author

Aldehyde groups can be generated in CNC surface also by the oxidation of the hydroxyl groups found on its chain. Literature reports the use of sodium periodate ( $\text{NaIO}_4$ ) to oxidize cellulose. This oxidation reaction cleaves the C2-C3 bond leading to the cellulose's glucopyranoside ring opening and the formation of a dialdehyde cellulose (Fig. 2.8). These aldehyde groups have high reactivity and can interact with desired enzyme for their immobilization (Siller *et al.*, 2015; Sun *et al.*, 2015; Yang, Chen e Ven, van de, 2015).

Figure 2.8 – Oxidation of CNC using sodium periodate ( $\text{NaIO}_4$ ) to form a dialdehyde cellulose.



Source: Elaborated by the author

## 2.7 References

ABREU, L. DE *et al.* Efficient purification-immobilization of an organic solvent-tolerant lipase from *Staphylococcus warneri* EX17 on porous styrene-divinylbenzene beads. **“Journal of Molecular Catalysis B: Enzymatic”**, v. 99, p. 51–55, 2014.

ADDORISIO, V. *et al.* Oxidation of phenyl compounds using strongly stable immobilized-stabilized laccase from *Trametes versicolor*. **Process Biochemistry**, v. 48, n. 8, p. 1174–1180, 2013.

AIT BRAHAM, S. *et al.* Cooperativity of covalent attachment and ion exchange on alcalase immobilization using glutaraldehyde chemistry: Enzyme stabilization and improved proteolytic activity. **Biotechnology Progress**, v. 35, n. 2, p. 1–4, 2019.

ALAMSYAH, G. *et al.* Effect of chitosan’s amino group in adsorption-crosslinking immobilization of lipase enzyme on resin to catalyze biodiesel synthesis. **Energy Procedia**, v. 136, p. 47–52, 2017.

ALBUQUERQUE, T. L. D. *et al.* Easy stabilization of interfacially activated lipases using heterofunctional divinyl sulfone activated-octyl agarose beads. Modulation of the immobilized enzymes by altering their nanoenvironment. **Process Biochemistry**, v. 51, n. 7, p. 865–874, 2016.

ANDRADES, D. DE *et al.* Immobilization and stabilization of different  $\beta$ -glucosidases using the glutaraldehyde chemistry: Optimal protocol depends on the enzyme. **International Journal of Biological Macromolecules**, v. 129, p. 672–678, 2019.

ANGKAWIDJAJA, C. *et al.* Crystal structure of a family I.3 lipase from *Pseudomonas sp.* MIS38 in a closed conformation. **FEBS Letters**, v. 581, n. 26, p. 5060–5064, 2007.

ARANA-PEÑA, S.; RIOS, N. S.; CARBALLARES, D.; *et al.* Effects of Enzyme Loading and Immobilization Conditions on the Catalytic Features of Lipase From *Pseudomonas fluorescens* Immobilized on Octyl-Agarose Beads. v. 8, n. February, p. 1–13, 2020.

ARANA-PEÑA, S.; RIOS, N. S.; MENDEZ-SANCHEZ, C.; *et al.* Use of polyethylenimine to produce immobilized lipase multilayers biocatalysts with very high volumetric activity using octyl-agarose beads : Avoiding enzyme release during multilayer production. **Enzyme and Microbial Technology**, v. 137, n. October 2019, p. 109535, 2020.

ARANA-PEÑA, S.; CARBALLARES, D.; CORBERAN, V. C.; *et al.* Multi-combibilipases: Co-immobilizing lipases with very different stabilities combining immobilization via interfacial activation and ion exchange. The reuse of the most stable co-immobilized enzymes after inactivation of the least stable ones. **Catalysts**, v. 10, n. 10, p. 1–23, 2020.

ARANA-PEÑA, S.; RIOS, N. S.; *et al.* Coimmobilization of different lipases: Simple layer by layer enzyme spatial ordering. **International Journal of Biological Macromolecules**, v. 145, p. 856–864, 2020.

ARANA-PEÑA, S.; CARBALLARES, D.; BERENQUER-MURCIA, Á.; *et al.* One pot use of combibilipases for full modification of oils and fats: Multifunctional and heterogeneous substrates. **Catalysts**, v. 10, n. 6, p. 605, 2020.

ARDAO, I.; ZENG, A. P. In silico evaluation of a complex multi-enzymatic system using one-pot and modular approaches: Application to the high-yield production of hydrogen from a synthetic metabolic pathway. **Chemical Engineering Science**, v. 87, p. 183–193, 2013.

BALAJI, V.; ARULAZHAGAN, P.; EBENEZER, P. Enzymatic bioremediation of polyaromatic hydrocarbons by fungal consortia enriched from petroleum contaminated soil and oil seeds. **Journal of Environmental Biology**, v. 35, n. 3, p. 521–529, 2014.

BARBOSA, O. *et al.* Heterofunctional supports in enzyme immobilization: From traditional immobilization protocols to opportunities in tuning enzyme properties. **Biomacromolecules**, v. 14, n. 8, p. 2433–2462, 2013.

BARBOSA, O.; ORTIZ, C.; BERENQUER-MURCIA, Á.; *et al.* Glutaraldehyde in biocatalysts design: A useful crosslinker and a versatile tool in enzyme immobilization. **RSC Advances**, v. 4, n. 4, p. 1583–1600, dez. 2014.

BAUTISTA, L. F.; MORALES, G.; SANZ, R. Biodegradation of polycyclic aromatic hydrocarbons (PAHs) by laccase from *Trametes versicolor* covalently immobilized on amino-functionalized SBA-15. **Chemosphere**, v. 136, p. 273–280, 2015.

BEBIĆ, J.; BANJANAC, K.; ČOROVIĆ, M.; *et al.* Immobilization of laccase from *Myceliophthora thermophila* on functionalized silica nanoparticles: Optimization and application in lindane degradation. **Chinese Journal of Chemical Engineering**, v. 28, n. 4, p. 1136–1144, 2020.

BEBIĆ, J.; BANJANAC, K.; RUSMIROVIĆ, J.; *et al.* Amino-modified kraft lignin microspheres as a support for enzyme immobilization. **RSC Advances**, v. 10, n. 36, p. 21495–21508, 2020.

BEZERRA, C. S. *et al.* Enzyme immobilization onto renewable polymeric matrixes: Past, present, and future trends. **Journal of Applied Polymer Science**, v. 132, n. 26, p. 1–15, 2015.

BOUDRANT, J.; WOODLEY, J. M.; FERNANDEZ-LAFUENTE, R. Parameters necessary to define an immobilized enzyme preparation. **Process Biochemistry**, v. 90, n. November, p. 66–80, 2020.

BREM, J. *et al.* Immobilization to improve the properties of *Pseudomonas fluorescens* lipase for the kinetic resolution of 3-aryl-3-hydroxy esters. **Process Biochemistry**, v. 47, p. 119–126, 2012.

BRENNA, E. *et al.* One-pot multi-enzymatic synthesis of the four stereoisomers of 4-methylheptan-3-ol. **Molecules**, v. 22, n. 10, p. 1–9, 2017.

- BRITOS, C. N. *et al.* Biodegradation of industrial dyes by a solvent, metal and surfactant-stable extracellular bacterial laccase. **Biocatalysis and Agricultural Biotechnology**, v. 14, n. March, p. 221–227, 2018.
- BRITOS, C. N.; TRELLES, J. A. Development of strong enzymatic biocatalysts for dye decolorization. **Biocatalysis and Agricultural Biotechnology**, v. 7, p. 228–233, 2016.
- CAI, Q. *et al.* Enhanced activity and stability of industrial lipases immobilized onto spherelike bacterial cellulose. **International Journal of Biological Macromolecules**, v. 109, p. 1174–1181, 2018.
- CAO, S. *et al.* Preparation of novel magnetic cellulose nanocrystal and its efficient use for enzyme immobilization. **Journal of Materials Chemistry B**, 2014.
- CAO, S.; HUANG, Y.; LI, X. *et al.* Preparation and Characterization of Immobilized Lipase from *Pseudomonas Cepacia* onto Magnetic Cellulose Nanocrystals. **Scientific Reports**, v. 6, p. 1–12, 2016.
- CAPARCO, A. A. *et al.* Protein-inorganic calcium-phosphate supraparticles as a robust platform for enzyme co-immobilization. **Biotechnology and Bioengineering**, v. 117, n. 7, p. 1979–1989, 2020.
- CASTILLO, G. F. D. DEL *et al.* Enzyme Immobilization in Polyelectrolyte Brushes: High Loading and Enhanced Activity Compared to Monolayers. **Langmuir**, v. 35, n. 9, p. 3479–3489, 2019.
- CAVELLO, I. A.; CONTRERAS-ESQUIVEL, J. C.; CAVALITTO, S. F. Immobilization of a keratinolytic protease from *Purpureocillium lilacinum* on genipin activated-chitosan beads. **Process Biochemistry**, v. 49, n. 8, p. 1332–1336, 2014.
- CHANG, X. *et al.* Tandem Biocatalysis by CotA-TJ102@UIO-66-NH<sub>2</sub> and Novozym 435 for Highly Selective Transformation of HMF into FDCA. **Transactions of Tianjin University**, v. 25, n. 5, p. 488–496, 2019.
- CHEN, Y. *et al.* Immobilization of lipase on porous monodisperse chitosan microspheres. **Biotechnology and Applied Biochemistry**, v. 62, n. 1, p. 101–106, 2014.
- CHRISTOPHER, L. P.; KUMAR, H.; ZAMBARE, V. P. Enzymatic biodiesel : Challenges and opportunities. **Applied Energy**, v. 119, p. 497–520, 2014.
- CRESTINI, C.; MELONE, F.; SALADINO, R. Novel multienzyme oxidative biocatalyst for lignin bioprocessing. **Bioorganic and Medicinal Chemistry**, v. 19, n. 16, p. 5071–5078, 2011.
- CRISTÓVÃO, R. O. *et al.* Immobilization of commercial laccase onto green coconut fiber by adsorption and its application for reactive textile dyes degradation. **Journal of Molecular Catalysis B: Enzymatic**, v. 72, n. 1–2, p. 6–12, 2011.
- DEB, S. *et al.* Chitosan – hyaluronic acid polyelectrolyte complex scaffold crosslinked with genipin for immobilization and controlled release of BMP-2. **Carbohydrate Polymers**, v. 115, p. 160–169, 2015.
- DEMIRKAN, E.; AVCI, T.; AYKUT, Y. Protease immobilization on cellulose monoacetate /chitosan-blended nanofibers. **Journal of Industrial Textiles**, v. 47, n. 8, p. 2092–2111, 2018.
- DHAKE, K. P. *et al.* Immobilization of Steapsin Lipase on Macroporous Immobead-350 for Biodiesel Production in Solvent Free System. **Research Paper - Biotechnology and**

**Bioprocess Engineering**, v. 17, p. 959–965, 2012.

DROZD, R. *et al.* Functionalized Magnetic Bacterial Cellulose Beads as Carrier for Lecitase® Ultra Immobilization. **Applied Biochemistry and Biotechnology**, v. 187, n. 1, p. 176–193, 2019.

DWIVEDDEE, B. P. *et al.* Development of Nanobiocatalysts through the Immobilization of Pseudomonas Department of Pharmaceutical Technology (Biotechnology), National Institute of Department of Pharmaceutical Technology (Process Chemistry), National Institute of Present address. **Bioresource Technology**, v. 239, p. 464–471, 2017.

ERNST, H. A. *et al.* A comparative structural analysis of the surface properties of asco-laccases. **PLoS ONE**, v. 13, n. 11, p. 1–27, 2018.

GAVEZZOTTI, P. *et al.* Synthesis of enantiomerically enriched dimers of vinylphenols by tandem action of laccases and lipases. **Advanced Synthesis and Catalysis**, v. 353, n. 13, p. 2421–2430, 2011.

GENNARI, A. *et al.* Magnetic cellulose: Versatile support for enzyme immobilization - A review. **Carbohydrate Polymers**, v. 246, n. March, p. 116646, 2020.

GONÇALVES, L. R. B. *et al.* Influence of mass transfer limitations on the enzymatic synthesis of  $\beta$ -lactam antibiotics catalyzed by penicillin G acylase immobilized on glioxil-agarose. **Bioprocess and Biosystems Engineering**, v. 31, n. 5, p. 411–418, 2008.

GUERBEROFF, G. K.; CAMUSSO, C. C. Effect of laccase from *Trametes versicolor* on the oxidative stability of edible vegetable oils. **Food Science and Human Wellness**, v. 8, n. 4, p. 356–361, 2019.

GULDHE, A. *et al.* Biocatalytic conversion of lipids from microalgae *Scenedesmus obliquus* to biodiesel using *Pseudomonas fluorescens* lipase. **FUEL**, v. 147, p. 117–124, 2015.

HAN, H. *et al.* Immobilization of Lipase from *Pseudomonas fluorescens* on Porous Polyurea and Its Application in Kinetic Resolution of Racemic 1-Phenylethanol. **ACS Applied Materials and Interfaces**, v. 8, n. 39, p. 25714–25724, 2016.

HAN, P.; ZHOU, X.; YOU, C. Efficient Multi-Enzymes Immobilized on Porous Microspheres for Producing Inositol From Starch. **Frontiers in bioengineering and biotechnology**, v. 8, n. May, p. 1–9, 2020.

HAUGLAND, J. O. *et al.* Laccase removal of 2-chlorophenol and sulfamethoxazole in municipal wastewater. **Water Environment Research**, p. 281–291, 2019.

INAGAKI, T.; UEDA, H. Stabilization of Multimeric Enzymes Via Immobilization and Further Cross-Linking With Aldehyde-Dextran. *In: Immobilization of Enzymes and Cells*. [s.l.: s.n.]. v. 61p. 49–51.

INCANI, V.; DANUMAH, C. Nanocomposites of nanocrystalline cellulose for enzyme immobilization. **Cellulose**. p. 191–200, 2013.

ISLAM, M. S. *et al.* Cellulose nanocrystal (CNC)-inorganic hybrid systems: Synthesis, properties and applications. **Journal of Materials Chemistry B**, v. 6, n. 6, p. 864–883, 2018.

JESIONOWSKI, T.; ZDARTA, J.; KRAJEWSKA, B. Enzyme immobilization by adsorption: A review. **Adsorption**, v. 20, n. 5–6, p. 801–821, 2014.

JIA, H. *et al.* The preparation and characterization of a laccase nanogel and its application in

- naphthoquinone synthesis. **ChemPlusChem**, v. 78, n. 5, p. 451–458, 2013.
- KADRI, T. *et al.* Biodegradation of polycyclic aromatic hydrocarbons (PAHs) by fungal enzymes: A review. **Journal of Environmental Sciences (China)**, v. 51, p. 52–74, 2017.
- KALLIO, J. P. *et al.* Structure-Function Studies of a *Melanocarpus albomyces* Laccase Suggest a Pathway for Oxidation of Phenolic Compounds. **Journal of Molecular Biology**, v. 392, n. 4, p. 895–909, 2009.
- KHANJANZADEH, H. *et al.* Surface chemical functionalization of cellulose nanocrystals by 3-aminopropyltriethoxysilane. **International Journal of Biological Macromolecules**, v. 106, p. 1288–1296, 2018.
- KHOABI, M. *et al.* Polyethyleneimine-modified superparamagnetic Fe<sub>3</sub>O<sub>4</sub> nanoparticles for lipase immobilization: Characterization and application. **Materials Chemistry and Physics**, v. 149, p. 77–86, 2015.
- KIM, HYUN JUNG *et al.* Biocompatible cellulose nanocrystals as supports to immobilize lipase. **Journal of Molecular Catalysis B: Enzymatic**, v. 122, p. 170–178, 2015.
- DOS SANTOS, K. P. *et al.* Modifying alcalase activity and stability by immobilization onto chitosan aiming at the production of bioactive peptides by hydrolysis of tilapia skin gelatin. **Process Biochemistry**, v. 97, n. April, p. 27–36, 2020.
- KOŁODZIEJCZAK-RADZIMSKA, A. *et al.* Laccase from *Trametes versicolor* supported onto mesoporous Al<sub>2</sub>O<sub>3</sub>: Stability tests and evaluations of catalytic activity. **Process Biochemistry**, v. 95, n. May, p. 71–80, 2020.
- LI, N. *et al.* Immobilizing laccase on modified cellulose/CF Beads to degrade chlorinated biphenyl in wastewater. **Polymers**, v. 10, n. 7, 2018.
- LIMA, G. V. *et al.* Applied Catalysis A , General Chemoenzymatic synthesis of ( S ) - Pindolol using lipases. **Applied Catalysis A, General**, v. 546, p. 7–14, 2017.
- LIMA, L. N. *et al.* Immobilization of *Pseudomonas fluorescens* lipase on hydrophobic supports and application in biodiesel synthesis by transesterification of vegetable oils in solvent - free systems. **Journal of industrial microbiology & biotechnology**, v. 42, n. 4, p. 523–535, 2015.
- LIU, H.; TEGE, G.; NIDETZKY, B. Glycosyltransferase Co-Immobilization for Natural Product Glycosylation: Cascade Biosynthesis of the C-Glucoside Nothofagin with Efficient Reuse of Enzymes. **Advanced Synthesis and Catalysis**, v. 363, p. 2157–2169, 2021.
- LIU, W.; LI, M.; YAN, Y. Heterologous expression and characterization of a new lipase from *Pseudomonas fluorescens* Pf0 – 1 and used for biodiesel production. **Scientific Reports**, n. July, p. 1–11, 2017.
- LOKHA, Y. *et al.* Modulating the properties of the lipase from *Thermomyces lanuginosus* immobilized on octyl agarose beads by altering the immobilization conditions. **Enzyme and Microbial Technology**, v. 133, n. October 2019, p. 109461, 2020.
- LONG, J. *et al.* Co-immobilization of  $\beta$ -fructofuranosidase and glucose oxidase improves the stability of Bi-enzymes and the production of lactosucrose. **LWT - Food Science and Technology**, v. 128, n. April 2019, p. 109460, 2020.
- LOPEZ-GALLEGO, F.; SCHMIDT-DANNERT, C. Multi-enzymatic synthesis. **Current Opinion in Chemical Biology**, v. 14, n. 2, p. 174–183, 2010.

- MAK, Y. W. Crosslinking of genipin and autoclaving in chitosan- based nanofibrous scaffolds : structural and physiochemical properties. **Journal of Materials Science**, v. 54, n. 15, p. 10941–10962, 2019.
- MANOEL, E. A. *et al.* Immobilization of lipases on hydrophobic supports involves the open form of the enzyme. **Enzyme and Microbial Technology**, v. 71, p. 53–57, 2015.
- MANZO, R. M. *et al.* Chemical improvement of chitosan-modified beads for the immobilization of *Enterococcus faecium* DBFIQ E36 l-arabinose isomerase through multipoint covalent attachment approach. **Journal of Industrial Microbiology and Biotechnology**, v. 42, n. 10, p. 1325–1340, 2015.
- MARSZAŁŁ, M. P.; SIÓDMIĄK, T. Immobilization of *Candida rugosa* lipase onto magnetic beads for kinetic resolution of (R,S)-ibuprofen. **Catalysis Communications**, v. 24, p. 80–84, 2012.
- MATEO, C. *et al.* Reversible enzyme immobilization via a very strong and nondistorting ionic adsorption on support-polyethylenimine composites. **Biotechnology and Bioengineering**, v. 68, n. 1, p. 98–105, 2000.
- MATTE, C. R. *et al.* Immobilization of *Thermomyces lanuginosus* lipase by different techniques on Immobead 150 support: Characterization and applications. **Applied Biochemistry and Biotechnology**, v. 172, n. 5, p. 2507–2520, 2014.
- MIGNEAULT, I. *et al.* Glutaraldehyde: Behavior in aqueous solution, reaction with proteins, and application to enzyme crosslinking. **BioTechniques**, v. 37, p. 790 - 802, 2004.
- MOHAMAD, N. R. *et al.* An overview of technologies for immobilization of enzymes and surface analysis techniques for immobilized enzymes. **Biotechnology and Biotechnological Equipment**, v. 29, n. 2, p. 205–220, 2015.
- MONTEIRO, R. R. C. *et al.* Immobilization of Lipase A from *Candida antarctica* onto Chitosan-Coated Magnetic Nanoparticles. **International Journal of Molecular Sciences**, v. 20, n. 16, p. 4018, 2019.
- MORAIS JÚNIOR, W. G. DE *et al.* Influence of different immobilization techniques to improve the enantioselectivity of lipase from *Geotrichum candidum* applied on the resolution of mandelic acid. **Molecular Catalysis**, v. 458, p. 89–96, 2018.
- MOROZOVA, O. V. *et al.* Laccase-mediator systems and their applications: A review. **Applied Biochemistry and Microbiology**, v. 43, n. 5, p. 523–535, 2007.
- NGUYEN, V. D. *et al.* Immobilization of  $\beta$ -galactosidase on chitosan-coated magnetic nanoparticles and its application for synthesis of lactulose-based galactooligosaccharides. **Process Biochemistry**, v. 84, n. April, p. 30–38, 2019.
- NOREEN, S. *et al.* Performance improvement of Ca-alginate bead cross- linked laccase from *Trametes versicolor* IBL-04. **BioResources**, v. 11, n. 1, p. 558–572, 2016.
- NUNES, L. *et al.* Immobilization and stabilization of a bimolecular aggregate of the lipase from *Pseudomonas fluorescens* by multipoint covalent attachment. **Process Biochemistry**, v. 48, n. 1, p. 118–123, 2013.
- OLIVEIRA, J. P. B. *et al.* Immobilization and characterization of latex cysteine peptidases on different supports and application for cow's milk protein hydrolysis. **Process Biochemistry**, v. 117, n. April, p. 180–190, 2022.



- OLIVEIRA, U. M. F. DE *et al.* Effect of the presence of surfactants and immobilization conditions on catalysts' properties of *Rhizomucor miehei* lipase onto chitosan. **Applied Biochemistry and Biotechnology**, v. 184, n. 4, p. 1263–1285, 2017.
- ORREGO, A. H. *et al.* Stabilization of immobilized lipases by intense intramolecular cross-linking of their surfaces by using aldehyde-dextran polymers. **International Journal of Molecular Sciences**, v. 19, n. 2, p. 1–16, 2018.
- OZYILMAZ, G.; TUKEL, S. S. Simultaneous co-immobilization of glucose oxidase and catalase in their substrates. **Applied Biochemistry and Microbiology**, v. 43, n. 1, p. 29–35, 2007.
- PEIRCE, S. *et al.* Development of simple protocols to solve the problems of enzyme coimmobilization. **RSC Advances**, v. 6, n. 66, p. 61707–61715, 2016.
- PENG, F. *et al.* Co-immobilization of multiple enzymes by self-assembly and chemical crosslinking for cofactor regeneration and robust biocatalysis. **International Journal of Biological Macromolecules**, v. 162, p. 445–453, 2020.
- PEREIRA, M. G. *et al.* Immobilized lipase from *Hypocrea pseudokoningii* on hydrophobic and ionic supports: Determination of thermal and organic solvent stabilities for applications in the oleochemical industry. **Process Biochemistry**, v. 50, n. 4, p. 561–570, 2015.
- PESSELA, B. C. C. *et al.* Increasing the binding strength of proteins to PEI coated supports by immobilizing at high ionic strength. **Enzyme and Microbial Technology**, v. 37, n. 3, p. 295–299, 2005.
- PIONTEK, K.; ANTORINI, M.; CHOINOWSKI, T. Crystal structure of a laccase from the fungus *Trametes versicolor* at 1.90-Å resolution containing a full complement of coppers. **Journal of Biological Chemistry**, v. 277, n. 40, p. 37663–37669, 2002.
- PRAMANIK, S. K. *et al.* Catalyzed degradation of polycyclic aromatic hydrocarbons by recoverable magnetic chitosan immobilized laccase from *Trametes versicolor*. **Chemosphere**, p. 100310, 2019.
- RAI, S. K.; KUMAR, V.; YADAV, S. K. Catalysis Science & Technology enzyme aggregates for the synthesis of high value. 2021.
- REKUĆ, A. *et al.* Laccase immobilization on the tailored cellulose-based Granocel carriers. **International Journal of Biological Macromolecules**, v. 42, n. 2, p. 208–215, 2008.
- REN, S. *et al.* Recent progress in multienzymes co-immobilization and multienzyme system applications. **Chemical Engineering Journal**, v. 373, n. February, p. 1254–1278, 2019.
- REN, S.; WANG, Z.; BILAL, M. *et al.* Co-immobilization multienzyme nanoreactor with cofactor regeneration for conversion of CO<sub>2</sub>. **International Journal of Biological Macromolecules**, v. 155, p. 110–118, 2020.
- RICCA, E.; BRUCHER, B.; SCHRITTWIESER, J. H. Multi-enzymatic cascade reactions: Overview and perspectives. **Advanced Synthesis and Catalysis**, v. 353, n. 13, p. 2239–2262, 2011.
- RIOS, N. S. *et al.* Strategies of covalent immobilization of a recombinant *Candida antarctica* lipase B on pore-expanded SBA-15 and its application in the kinetic resolution of (R,S)-Phenylethyl acetate. **Journal of Molecular Catalysis B: Enzymatic**, v. 133, p. 246–258, 2016.

- RIOS, N. S. *et al.* Biotechnological potential of lipases from *Pseudomonas*: Sources, properties and applications. **Process Biochemistry**, v. 75, n. August, p. 99–120, 2018.
- RIOS, N. S.; ARANA-PEÑA, S.; *et al.* Increasing the enzyme loading capacity of porous supports by a layer-by-layer immobilization strategy using PEI as glue. **Catalysts**, v. 9, n. 7, p. 576, 2019.
- RIOS, N. S.; MENDEZ-SANCHEZ, C.; *et al.* Immobilization of lipase from *Pseudomonas fluorescens* on glyoxyl-octyl-agarose beads: Improved stability and reusability. **Biochimica et Biophysica Acta (BBA) - Proteins and Proteomics**, v. 1867, n. 9, p. 741–747, set. 2019.
- RODRIGUES, R. C. *et al.* Immobilization of lipases on hydrophobic supports: immobilization mechanism, advantages, problems, and solutions. **Biotechnology Advances**, v. 37, n. 5, p. 746–770, set. 2019.
- ROMERO-GUIDO, C.; BAEZ, A.; TORRES, E. Dioxygen activation by laccases: Green chemistry for fine chemical synthesis. **Catalysts**, v. 8, n. 6, 2018.
- ROSA-GARZON, N. G. DA *et al.* Amino acid supplementation improves the production of extracellular peptidases by *Aspergillus section flavi* and their ionic immobilization. **Brazilian Archives of Biology and Technology**, v. 63, 2020.
- RUEDA, N. *et al.* Chemical amination of lipases improves their immobilization on octyl-glyoxyl agarose beads. **Catalysis Today**, 2015.
- RUEDA, N. *et al.* Improved performance of lipases immobilized on heterofunctional octyl-glyoxyl agarose beads. **RSC Advances**, v. 5, n. 15, p. 11212–11222, 2015.
- RUEDA, N.; DOS SANTOS, C. S.; RODRIGUEZ, M. D. *et al.* Enzymatic Reversible immobilization of lipases on octyl-glutamic agarose beads : A mixed adsorption that reinforces enzyme immobilization. **Journal of Molecular Catalysis. B, Enzymatic**, v. 128, p. 10–18, 2016.
- SAMPAIO, L. M. P. *et al.* Laccase immobilization on bacterial nanocellulose membranes: Antimicrobial, kinetic and stability properties. **Carbohydrate Polymers**, v. 145, p. 1–12, jul. 2016.
- SÁNCHEZ-OTERO, M. G. *et al.* Polypropylene as a selective support for the immobilization of lipolytic enzymes: hyper-activation, purification and biotechnological applications. **Journal of Chemical Technology and Biotechnology**, v. 97, n. 2, p. 436–445, 2022.
- SANKAR, K. *et al.* A novel method for improving laccase activity by immobilization onto copper ferrite nanoparticles for lignin degradation. **International Journal of Biological Macromolecules**, v. 152, p. 1098–1107, 2020.
- SANTOS, J. C. S. *et al.* Characterization of supports activated with divinyl sulfone as a tool to immobilize and stabilize enzymes via multipoint covalent attachment . Application to chymotrypsin. **RSC Advances**, v. 5, n. 27, p. 20639–20649, 2015.
- SANTOS, J. C. S. DOS *et al.* Importance of the Support Properties for Immobilization or Purification of Enzymes. **CHEM CAT CHEM**, v. 7, n. 16, p. 2413–2432, 2015.
- SANTOS, J. C. S. DOS *et al.* Immobilization of CALB on activated chitosan: Application to enzymatic synthesis in supercritical and near-critical carbon dioxide. **Biotechnology Reports**, v. 14, p. 16–26, 2017.
- SATHISHKUMAR, P. *et al.* Laccase immobilization on cellulose nanofiber : The catalytic

efficiency and recyclic application for simulated dye effluent treatment. **Journal of Molecular Catalysis. B, Enzymatic**, v. 100, p. 111–120, 2014.

SCHEIBEL, D. M.; GITSOV, I. Unprecedented Enzymatic Synthesis of Perfectly Structured Alternating Copolymers via “green” Reaction Cocatalyzed by Laccase and Lipase Compartmentalized within Supramolecular Complexes. **Biomacromolecules**, v. 20, n. 2, p. 927–936, 2019.

SHARMA, A. *et al.* Commercial application of cellulose nano-composites – A review. **Biotechnology Reports**, v. 21, n. 2018, p. e00316, 2019.

SIAR, E. H. *et al.* Solid phase chemical modification of agarose glyoxyl-ficin: Improving activity and stability properties by amination and modification with glutaraldehyde. **Process Biochemistry**, v. 73, n. May, p. 109–116, 2018.

SILLER, M. *et al.* Effects of periodate oxidation on cellulose polymorphs. **Cellulose**, v. 22, n. 4, p. 2245–2261, 2015.

SILVA-TORRES, O. *et al.* Enhanced laccase activity of biocatalytic hybrid copper hydroxide nanocages. **Enzyme and Microbial Technology**, v. 128, n. March, p. 59–66, 2019.

SILVA DIAS, G. *et al.* Immobilization of *Pseudomonas cepacia* lipase on layered double hydroxide of Zn/Al-Cl for kinetic resolution of rac-1-phenylethanol. **Enzyme and Microbial Technology**, v. 130, n. March, p. 109365, 2019.

SILVA, J. A. *et al.* Immobilization of *Candida antarctica* lipase B by covalent attachment on chitosan-based hydrogels using different support activation strategies. **Biochemical Engineering Journal**, v. 60, p. 16–24, 2012.

SIQUEIRA, N. M. *et al.* Poly (lactic acid)/chitosan fiber mats: Investigation of effects of the support on lipase immobilization. **International Journal of Biological Macromolecules**, v. 72, p. 998–1004, 2015.

SONI, S. *et al.* Kinetic resolution of (RS)-1-chloro-3-(4-(2-methoxyethyl)phenoxy)propan-2-ol: a metoprolol intermediate and its validation through homology model of *Pseudomonas fluorescens* lipase. **RSC Advances**, v. 7, p. 36566–36574, 2017.

SONI, S.; DWIVEDEE, B. P.; SHARMA, V. K. Exploration of the expeditious potential of *Pseudomonas fluorescens* lipase in the kinetic resolution of racemic intermediates and its validation through molecular docking. **CHIRALITY**, v. 30, p. 85–94, 2018.

SOUZA, L. T. DE A. *et al.* Immobilization of *Moniliella spathulata* R25L270 lipase on ionic, hydrophobic and covalent supports: Functional properties and hydrolysis of sardine oil. **Molecules**, v. 22, n. 10, p. 1508, 2017.

SULAIMAN, S. *et al.* A Review: Potential Usage of Cellulose Nanofibers (CNF) for Enzyme Immobilization via Covalent Interactions. **Applied Biochemistry and Biotechnology**, v. 175, n. 4, p. 1817–1842, 2014.

SULMAN, E. M.; MATVEEVA, V. G.; BRONSTEIN, L. M. Design of biocatalysts for efficient catalytic processes. **Current Opinion in Chemical Engineering**, v. 26, p. 1–8, 2019.

SUN, B. *et al.* Sodium periodate oxidation of cellulose nanocrystal and its application as a paper wet strength additive. **Cellulose**, v. 22, n. 2, p. 1135–1146, 2015.

TALEKAR, S. *et al.* Carrier free co-immobilization of alpha amylase, glucoamylase and

- pullulanase as combined cross-linked enzyme aggregates (combi-cleas): a tri-enzyme biocatalyst with one pot starch hydrolytic activity. **Bioresource Technology**, v. 147, p. 269–275, 2013.
- TARDIOLI, P. W. *et al.* Hydrolysis of proteins by immobilized-stabilized Alcalase-Glyoxyl agarose. **Biotechnology progress**, v. 19, n. 2, p. 352–360, 2003.
- TORRES, P.; BATISTA-VIERA, F. Production of D-tagatose and D-fructose from whey by co-immobilized enzymatic system. **Molecular Catalysis**, v. 463, n. July 2018, p. 99–109, 2019.
- TOUAHAR, I. E. *et al.* Characterization of combined cross-linked enzyme aggregates from laccase, versatile peroxidase and glucose oxidase, and their utilization for the elimination of pharmaceuticals. **Science of the Total Environment**, v. 481, n. 1, p. 90–99, 2014.
- UTH, C. *et al.* A Chemoenzymatic Approach to Protein Immobilization onto Crystalline Cellulose Nanoscaffolds. v. 53, n. 46, p. 12618–12623, 2014.
- VERA, M. Multienzymatic immobilization of laccases on polymeric microspheres : A strategy to expand the maximum catalytic efficiency. **Journal of Applied Polymer Science**, v. 137, n. 47, p. 49562, 2020.
- WANG, D. A critical review of cellulose-based nanomaterials for water purification in industrial processes. **Cellulose**, v. 26, n. 2, p. 687–701, 2019.
- WANG, J. *et al.* Facile self-assembly of magnetite nanoparticles on three-dimensional graphene oxide-chitosan composite for lipase immobilization. **Biochemical Engineering Journal**, v. 98, p. 75–83, 2015.
- WELLINGTON, K. W. *et al.* Laccase-Catalyzed C-S and C-C Coupling for a One-Pot Synthesis of 1,4-Naphthoquinone Sulfides and 1,4-Naphthoquinone Sulfide Dimers. **ChemCatChem**, v. 5, n. 6, p. 1570–1577, 2013.
- XIA, T. T. *et al.* Improved performance of immobilized laccase on amine-functioned magnetic Fe<sub>3</sub>O<sub>4</sub> nanoparticles modified with polyethylenimine. **Chemical Engineering Journal**, v. 295, p. 201–206, 2016.
- XIE, J.; ZHANG, Y.; SIMPSON, B. Food enzymes immobilization: novel carriers, techniques and applications. **Current Opinion in Food Science**, v. 43, n. 7, p. 27–35, 2022.
- YANG, H.; CHEN, D.; VEN, T. G. M. VAN DE. Preparation and characterization of sterically stabilized nanocrystalline cellulose obtained by periodate oxidation of cellulose fibers. **Cellulose**, v. 22, n. 3, p. 1743–1752, 2015.
- YOUSEFI, M.; MOHAMMADI, M.; HABIBI, Z. Enantioselective resolution of racemic ibuprofen esters using different lipases immobilized on octyl sepharose. **“Journal of Molecular Catalysis. B, Enzymatic”**, v. 104, p. 87–94, 2014.
- YU, X. *et al.* Co-immobilization of multi-enzyme on reversibly soluble polymers in cascade catalysis for the one-pot conversion of gluconic acid from corn straw. **Bioresource Technology**, v. 321, n. October 2020, p. 124509, 2021.
- ZERVA, A. *et al.* Degradation of olive mill wastewater by the induced extracellular ligninolytic enzymes of two wood-rot fungi. **Journal of Environmental Management**, v. 203, p. 791–798, 2017.
- ZHANG, H. *et al.* Can graphene oxide improve the performance of biocatalytic membrane?

**Chemical Engineering Journal**, v. 359, n. November, p. 982–993, 2019.

ZHANG, Y. *et al.* Synthesis of mitomycin analogs catalyzed by coupling of laccase with lipase and the kinetic model. **Journal of Chemical Technology and Biotechnology**, v. 95, n. 5, p. 1421–1430, 2020.

ZHAO, F. *et al.* Co-immobilization of multi-enzyme on control-reduced graphene oxide by non-covalent bonds: An artificial biocatalytic system for the one-pot production of gluconic acid from starch. **Green Chemistry**, v. 16, n. 5, p. 2558–2565, 2014.

ZHU, H. *et al.* Diethylaminoethyl Sepharose (DEAE-Sepharose) microcolumn for enrichment of glycopeptides. **Analytical and Bioanalytical Chemistry**, v. 409, n. 2, p. 511–518, 2017.

ZHU, P. *et al.* Preparation and application of a chemically modified laccase and copper phosphate hybrid flower-like biocatalyst. **Biochemical Engineering Journal**, v. 144, p. 235–243, 2019.

# Chapter 3

**Co-immobilization of lipase and laccase on agarose-based supports via layer-by-layer strategy: effect of diffusional limitations**

### 3.1 Abstract

Co-immobilized enzymes present desirable advantages to performing cascade reactions when employed in one-pot processes, mainly because of the shorter lag times owing to better reagent diffusion across the active sites of the different enzymes. But high product yields require high enzyme loads, usually achieved with high surface area and porous supports, where diffusional limitations may be introduced or increased. Heterogeneous biocatalysts were prepared by co-immobilizing *Pseudomonas fluorescens* lipase (PFL) and *Aspergillus sp.* Laccase (Novozymes 51003) on two agarose-based supports, DEAE-Sepharose and Octyl-agarose. A layer-by-layer strategy was used by adding polyethyleneimine (PEI) to allow the attachment of the upper enzyme layer onto the lower adjacent layer. A final step, crosslinking with glutaraldehyde, was performed to prevent enzyme leaching under harsh environmental conditions. The heterogeneous biocatalysts showed lower temperature dependence and a significant increase in thermal stability at 50 °C. No internal mass transfer effects were observed when a low protein load was used during co-immobilization (2 mg<sub>protein</sub>/g<sub>support</sub> of each enzyme). However, increasing the enzyme load (more than 10 mg<sub>protein</sub>/g<sub>support</sub>) promoted internal diffusion limitations. The layer-by-layer strategy defined in this work enabled the preparation of a multi-enzymatic heterogeneous biocatalyst with high activity, thermal stability, and no diffusional limitations, depending on enzyme concentration.

**Keywords:** Lipase from *Pseudomonas fluorescens*, laccase from *Aspergillus sp.*, cascade reactions, PEI coating, layer-by-layer strategy

### 3.2 Introduction

There has been a strong drive in modern processes involving enzymatic synthesis toward the employment of heterogeneous biocatalysts in reaction catalysis due to two main advantages: their easy recovery and reuse following the reaction process and the possibility of performing industrial processes in continuous mode (Bolívar, Eisl e Nidetzky, 2015). In this context, one-pot syntheses of high added-value products are one of the technical solutions that have shown the most significant potential in the field of applied bioprocess engineering. For this purpose, the use of heterogeneous biocatalysts containing co-immobilized enzymes in cascade reactions or the complete modification of heterogeneous substrates performed in one reactor has been constantly and intensively researched (Arana-Peña, Carballares, *et al.*, 2020; Sulman, Matveeva e Bronstein, 2019). Multiple enzymes are simultaneously immobilized onto the same particle during co-immobilization in supports. Therefore, intermediate products of cascade reactions do not need to diffuse into the reaction mixture to be consumed by different enzymes, avoiding the time lag experienced in other processes (Rios, Arana-peña, *et al.*, 2019). Consequently, an enhancement in reaction rates is observed, rendering such biocatalytic systems considerably more efficient than their conventional counterparts (Arana-Peña *et al.*, 2019; Hwang e Lee, 2019; Peirce *et al.*, 2016).

Several enzymes have already been co-immobilized onto different supports by other techniques and strategies reported in the literature (Han, Zhou e You, 2020; Ren *et al.*, 2019; Vera, 2020; Yu *et al.*, 2021). Nevertheless, lipase-laccase biocatalytic systems are not often reported. With this in mind, the co-immobilization of lipase and laccase is a promising area of research since they can work simultaneously in cascade reactions in the synthesis of structured copolymers (Scheibel e Gitsov, 2019), enantiomerically-enriched compounds (Gavezzotti *et al.*, 2011), and pharmaceuticals (Zhang *et al.*, 2020).

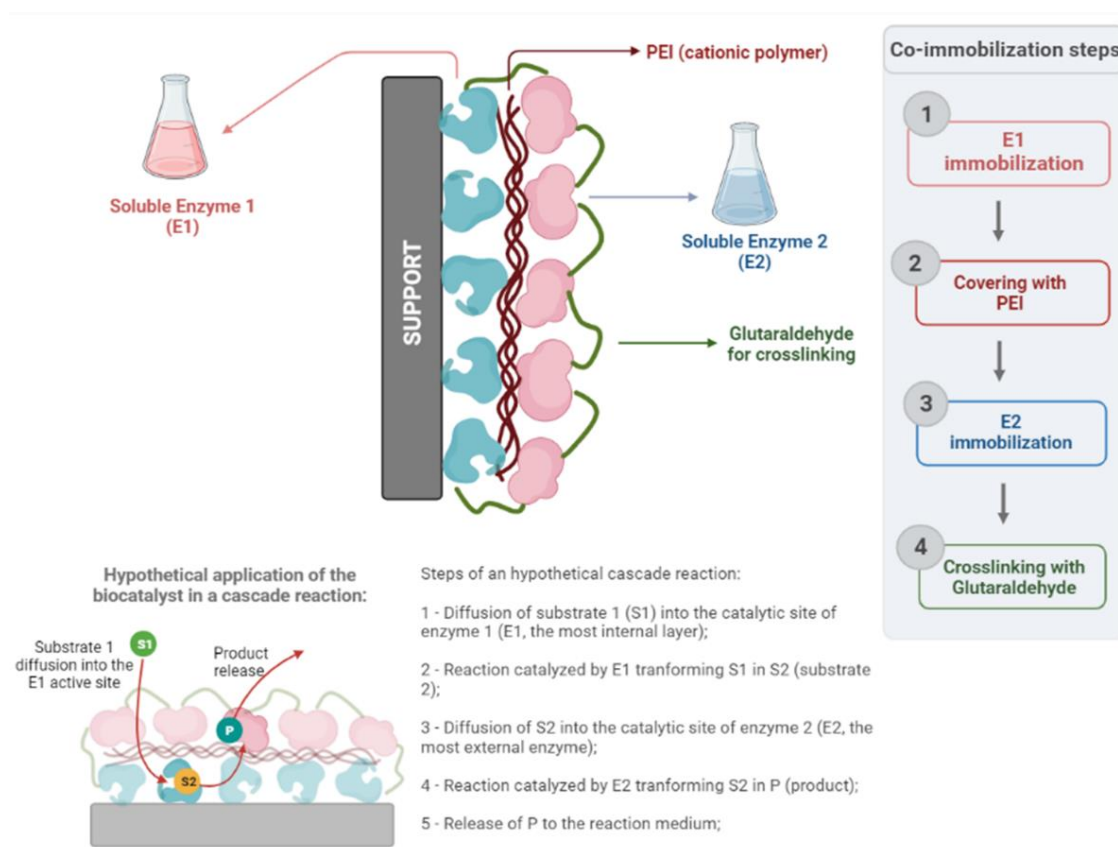
The production of an efficient multi-active heterogeneous biocatalyst based on the co-immobilization of lipase and laccase using a layer-by-layer strategy is addressed in this paper. In the proposed approach, one layer of one enzyme is alternately immobilized on top of one layer of the other enzyme to increase the loading capacity of the support (Rios, Arana-Peña, *et al.*, 2019). To reach this goal, the first enzyme layer was coated with polyethylenimine (PEI), a multicationic polymer with primary, secondary, and tertiary amino groups (Virgen-Ortíz *et al.*, 2017). The use of PEI as an intermediate allows the immobilization of the second enzyme layer via ion exchange (Forrest, Elmore e Palmer, 2007; Onda, Ariga e Kunitake, 1999;



Rodríguez e Rivas, 2004; Virgen-Ortíz *et al.*, 2017). This enabled the manufacture of a highly-active biocatalyst containing different but well-ordered enzymes since there was only one enzyme type in each layer. Another advantage of this strategy is the process flexibility due to the possibility of rearranging the order of the immobilized enzymes within each layer (Arana-Peña, Rios, *et al.*, 2020).

Although the use of 10% PEI between the two enzyme layers has been shown to strongly attach the second enzyme layer (Arana-Peña, Rios, *et al.*, 2020; Arana-peña, Rios, Mendez-sanchez, *et al.*, 2020; Rios, Arana-Peña, *et al.*, 2019), in order to prevent enzyme release under drastic pH or ionic strength conditions, a final crosslinking treatment is needed (Rios, Arana-Peña, *et al.*, 2019). For instance, the use of glutaraldehyde for such multi-crosslinking in systems containing protein/PEI has shown beneficial results (Arana-peña, Rios, Mendez-sanchez, *et al.*, 2020; Wang *et al.*, 2020), since "Schiff's base" is formed between primary amino groups in PEI and GA. Fig. 3.1 shows a schematic representation of the co-immobilization (using the over cited layer-by-layer strategy) of two enzymes. This figure includes also an hypothetical application (cascade reaction) for the multi-active biocatalyst. In such hypothetical cascade reaction, the product of the catalysis performed by the first enzyme works as substrate for the second enzyme catalysis.

Figure 3.1 – Schematic representation of the layer-by-layer strategy used for the co-immobilization of the enzymes and a hypothetical application of the multi-active biocatalyst in a cascade reaction.



Source: Elaborated by the author.

Last but not least, to produce efficient heterogeneous biocatalysts with a high concentration of active proteins, internal and external diffusion effects in the particles must be investigated. Two main phenomena can occur in the system by increasing the protein load. First, there may be an increase in the reaction rate. With the increase in  $E_0$  value (the number of enzyme molecules in the biocatalyst preparation), the value of  $V_{max}$  also increases. If the reaction rate is lower than the mass transfer rates, the former is the determinant step in the process, and hence, the diffusional effects can be neglected. From a certain point, this progressive increase in protein load can cause diffusion to become a limiting factor since the mass transfer rate should be slower than that of the Reaction itself (Doran, 2013). In other words, if the reaction rate is higher than the mass transfer rate, the latter is the governing step in the process. In this scenario, the substrate can be consumed before penetrating the inner structures of the biocatalyst, negatively affecting the reaction rates (Doran, 2013). The second phenomenon triggered by higher protein loads is the increase in steric hindrances caused by the

insertion of more enzyme molecules inside the particle pores. Both phenomena involve the intensification of mass transfer effects. When reaction and mass transfer limitations co-occur in a porous biocatalyst, the substrate concentration inside the biocatalyst is different from that of its surface. This is why the observed rates decrease whenever internal diffusion effects are present (Bódalo *et al.*, 1986).

The phenomenon, as mentioned earlier, characterizes diffusional effects in the particles. Fluid dynamics can control external diffusion in the reactor, specifically concerning stirring efficiency (Bolivar, Eisl e Nidetzky, 2015). Efficient stirring can decrease the thickness of the boundary layer on the particle surface, eliminating the effects of external diffusion (Doran, 2013). The external reactor conditions do not control internal diffusion mechanisms since the latter depends on the internal structural characteristics of the particle, such as porosity and tortuosity, among others (Bódalo *et al.*, 1986; Bolivar, Eisl e Nidetzky, 2015).

Notably, the activity of heterogeneous biocatalysts, which includes co-immobilized enzymes, can be decreased by internal or external mass transfer effects or by the strong interactions between enzyme and support caused by an excessive rigidity or distortion in the enzyme structure (Ferreira *et al.*, 2003; Oliveira *et al.*, 2017; Souza *et al.*, 2017). In this context, this research aims to prepare an efficient lipase-laccase co-immobilized biocatalyst using agarose-based supports and investigate if the internal diffusional effects limit its application. First, the design of a multi-active biocatalyst was studied by testing two different supports and the order of enzyme immobilization using strategies based on a layer-by-layer approach. Then, a multi-active and thermally stable biocatalyst was produced using the best strategy for enzyme co-immobilization. Afterward, two synthetic substrates (*p*NPB for lipase and ABTS for laccase) were used as model reactions to investigate internal diffusion limitations. Finally, the influence of protein load (used during co-immobilization) on those substrates' diffusion was analyzed to establish conditions in which the reaction occurred in the absence of mass transfer limitations. These diffusion studies may provide a basis for future research with other substrates of industrial interest and the application of this biocatalyst in a cascade reaction.

In recent years, agarose-based supports have been the most studied support for enzyme immobilization (Albuquerque *et al.*, 2016; Santos *et al.*, 2015; Siar *et al.*, 2018; Zucca, Fernandez-Lafuente e Sanjust, 2016), owing to their high porosity, mechanical resistance, and inertness (Zucca, Fernandez-Lafuente e Sanjust, 2016). Moreover, it was also selected due to the high surface area (Zucca, Fernandez-Lafuente e Sanjust, 2016), which allowed high enzyme loads when diffusional limitations are more prone. In this paper, the enzymes were immobilized

on two agarose-based supports: agarose modified with anion-exchange diethylaminoethyl reactive groups (DEAE-agarose) and agarose modified with hydrophobic octyl groups (Octyl-agarose). Octyl-Agarose (OA) was chosen as the support to this end due to its broad applicability in the immobilization of different lipases, including PFL, via interfacial activation (Arana-Peña, Rios, *et al.*, 2020; Lokha *et al.*, 2020; Rios, Arana-Peña, *et al.*, 2019).

### 3.3 Materials and methods

#### 3.3.1 Materials

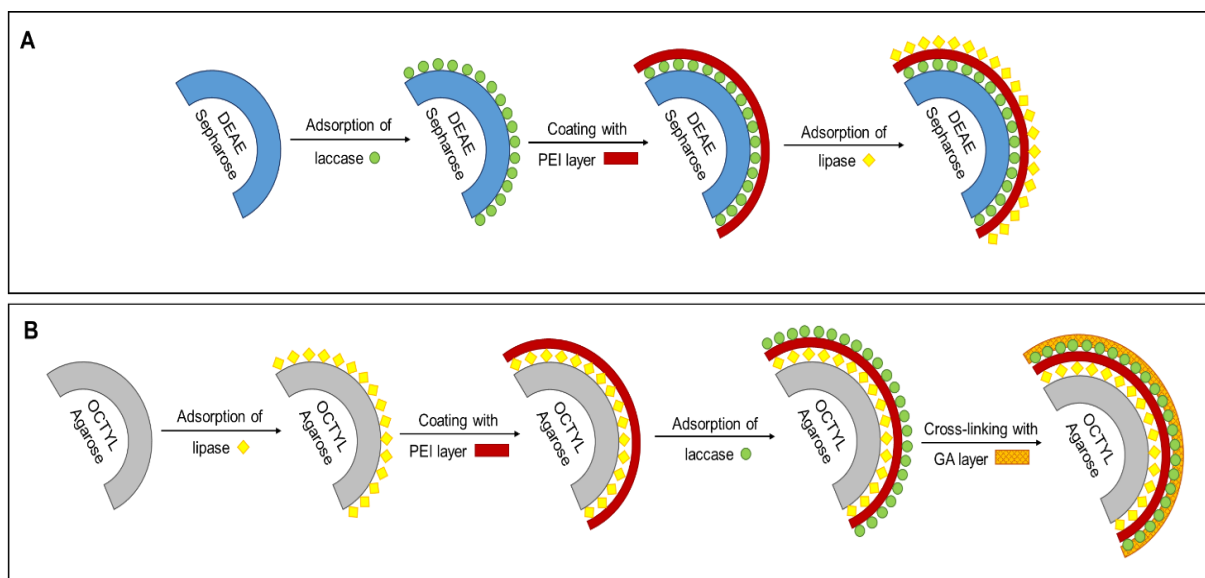
Amano Lipase from *Pseudomonas fluorescens* EC 3.1.1.3 (PFL, isoelectric point at pH 4 (Rios *et al.*, 2018)), polyethyleneimine (PEI), *p*-nitrophenyl butyrate (*p*NPB), and 2,2'-Azino-bis (3-ethylbenzothiazoline-6-sulfonic acid) diammonium salt (ABTS) were purchased from Sigma-Aldrich (Brazil). Laccase from *Aspergillus* sp. was purchased from Novozymes (Novozym 51003, isoelectric point at pH 4 (Bebić *et al.*, 2020)). GE Healthcare (Brazil) supplied the immobilization supports (DEAE-Sepharose and Octyl-agarose). All other reagents were of analytical grade.

#### 3.3.2 Methods

##### 3.3.2.1 Co-immobilization of laccase and lipase

Two different protocols based on a layer-by-layer strategy were studied to co-immobilize laccase and lipase onto agarose-based supports (DEAE-agarose or Octyl-agarose). A different enzyme order was employed for each protocol based on enzyme-support interactions (Othman, Correa-duarte e Moldes, 2016; Rios, Arana-Peña, *et al.*, 2019). Fig. 3.2 presents a schematic diagram of the two protocols used for co-immobilization. A commercial extract (containing 16.76 mg<sub>protein</sub>/mL and 410.9 U<sub>ABTS</sub>/mL) was used to prepare the immobilization solution for laccase. For PFL, a solution was prepared (containing 6.5 mg<sub>protein</sub>/mL and 20.5 U<sub>pNPB</sub>/mL) from the commercial powder used to prepare the immobilization solution.

Figure 3.2 - The two reversed layer-by-layer strategies followed for the co-immobilization of lipase (PFL) and laccase (Lac) proposed in the current study. (A) Protocol I: DEAE-Sepharose-laccase-PEI-lipase (DEAE-Lac-PEI-PFL); (B) Protocol II: Octyl-Agarose-lipase-PEI-laccase-GA (OA-PFL-PEI-Lac-GA). PEI: polyethyleneimine; GA: glutaraldehyde; DEAE: diethylaminoethyl.



Source: Elaborated by the author.

#### I. Protocol I: DEAE-Sepharose – Laccase – PEI – Lipase (DEAE-Lac-PEI-PFL):

The co-immobilization procedure onto DEAE-Sepharose via the first protocol was performed in three steps: laccase immobilization, PEI coating, and lipase immobilization. For each immobilization step, the yield (IY) was defined as the difference between the enzyme activity on the supernatant (soluble enzyme) before and after the immobilization, related to the initial activity of the enzyme solution (Silva *et al.*, 2012). A 5 mM Sodium phosphate buffer pH 7.0 was used to immobilize lipase (Rios, Arana-Peña, *et al.*, 2019). For laccase immobilization, the same sodium phosphate buffer was used with the addition of 1mM  $\text{CuSO}_4 \cdot 5\text{H}_2\text{O}$  (Baldrian e Gabriel, 2002; Sankar *et al.*, 2020).

The first step was the adsorption of laccase in DEAE-Sepharose particles at pH 7. For that purpose, the particles were suspended in a laccase solution (2 mg of laccase per g of the support) and gently stirred for 1h at 25 °C. Then, samples were withdrawn from the supernatant, and the enzymatic activity was determined. The support containing the immobilized laccase (DEAE-Lac) was filtered and washed with distilled water. Next, the

DEAE-Sepharose containing the immobilized laccase was coated with polyethyleneimine (PEI). Literature reports (Arana-Peña, Rios, *et al.*, 2020; Arana-peña, Rios, Mendez-sanchez, *et al.*, 2020; Rios, Arana-Peña, *et al.*, 2019) that using 10% PEI as an intermediate between the two enzyme layers has attached the second enzyme layer preventing its release.

The immobilized preparation was suspended in 10% (w/v) PEI solution at pH 7.0 and gently stirred overnight at 4 °C (Rios, Arana-Peña, *et al.*, 2019). In this case, lower PEI concentrations were tested due to the drastic activity loss observed after 10% PEI covering. Subsequently, the DEAE-Sepharose-Laccase-PEI (DEAE-Lac-PEI) preparation was filtered and thoroughly washed with distilled water. The lipase adsorption at pH 7 onto DEAE-Lac-PEI was conducted by suspending the particles in a lipase solution (2 mg of lipase per 1 g of support). The mixture was then stirred for 1 h at 25 °C, and samples were withdrawn from the supernatant to monitor the catalytic activity of the soluble lipase. Lastly, the DEAE-Sepharose-Laccase-PEI-Lipase (DEAE-Lac-PEI-PFL) preparation was filtered, thoroughly washed with distilled water, and stored at 4 °C.

## II. Protocol II: Octyl-Agarose (OA) – Lipase – PEI – Laccase – GA (OA-PFL-PEI-Lac-GA):

In this second protocol, using Octyl-Agarose as the support, the co-immobilization procedure was performed similarly to the first one, but with the addition of a fourth step consisting of a crosslinking reaction with glutaraldehyde. In this case, the first enzyme to be immobilized was lipase, followed by laccase immobilization. The buffers used were the same as used in the first protocol. Initially, a protein load of 2 mg<sub>protein</sub>/g<sub>support</sub> of each enzyme was employed. Next, to evaluate the influence of protein load on internal diffusion, the amount of protein varied from 2 to 20 mg<sub>protein</sub>/g<sub>support</sub> of each enzyme. Immobilization yield (IY) was again defined as the difference between the catalytic activity of the soluble enzyme before and after immobilization, related to the initial activity of the enzyme solution (Silva *et al.*, 2012).

Layer-by-layer heterogeneous biocatalysts (protocol II) were prepared according to a four-step protocol. The first step was PFL adsorption onto Octyl-Agarose (OA). For that, the support was suspended in a PFL solution (whose PFL concentration depended on the protein load tested) and gently stirred for an appropriate time (which ranged from 1 to 15 h depending on the protein load) at 25 °C. Following the adsorption process, samples were withdrawn from the supernatant to determine the enzyme activity. Next, the support containing the adsorbed PFL (OA-PFL) was filtered and washed with distilled water. Subsequently, the immobilized

lipase was suspended in 10% (w/v) PEI solution at pH 7.0 and stirred overnight at 4 °C. The Octyl-Agarose-PFL-PEI (OA-PFL-PEI) preparation was filtered and washed with distilled water. A similar process was followed for the immobilization of laccase by adsorption: the OA-PFL-PEI particles were suspended in the laccase solution and stirred for an appropriate time (1-15 hours, depending on the protein load) at 25 °C. Samples were also withdrawn from the supernatant to determine enzyme activity. The obtained Octyl-Agarose-Lipase-PEI-Laccase (OA-PFL-PEI-LAC) was filtered and washed with distilled water. Finally, a crosslinking with glutaraldehyde was performed. To this end, the co-immobilized preparation (OA-PFL-PEI-LAC) was suspended in a 1% GA solution at pH 7.0 in 50 mM sodium phosphate buffer and incubated for 1h at 25 °C (Arana-Peña, Rios, *et al.*, 2020). These conditions were selected since they allowed a complete modification of primary amino groups of the proteins with just one molecule of glutaraldehyde (Arana-peña, Rios, Mendez-sanchez, *et al.*, 2020; Barbosa *et al.*, 2014; Migneault *et al.*, 2004). The final immobilized PFL/Laccase preparations were thoroughly washed with distilled water and stored at 4 °C.

### 3.3.2.2 Soluble enzyme and heterogeneous biocatalysts activity

Enzyme reactions were performed in a glass cuvette placed in a spectrophotometer (BioMate™ 3) with an internal stirrer controlled by an Air-cooled Peltier Accessory (Fig. S3.1). Experimental conditions were defined by determining the proper stirring speed rate to avoid external mass transfer limitations (Gonçalves *et al.*, 2008; Gonçalves, Giordano e Giordano, 1997).

#### I. Lipase activity

The activity of the soluble and immobilized lipases was quantified by monitoring the linear rate of hydrolysis of 50 mM *p*-nitrophenyl butyrate (*p*-NPB) performed in 25 mM phosphate buffer (pH 7.0) at 25 °C (Arana-peña, Rios, Carballares, *et al.*, 2020). The colored product of this reaction (*p*-nitrophenol, *p*-k NP) was monitored over time at 348 nm. One unit of lipase activity corresponds to the hydrolysis of 1 μmol of *p*-NPB per minute at 25 °C.

#### II. Laccase activity

The activities of the soluble and immobilized laccases were quantified according to the methodology described in the literature (Addorisio *et al.*, 2013) with modifications. The linear oxidation rate of 3 mM 2,2'-Azino-bis (3-ethylbenzothiazoline-6-sulfonic acid diammonium salt (ABTS) was performed in 10 mM acetate buffer at pH 4.5 containing 1mM CuSO<sub>4</sub>·5H<sub>2</sub>O at 25 °C. The quantification of ABTS oxidation was measured by spectrophotometer at 418 nm. One unit of laccase activity corresponds to the oxidation of 1µmol of ABTS per minute at 25 °C.

#### 3.3.2.3 Protein concentration

The protein concentration was determined using the Bradford protocol (Bradford, 1976), based on spectrophotometric measurements at 585 nm of samples previously incubated in 1mL of Bradford reagent for 10 min. The protein concentration was quantified via calibration curves once determined using bovine serum albumin (BSA) as the standard protein.

#### 3.3.2.4 SDS-PAGE analysis

Electrophoresis was performed for both enzymes in their soluble and immobilized forms according to the methods from the literature (Laemmli, 1970). A 12% polyacrylamide gel was placed in a Miniprotein tetra-cell (Biorad) electrophoresis unit. Enzymes samples were incubated in the loading buffer (2% SDS and 10% mercaptoethanol) at 100 °C for 10 min. In the case of the immobilized enzymes, the biocatalyst was resuspended in the loading buffer, so all non-covalently attached enzymes could be released to the supernatant (Barbosa *et al.*, 2012). A low-molecular-weight (14.4 – 97 kDa) marker (GE - Healthcare Life sciences) was used for identification purposes. Coomassie brilliant blue was used for the staining procedure.

#### 3.3.2.5 Thermal stability

The thermal stabilities of the soluble and immobilized enzymes were performed at 50 °C in a 50mM Tris-HCl pH 7.0 buffer for 48 hours (Arana-peña, Rios, Carballares, *et al.*, 2020). Samples were periodically withdrawn, and the activity determination for both enzymes was performed using their specific substrates (*p*NPB for lipase and ABTS for laccase). Then, their relative activity was calculated, considering the initial activity values to be 100%.



### 3.3.2.6 Temperature dependence of the heterogeneous biocatalysts' activity

The influence of temperature on the catalytic activity of the soluble and immobilized preparations was studied in the temperature range of 25 – 50 °C. For that purpose, the catalytic activity of both enzymes (lipase and laccase) was determined under each temperature. The experiment was carried out for enzymes immobilized at a concentration of 2 and 4 mg/g of the carrier. The dependence of soluble enzyme activity on temperature was determined for comparative purposes.

### 3.3.2.7 Diffusivity analysis

Diffusivity (solute A through a solvent B) for the substrate of PFL (pNPB) was calculated using the Wilke-Chang correlation, demonstrated in Equation 3.1 (Guo e Xu, 2006; Wilke e Chang, 1955):

$$D_{AB} = 7.4 \cdot 10^{-8} \frac{(x \cdot M_B)^{1/2} \cdot T}{\eta_B \cdot V_A^{0.6}} \quad (3.1)$$

Where  $D_{AB}$  (cm<sup>2</sup>/s) is the diffusion coefficient of solute A (pNPB) in solvent B, since the reaction was performed in a diluted solution (25 mM sodium phosphate buffer prepared in distilled water), parameters of solvent B were considered as for water. X (dimensionless) is the association parameter (= 2.60, (Wilke e Chang, 1955)),  $M_B$  is the solvent molecular weight (18.015 g/mol), T is the temperature (298, 15 K) and  $\eta_B$  is the solvent viscosity (0.891 cP).  $V_A$  is the molar volume of the solute at its normal boiling temperature (cm<sup>3</sup>/mol). For pNPB, an approximate value was obtained by dividing the molar weight (209.20 g/mol) by the manufacturer's density (1.19 g/mL at 20 °C). For ABTS, the diffusion coefficient is reported in literature as  $3.22 \times 10^{-6}$  cm<sup>2</sup>/s (Fei *et al.*, 2006).

Since the Wilke-Chang correlation is used for homogeneous systems, it was necessary to adjust the calculated coefficient for a heterogeneous system, such as the one used in this work. In heterogeneous catalysis, an effective diffusivity can be calculated by using the following equation (Eq. 3.2) (Arıkaya, Ünlü e Takaç, 2019):

$$D_{AB_e} = D_{AB} \frac{\varepsilon_p}{\tau} \sigma \quad (3.2)$$

Where  $D_{AB_e}$  is the effective diffusivity ( $\text{cm}^2/\text{s}$ );  $\varepsilon_p$  and  $\tau$  are the porosity and the tortuosity of the particle, respectively; and  $\sigma$  is the constriction factor, which can be neglected when the radius of the pore (about 37 nm (Barrande, Bouchet e Denoyel, 2007)) is larger than the molecule of solute (Arıkaya, Ünlü e Takaç, 2019). The values of porosity ( $\varepsilon_p = 94.5\%$ ) and tortuosity ( $\tau = 1.32$ ) of the particle were taken from literature (Barrande, Bouchet e Denoyel, 2007; Gonçalves *et al.*, 2008).

To calculate the observable Thiele modulus  $\Phi$  (also known as Weisz's modulus) Equation 3.3 was used (Doran, 2013). To standardize all the calculations of observed reactions rate ( $r_{a,obs}$ ) herein, it was considered that 1g of immobilized enzyme was used for the Reaction of both enzymes.

$$\Phi = \left(\frac{V_P}{S_P}\right)^2 \frac{r_{A,obs}}{D_{AB_e} \cdot C_{As}} \quad (3.3)$$

Where  $V_P$  and  $S_P$  are the particle's volume and the external surface area, calculated considering the diameter of the particle as 90  $\mu\text{m}$  (supplied by the producer);  $r_{A,obs}$  is the observed rate for the Reaction; and  $C_{As}$  is the substrate concentration at the particle surface, which can be considered equal to the bulk concentration when no external diffusion is present in the system.

### 3.4 Results and discussion

#### 3.4.1 Production and characterization of heterogeneous biocatalyst containing lipase and laccase

##### 3.4.1.1 Co-immobilization of lipase and laccase onto agarose-based supports

The multi-enzyme biocatalyst was prepared by the two strategies via the co-immobilization of laccase (Lac) and lipase (PFL), using 2  $\text{mg}_{\text{protein}}/\text{g}_{\text{support}}$  in each enzyme layer. In immobilization solutions, soluble Lac presented activity of  $4.54 \pm 0.01 \text{ U}_{\text{ABTS}}/\text{mL}$  and soluble

PFL presented  $1.44 \pm 0.05 U_{p\text{NPB}}/\text{mL}$  of activity. The first strategy followed a three-step procedure, using DEAE-Sephrose as support. In this case, laccase (Lac) was immobilized by adsorption on DEAE-Sephrose, with an immobilization yield (%) of  $97.49 \pm 0.75$ . Then, different PEI concentrations (0.1, 1.0, and 10%) were used in the coating of the DEAE-Lac preparation, which would provide an adequate surface for the immobilization of the second enzyme (PFL). As a result, the heterogeneous biocatalyst (DEAE-Lac-PEI-PFL) was produced. The yields (IY, %) obtained for lipase immobilization onto the DEAE-Lac covered with PEI 10%, PEI 1%, and PEI 0.1% were  $49.30 \pm 1.73$ ,  $61.1 \pm 1.09$  and  $59.33 \pm 0.16$ , respectively. The biocatalysts' activities determined in each step are shown in Table 3.1. A remarkable loss in laccase activity (over 97% of its initial value) was observed after coating with high concentrations of PEI (1% and 10%). Other authors have also reported similar issues, such as the difficult access of ABTS and other ions to laccase after PEI coating due to the ion-exchange effect it promotes (Zhang *et al.*, 2015). Therefore, partition effects are probably the reason for such a drastic activity reduction after co-immobilization under these conditions. Substrate access to the active site of laccase, which is located under the PEI layer, may have been hindered due to the electrostatic interaction between the negatively-charged substrate ABTS (Kadnikova e Kostić, 2002) and the layer of the positively-charged polymer PEI (Khoobi *et al.*, 2016). When the PEI concentration was low (0.1%), the activity loss was much lower (around 30%), confirming that partition effects must be considered when using high PEI concentrations. Regardless, under all conditions, the immobilization yields obtained for PFL were not particularly high, resulting in low activity values for both biocatalysts. Thus, in the best scenario (0.1% PEI), this strategy results in a heterogeneous biocatalyst with low lipase activity than laccase. Furthermore, the intrinsic hindrances of the system led us to abandon this first strategy (not performing the final crosslinking step) and search for another strategy to prepare the multi-enzyme biocatalyst.

Table 3.1 - Catalytic activity for both enzymes in each stage of the 3-step immobilization process using DEAE as support.

Heterogeneous biocatalysts	laccase activity ( $U_{ABTS/g}$ )			lipase activity ( $U_{pNFB/g}$ )		
	PEI 10%	PEI 1%	PEI 0.1%	PEI 10%	PEI 1%	PEI 0.1%
<b>DEAE-Lac</b>	————— $27.6 \pm 2.3$ —————					
<b>DEAE-Lac-PEI</b>	$0.27 \pm 0.02$	$0.61 \pm 0.02$	$20.04 \pm 0.12$			
<b>DEAE-Lac-PEI-PFL</b>	undetectable	$0.74 \pm 0.01$	$11.25 \pm 0.01$	$2.64 \pm 0.43$	$3.71 \pm 0.28$	$1.96 \pm 0.52$

Source: Elaborated by the author.

In the second immobilization strategy, the order of enzyme co-immobilization was inverted. PFL adsorption was the first step of the process, followed by PEI coating and, finally, laccase immobilization. The PEI layer would be on top of PFL and below the laccase layer. Therefore, partition effects due to electrostatic interactions between PEI and the laccase substrate should not be observed. Thus, PEI at a concentration of 10% could be used without causing partition effects. After laccase immobilization onto OA-PFL-PEI, a fourth step (glutaraldehyde crosslinking) was also performed to promote covalent linkages between the enzyme and the support. This would also prevent enzyme leaching under harsh conditions (Barbosa *et al.*, 2014; Vazquez-Ortega *et al.*, 2018). Immobilization yields of  $90.94 \pm 0.45$  % and  $96.75 \pm 0.28$  % were achieved for lipase and laccase, respectively. The immobilization yield for PFL was significantly higher when compared to the first strategy (DEAE-Sepharose support), but for laccase, it was similar. Table 3.2 shows the values of the biocatalyst activity obtained in each step of the co-immobilization procedure.

Table 3.2 - Catalytic activities for both enzymes in each stage of the 4-steps co-immobilization process using octyl-agarose as support.

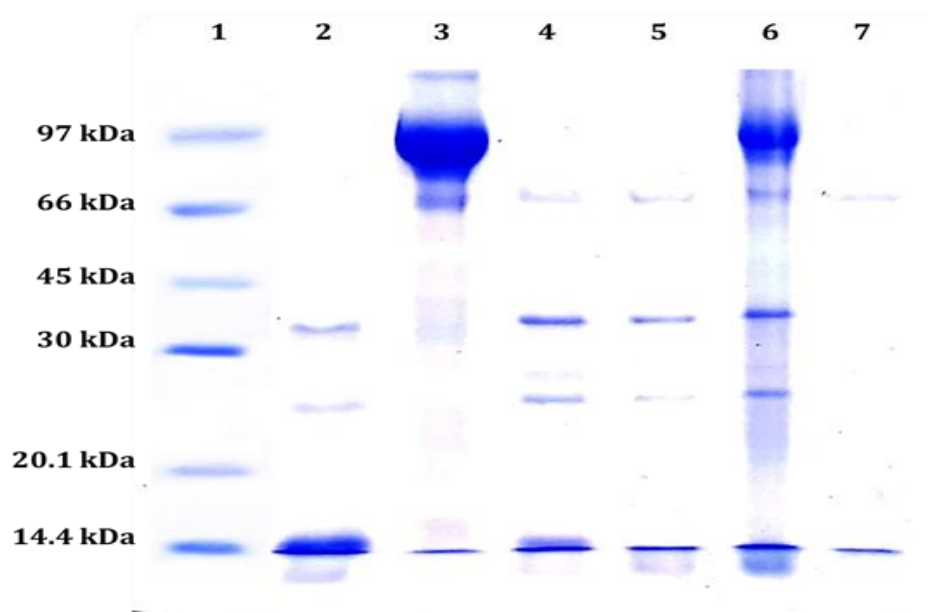
<b>Heterogeneous biocatalysts</b>	lipase activity (U <sub>pNPB</sub> /g)	laccase activity (U <sub>ABTS</sub> /g)
<b>OA-PFL</b>	20.28 ± 0.42	-
<b>OA-PFL-PEI</b>	20.67 ± 0.54	-
<b>OA-PFL-PEI-Lac</b>	13.8 ± 0.13	11.93 ± 0.06
<b>OA-PFL-PEI-Lac-GA</b>	14.26 ± 0.11	10.63 ± 0.03

Source: Elaborated by the author.

The PFL immobilized in Octyl-Agarose maintained its activity after the coating process with the first layer of PEI and retained around 70% of its initial activity after all the steps. In comparison, laccase kept almost 90% of its activity after the co-immobilization procedure. The use of Octyl-Agarose as support enabled to obtain a biocatalyst that showed high hydrolytic and oxidative activities. Thus, we proceeded with the present study by using this second strategy, using Octyl-Agarose as the co-immobilization support.

An electrophoresis (SDS-PAGE) analysis of the enzyme samples was carried out after each step of the co-immobilization process (Fig. 3.3). Lane 2 shows a band around 33kDa, which corresponds to PFL (Rios *et al.*, 2018), and lane 3 shows the band corresponding to laccase, at around 85kDa (Berka *et al.*, 1997). From lane 4 onwards, the presence of bands indicates enzyme desorption since the biocatalyst obtained after each step of co-immobilization was assayed. The PFL adsorbed on OA after the first step of co-immobilization can be seen in lane 4. Then, OA-bound lipase, lipase was coated with PEI in the second step, and the enzyme remained adsorbed to the support, as seen in lane 5. The insertion and immobilization of laccase by adsorption in the third step is seen in lane 6. Finally, after crosslinking with glutaraldehyde (lane 7), the absence of bands of laccase (~85 kDa) and PFL (~33 kDa) indicates the formation of covalent bonds, which prevents the leaching of both enzymes from the support under harsh environmental conditions. In addition, the formation of a dimer of PFL, observed at around 66 kDa, is reported in the literature as a result of the Maillard reaction (Rios, Arana-Peña, *et al.*, 2019).

Figure 3.3 - SDS-page of the soluble enzymes and the biocatalysts in each stage of the 4-step co-immobilization process using Octyl-agarose as support. Lanes: (1) Molecular weight marker; (2) Soluble PFL, molecular weight around 33 kDa; (3) Soluble Laccase, molecular weight around 85 kDa; (4) OA-PFL; (5) OA-PFL-PEI; (6) OA-PFL-PEI-Lac; (7) OA-PFL-PEI-Lac-GA.



Source: Elaborated by the author.

#### 3.4.1.2 Thermal stability at 50 °C

The thermal stability of soluble enzymes and heterogeneous biocatalysts was assayed by incubating them at 50 °C and pH 7 for 48 h (inactivation profile is shown in Fig. S3.2). The immobilization procedure remarkably improved the thermal stability of both enzymes. While soluble PFL retained around 70% of its initial activity after 24 hours of incubation, preserving this percentage up to 48 hours, the immobilized PFL retained its activity during the complete thermal inactivation assay (48 h). There is clear evidence in the literature that treatment with glutaraldehyde significantly improves the thermal stability of enzymes (Rios, Arana-Peña, *et al.*, 2019), which explains the results obtained in the present study for PFL immobilized onto Octyl-agarose and coated with PEI. In the case of laccase, the four-step immobilization procedure also positively affected its thermal stability. Soluble Laccase

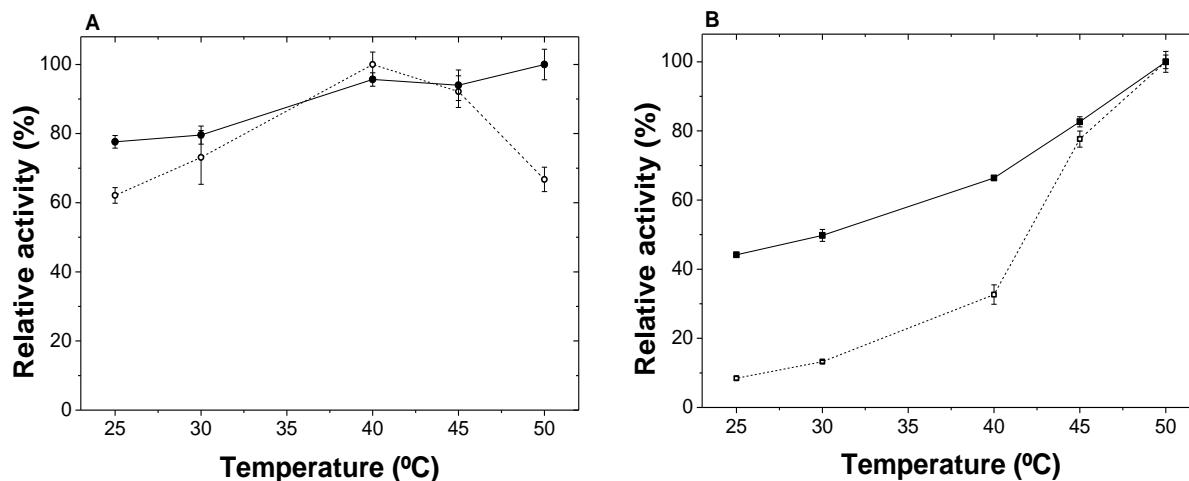
preserved about 17.6 % of its initial activity after 24 hours of incubation and lost almost its complete activity after 48 hours of thermal inactivation (keeping only 2.16% of it).

On the other hand, immobilized laccase kept about 69.3 % of its initial activity after 24 hours of incubation (more than 3 times the percentage obtained for soluble laccase) and more than 20% after 48 hours. The literature also reports thermal stability improvements after laccase immobilization. Some authors report an increase in the thermal stability of the enzyme at different temperatures and pHs when it is covalently immobilized via glutaraldehyde crosslinking (Bezerra *et al.*, 2015; Patel *et al.*, 2014). However, thermal stability is also dependent on the type of support used for immobilization. For instance, laccase immobilized onto mesostructured siliceous cellular foams showed a thermostability similar to the soluble enzyme (Rekuć *et al.*, 2009).

#### *3.4.1.3 Temperature-dependent activity profiles of soluble and immobilized enzymes*

Since temperature is one of the most critical reaction conditions, its effect on the catalytic performance of the soluble and immobilized enzymes was quantified by measuring the lipase and laccase activities between 25 and 50°C (Fig 3.4). For comparison purposes, the relative activity was expressed for each biocatalyst by considering the maximum activity value as 100%. For the soluble PFL (Fig. 3.4A), the highest activity was observed at 40 °C, whereas, for the heterogeneous biocatalyst, the optimum temperature may be equal to or higher than 50 °C. In the case of laccase (Fig 3.4B), the optimum temperature for both soluble and heterogeneous biocatalysts can also be equal to or higher than 50 °C.

Figure 3.4 - Temperature dependence of PFL (A) and Laccase (B) activity profiles. Hollow shapes and dashed lines: soluble enzyme; Solid shapes and solid lines: heterogeneous biocatalyst (2 mg<sub>protein</sub>/g<sub>support</sub> of each enzyme).



Source: Elaborated by the author.

From the results presented in Fig. 3.4, the natural logarithm of the reaction rate as a function of the inverse of temperature, i.e.,  $\ln(V) \times 1/T$ , was plotted according to the Arrhenius equation. For the soluble PFL, rate values were only taken up to the temperature of 40 °C because, under higher temperatures, enzyme deactivation may occur. All rate values (25 °C – 50 °C) were considered for laccase since no enzyme deactivation was observed in this temperature range.

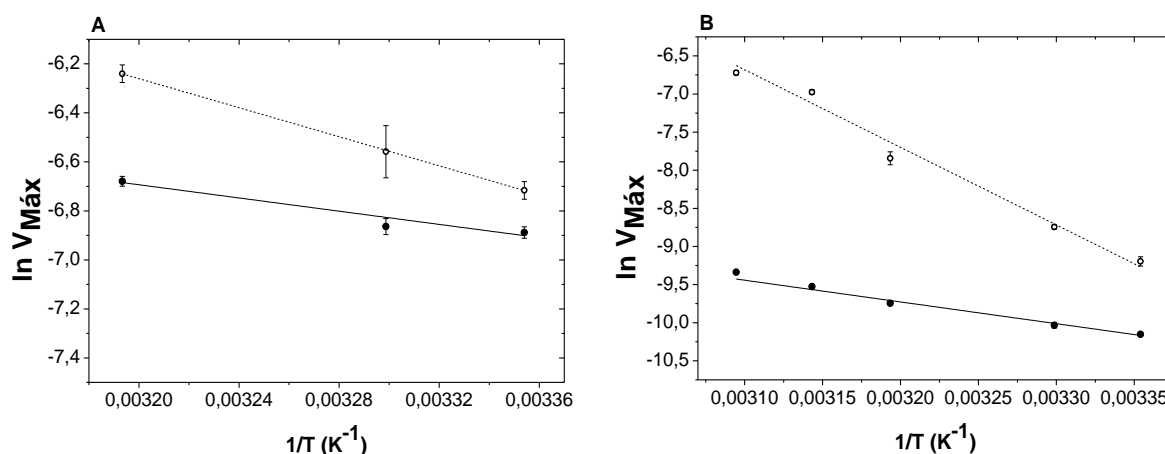
The activation energy was calculated from the slope ( $-E_a/R$ ) of the graphs shown in Fig. 3.5 for each enzyme. The values of activation energy for the heterogeneous biocatalysts (2 mg<sub>protein</sub>/g<sub>support</sub> of each enzyme) were 11.21 and 23.71 kJ/mol for PFL and Laccase, respectively. These values are lower than those for the soluble enzymes, 24.65 and 84.62 kJ/mol for PFL and Laccase, respectively, which is a trend reported by different literature authors. The decrease in  $E_a$  values determined for support-bound enzymes indicates that the temperature dependence decreases after immobilization (Ahmed *et al.*, 2019; Ahmed, Hashem e Saleh, 2013; Chiou e Wu, 2004; Yan *et al.*, 2010). Thus, the results of this work demonstrate that soluble PFL presents a higher temperature dependence than its immobilized counterpart. PFL heterogeneous biocatalyst is less sensitive to temperature changes since it retains more than 90% of their maximum activity in a higher temperature range (as seen in Fig. 3.4A).

Similarly, the laccase heterogeneous biocatalyst also showed a lower temperature dependence than the soluble laccase. Thus, enzyme immobilization enabled an apparent



increase in their catalytic effectivity in a broader temperature range. This lower temperature dependence is a desired feature for industrial purposes since reactions can be performed in a wide range of temperatures while still conserving a high percentage (enzyme activity).

Figure 3.5 - Plot of  $\ln(V_{\max})$  versus  $1/T$  for calculating the activation energy via the Arrhenius equation for PFL (A) and Laccase (B). Hollow shapes and dashed lines: soluble enzyme; Solid shapes and lines: heterogeneous biocatalyst containing  $2 \text{ mg}_{\text{protein}}/\text{g}_{\text{support}}$  of each enzyme.

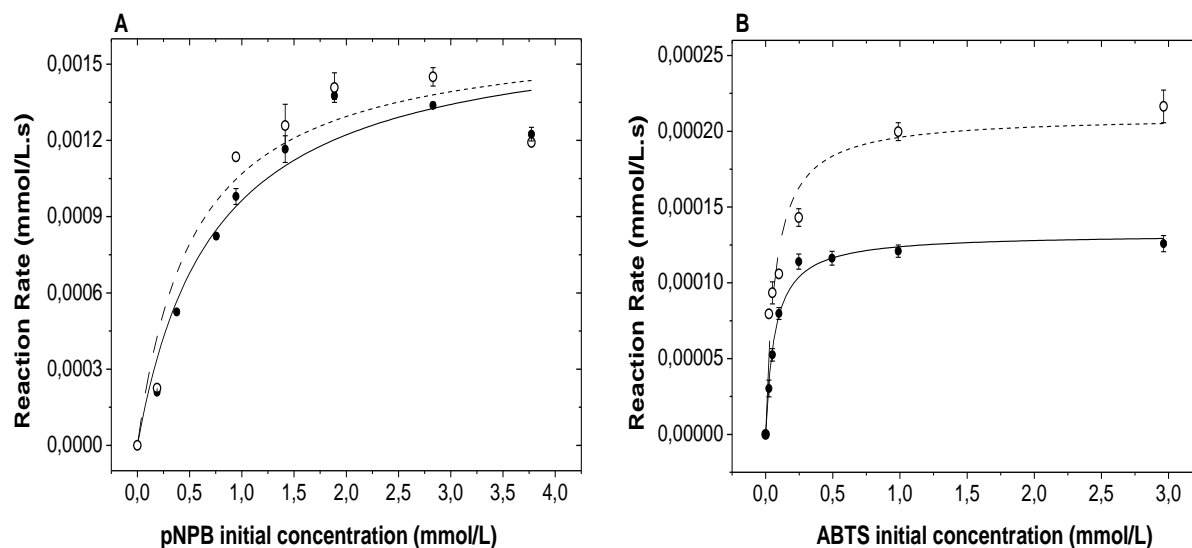


Source: Elaborated by the author.

### 3.4.2 Reaction and Diffusion analysis

The effects of reaction parameters and intraparticle diffusion were analyzed. First, in order to estimate the kinetic parameters for both substrates, reactions were performed using a low protein load of the soluble and heterogeneous biocatalysts ( $2 \text{ mg}_{\text{protein}}/\text{g}_{\text{support}}$  of each enzyme) at different substrate concentrations (Fig. 3.6). For each enzyme, the same amount of protein in its soluble and immobilized forms was used in the reactions.

Figure 3.6 - Michaelis-Menten fit of PFL (A) and laccase (B) data. Open circle: Soluble enzyme; Solid circle: heterogeneous biocatalysts; Dashed line: fitting for the soluble enzyme; Solid line: fitting for the heterogeneous biocatalysts.



Source: Elaborated by the author.

Table 3.3 - Kinetic parameters from the Michaelis-Menten model adjustment using the values obtained from the reactions for both enzymes performed at different substrate concentrations.

	PFL		Laccase	
	Soluble	Co-immobilized	Soluble	Co-immobilized
$V_{\text{máx}}$ ( $10^{-3}$ mmol/L.s)	$1.64 \pm 0.16$	$1.67 \pm 0.11$	$0.21 \pm 0.01$	$0.13 \pm 0.004$
$K_m$ (mmol/L)	$0.53 \pm 0.20$	$0.73 \pm 0.14$	$0.072 \pm 0.014$	$0.068 \pm 0.0081$
$R^2$	0.84	0.92	0.88	0.96

Source: Elaborated by the author.

The Michaelis-Menten model was able to describe the reactions catalyzed by PFL and laccase (see Table 3.3 and Fig. 3.6) reasonably well, both in their soluble ( $R^2 \geq 0.84$ ) and immobilized ( $R^2 \geq 0.92$ ) forms, under the substrate concentrations investigated. For PFL, the soluble and heterogeneous biocatalysts seemed to follow the same behavior as the *p*NPB concentration increased, with very similar reaction rates. The  $V_{\text{max}}$  values were also similar (around  $1.6 \times 10^{-3}$  mmol/L.s), but the  $K_m$  increased, indicating that the enzyme's affinity for the

substrate may have decreased slightly after immobilization. Nevertheless, the overall results of reaction rates were not affected by the immobilization process (Valencia, Pinto e Almonacid, 2014). The similarity between the  $V_{\max}$  values for lipase might indicate the absence of internal diffusion limitations in this system for *p*NPB hydrolysis.

For laccase, on the other hand, very different rates were obtained for the soluble and the heterogeneous biocatalyst. The most remarkable discrepancy was that the observed rate decreased when using higher ABTS concentrations, which consequently caused a decrease in  $V_{\max}$  of the immobilized enzyme. This decrease should not be linked to differences in affinity following immobilization since the values of  $K_m$  for both biocatalysts are very similar (around 0.07 mmol/L). However, the immobilization process may have caused important changes in the enzyme structure, probably leading to inactivation. This decrease in reaction rate could also result from blocking the active site of immobilized laccase followed by glutaraldehyde crosslinking. Either way, the number of active enzyme molecules ( $E_o$ , proportional to  $V_{\max}$  in the Michaelis-Menten model) was lowered. Additionally, unlike lipase, the decrease in the observed reaction rates for the immobilized laccase can also be related to intraparticle diffusion limitations.

Thus, the intraparticle diffusion effects were also analyzed for the immobilized enzymes. The literature provides the diffusivity value for the laccase substrate ABTS in sodium acetate buffer at pH 4.0, used as the reaction medium, as shown in Table 3.4 (Fei *et al.*, 2006). As for the *p*NPB, the PFL substrate, the diffusivity may be calculated using the Wilke-Chang correlation (Equation 3.1). Then, the approximated *p*NPB diffusivity value was calculated and presented in Table 3.4.

The effective diffusivity values for both substrates could then be calculated (Table 3.4). The estimated values for the Weisz modulus ( $\Phi$ ) were also calculated, as shown in Table 3.4. Since  $\Phi < 0.3$  (Weisz criteria, (Doran, 2013)) for both enzymes, internal diffusion effects can be considered negligible, probably due to the low protein load of 2 mg<sub>protein</sub>/g<sub>support</sub> of each enzyme. Thus, the decrease in the  $V_{\max}$  for the immobilized laccase (Fig. 3.6B) is likely to be linked to the inactivation or the blockage of the active sites of enzyme molecules during the co-immobilization process.

Table 3.4 - Diffusivity parameters for PFL and Laccase using pNPB and ABTS as substrates, respectively.  $D_{AB}$  ( $\text{cm}^2/\text{s}$ ) is the diffusion coefficient of solute A in solvent B.  $D_{ABe}$  ( $\text{cm}^2/\text{s}$ ) is the effective diffusivity, considering the specificities of the agarose-based support.  $\Phi$  (dimensionless) is Weisz's modulus calculated at the maximum tested substrate concentration.

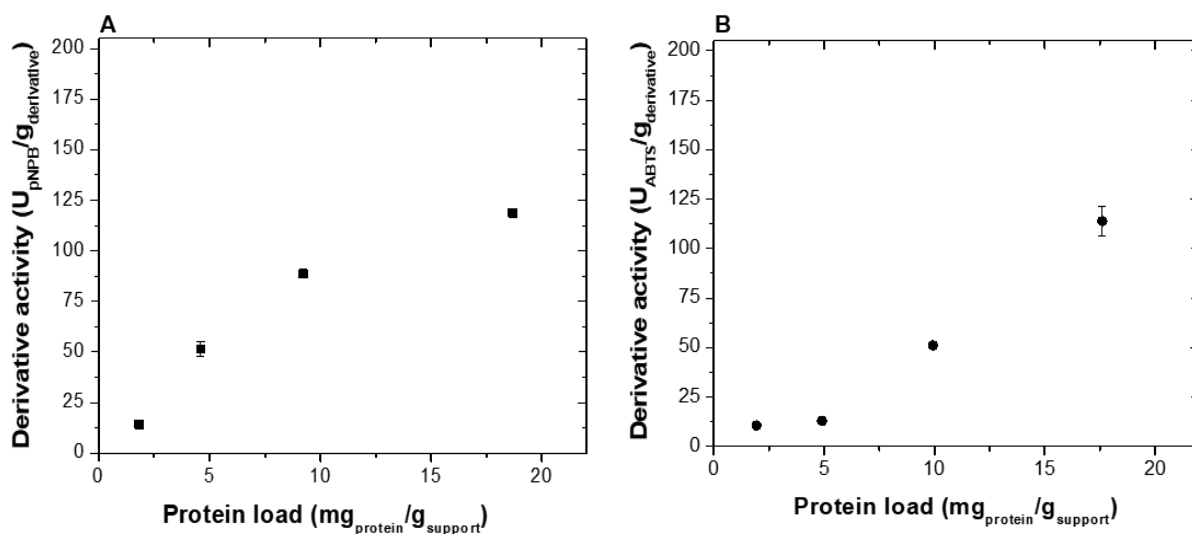
	$D_{AB}$ ( $\text{cm}^2/\text{s}$ )	$D_{ABe}$ ( $\text{cm}^2/\text{s}$ )	$\Phi$ (dimensionless)
<b>PFL</b>	$7.63 \times 10^{-6}$	$5.46 \times 10^{-6}$	$3.21 \times 10^{-2}$
<b>Laccase</b>	$3.22 \times 10^{-6}$	$2.31 \times 10^{-6}$	$4.38 \times 10^{-3}$

Source: Elaborated by the author.

### 3.4.3 Influence of internal mass transfer at high enzyme loadings

In this work, internal mass transfer limitations were assessed by varying the initial protein load during co-immobilization (2 to 20  $\text{mg}_{\text{protein}}/\text{g}_{\text{support}}$  for each enzyme) and keeping similar concentrations for both enzymes. In the case of the PFL, the first enzyme layer, the immobilization yield was around 90% for all protein loads studied. For laccase, the second enzyme layer, the yield obtained using 2 – 10  $\text{mg}_{\text{protein}}/\text{g}_{\text{support}}$  of protein load was higher than 96%. However, it was observed that the yield decreased when using a 20  $\text{mg}_{\text{protein}}/\text{g}_{\text{support}}$  load, reaching the value of 88.1%. To provide more binding spots between laccase and the PEI layer, a higher content of PEI (20%) was tested (results not shown). But the immobilization yield did not increase, which indicates that the limit for laccase linkage onto this support had been reached. Since the obtained immobilization yields were consistently lower than 100%, the total value of protein load attached to the support during the co-immobilization (used in Fig. 3.7 as the abscissa for both graphs) is always lower than the initial protein load used.

Figure 3.7 - The activity of the heterogeneous biocatalysts. PFL activity (A) and Laccase activity (B) as a function of enzyme load on the support.



Source: Elaborated by the author.

Fig. 3.7 shows the activity for each immobilized enzyme as a function of the immobilized protein load. In a system with no internal diffusion limitations, the catalytic activity should be proportional to the protein load since  $V_{max}$  is proportional to the enzyme concentration ( $E_0$ ). For PFL (Fig. 3.7A), the activity increases with increasing protein load up to 10 mg<sub>protein</sub>/g<sub>support</sub>. Over this point, the increase in activity is no longer dependent on protein load, suggesting that internal mass transfer limitations may be a limiting factor when 10-20 mg<sub>protein</sub>/g<sub>support</sub> is used in the biocatalyst preparation (Gonçalves *et al.*, 2008). Weisz modulus ( $\Phi$ ) was also calculated for the pNPB hydrolysis, and the results are shown in Table 3.5. For PFL,  $\Phi < 0.3$  for all the biocatalysts prepared using 2 to 10 mg<sub>protein</sub>/g<sub>support</sub>, and therefore, internal diffusion can be considered negligible. When the biocatalyst was prepared with 20 mg<sub>protein</sub>/g<sub>support</sub>, intraparticle mass transfer effects cannot be neglected since  $\Phi > 0.3$ .

For laccase (Fig. 3.7B), a maximum protein load of 17.6 mg<sub>protein</sub>/g<sub>support</sub> was achieved after immobilization when an initial load of 20 mg<sub>protein</sub>/g<sub>support</sub> was used. The increase in laccase activity seems to be proportional to the increase in protein load up to this point, which could indicate that no intraparticle mass transfer effects take place in the system for all studied conditions using ABTS as substrate. However, the Weisz modulus calculated for the ABTS oxidation (Table 3.5) using the biocatalyst prepared with 20 mg<sub>protein</sub>/g<sub>support</sub> was  $\Phi > 0.3$ , so intraparticle diffusion effects should be considered for this system.

All the results presented in Fig. 3.7 and Table 3.5 are essential to the understanding of the effect of enzyme load on biocatalyst activity. This information would subside the choice of conditions under which the reactions will occur in the absence of mass transfer effects. In the case of the model reactions (pNPB hydrolysis and ABTS oxidation) here investigated, the biocatalyst is the one prepared by the co-immobilization of PFL and laccase using 10  $\text{mg}_{\text{protein}}/\text{g}_{\text{substrate}}$  of each enzyme. It is important to mention that the use of these synthetic substrates provides a basis for future research on applying such multi-active biocatalysts to catalyze reactions of interest on the industrial scale.

Table 3.5 - Weisz's modulus ( $\Phi$ , dimensionless) was calculated for reactions using heterogeneous biocatalysts obtained from immobilization with different initial protein loads.

Initial protein load ( $\text{mg}_{\text{protein}}/\text{g}_{\text{support}}$ )	$\Phi$ (dimensionless)	
	PFL	Laccase
2	$3.92 \times 10^{-2}$	$3.04 \times 10^{-2}$
5	$1.41 \times 10^{-1}$	$3.73 \times 10^{-2}$
10	$2.43 \times 10^{-1}$	$1.46 \times 10^{-1}$
20	$3.26 \times 10^{-1}$	$3.26 \times 10^{-1}$

Source: Elaborated by the author.

### 3.5 Conclusions

The co-immobilization of laccase and PFL using a layer-by-layer strategy showed to be appropriate for the immobilization of these two enzymes by taking advantage of the different interactions between the supports and the enzymes and between PEI and the enzymes. The strategy using Octyl-agarose as support proved to be the most appropriate for producing such multi-active heterogeneous biocatalyst. The final step of crosslinking with glutaraldehyde formed covalent bonds that prevent the leaching of both enzymes under harsh conditions. As intended, the immobilization process increased the thermal stability of both enzymes, especially lipase, which remained at 100% of its initial activity even after 48 hours at 50 °C. Enzyme

immobilization also showed a positive effect on decreasing the catalytic activity dependence on temperature. No internal mass transfer limitations were observed when the heterogeneous biocatalysts containing low protein load ( $2 \text{ mg}_{\text{protein}}/\text{g}_{\text{support}}$  of each enzyme) were used to catalyze the reactions of *p*NPB hydrolysis and ABTS oxidation. However, higher protein loads may cause diffusional limitations in the system, which can impact the production of industrial biocatalysts with high activities. Moreover, the diffusion limitation is not only caused by the increase in enzyme concentration but also depends on the reaction to be catalyzed.

### 3.6 Acknowledgments

The authors would like to acknowledge the Brazilian Research Agencies CNPq (Conselho Nacional de Desenvolvimento Científico e Tecnológico), CAPES (Coordenação de Aperfeiçoamento de Pessoal de Nível Superior), and FUNCAP (Fundação Cearense de Apoio ao Desenvolvimento Científico e Tecnológico) for the financial support.

### 3.7 References

- ADDORISIO, V. *et al.* Oxidation of phenyl compounds using strongly stable immobilized-stabilized laccase from *Trametes versicolor*. **Process Biochemistry**, v. 48, n. 8, p. 1174–1180, 2013.
- AHMED, S. A. *et al.* Catalytic , kinetic and thermodynamic properties of free and immobilized caseinase on mica glass-ceramics. **Heliyon**, v. 5, n. May, p. e01674, 2019.
- AHMED, S. A.; HASHEM, A. M.; SALEH, S. A. Biochemical studies on immobilized fungal  $\beta$ -Glucosidase. **Brazilian Journal of Chemical Engineering**, v. 30, n. 04, p. 747–758, 2013.
- ALBUQUERQUE, T. L. D. *et al.* Easy stabilization of interfacially activated lipases using heterofunctional divinyl sulfone activated-octyl agarose beads. Modulation of the immobilized enzymes by altering their nanoenvironment. **Process Biochemistry**, v. 51, n. 7, p. 865–874, 2016.
- ARANA-PEÑA, S. *et al.* New applications of glyoxyl-octyl agarose in lipases co-immobilization: Strategies to reuse the most stable lipase. **International Journal of Biological Macromolecules**, v. 131, p. 989–997, 2019.
- ARANA-PEÑA, S.; CARBALLARES, D.; *et al.* One pot use of combilipases for full modification of oils and fats: Multifunctional and heterogeneous substrates. **Catalysts**, v. 10, n. 6, p. 605, 2020.
- ARANA-PEÑA, S.; RIOS, N. S.; *et al.* Coimmobilization of different lipases: Simple layer by layer enzyme spatial ordering. **International Journal of Biological Macromolecules**, v.

145, p. 856–864, 2020.

ARANA-PEÑA, S.; RIOS, N. S.; CARBALLARES, D.; *et al.* Effects of Enzyme Loading and Immobilization Conditions on the Catalytic Features of Lipase From *Pseudomonas fluorescens* Immobilized on Octyl-Agarose Beads. v. 8, n. February, p. 1–13, 2020.

ARANA-PEÑA, S.; RIOS, N. S.; MENDEZ-SANCHEZ, C.; *et al.* Use of polyethylenimine to produce immobilized lipase multilayers biocatalysts with very high volumetric activity using octyl-agarose beads : Avoiding enzyme release during multilayer production. **Enzyme and Microbial Technology**, v. 137, n. October 2019, p. 109535, 2020.

ARIKAYA, A.; ÜNLÜ, A. E.; TAKAÇ, S. Use of deep eutectic solvents in the enzyme catalysed production of ethyl lactate. **Process Biochemistry**, v. 84, n. February, p. 53–59, 2019.

BALDRIAN, P.; GABRIEL, J. Copper and cadmium increase laccase activity in *Pleurotus ostreatus*. **FEMS Microbiology Letters**, v. 206, p. 69–74, 2002.

BARBOSA, O. *et al.* The slow-down of the CALB immobilization rate permits to control the inter and intra molecular modification produced by glutaraldehyde. **Process Biochemistry**, v. 47, n. 5, p. 766–774, 2012.

BARBOSA, O.; ORTIZ, C.; BERENQUER-MURCIA, Á. *et al.* Glutaraldehyde in biocatalysts design: A useful crosslinker and a versatile tool in enzyme immobilization. **RSC Advances**, v. 4, n. 4, p. 1583–1600, dez. 2014.

BARRANDE, M.; BOUCHET, R.; DENOYEL, R. Tortuosity of porous particles. **Analytical Chemistry**, v. 79, n. 23, p. 9115–9121, 2007.

BEBIĆ, J. *et al.* Immobilization of laccase from *Myceliophthora thermophila* on functionalized silica nanoparticles: Optimization and application in lindane degradation. **Chinese Journal of Chemical Engineering**, v. 28, n. 4, p. 1136–1144, 2020.

BERKA, R. M. *et al.* Characterization of the gene encoding an extracellular laccase of *Myceliophthora thermophila* and analysis of the recombinant enzyme expressed in *Aspergillus oryzae*. **Applied and Environmental Microbiology**, v. 63, n. 8, p. 3151–3157, 1997.

BEZERRA, T. M. D. S. *et al.* Covalent immobilization of laccase in green coconut fiber and use in clarification of apple juice. **Process Biochemistry**, v. 50, n. 3, p. 417–423, 2015.

BÓDALO, A. *et al.* Analysis of diffusion effects on immobilized enzymes on porous supports with reversible Michaelis-Menten kinetics. **Enzyme and Microbial Technology**, v. 8, n. 7, p. 433–438, 1986.

BOLIVAR, J. M.; EISL, I.; NIDETZKY, B. Advanced characterization of immobilized enzymes as heterogeneous biocatalysts. **Catalysis Today**, v. 259, p. 66–80, 2015.

BRADFORD, M. M. A Rapid and Sensitive Method for the Quantitation of Microgram Quantities of Protein Utilizing the Principle of Protein-Dye Binding. **Analytical Biochemistry**, v. 72, p. 248–254, 1976.

CHIOU, S. H.; WU, W. T. Immobilization of lipase on chitosan with activation of the hydroxyl groups. **Biomaterials**, v. 25, n. 2, p. 197–204, 2004.



DORAN, P. M. **Bioprocess Engineering Principles**. second ed. Oxford: Elsevier, 2013.

FEI, J. *et al.* Two Polymerizable Derivatives of 2,2'-Azino-bis(3-ethylbenzthiazoline-6-sulfonic acid). **ORGANIC LETTERS**, v. 8, n. 1, p. 3–6, 2006.

FERREIRA, L. *et al.* Influence of different silica derivatives in the immobilization and stabilization of a *Bacillus licheniformis* protease (Subtilisin Carlsberg). **Journal of Molecular Catalysis B: Enzymatic**, v. 21, n. 4–6, p. 189–199, 2003.

FORREST, S. R.; ELMORE, B. B.; PALMER, J. D. Activity and lifetime of organophosphorous hydrolase (OPH) immobilized using layer-by-layer nano self-assembly on silicon microchannels. **Catalysis Today**, v. 120, n. 1, p. 30–34, 2007.

GAVEZZOTTI, P. *et al.* Synthesis of enantiomerically enriched dimers of vinylphenols by tandem action of laccases and lipases. **Advanced Synthesis and Catalysis**, v. 353, n. 13, p. 2421–2430, 2011.

GONÇALVES, L. R. B. *et al.* Influence of mass transfer limitations on the enzymatic synthesis of  $\beta$ -lactam antibiotics catalyzed by penicillin G acylase immobilized on glioxil-agarose. **Bioprocess and Biosystems Engineering**, v. 31, n. 5, p. 411–418, 2008.

GONÇALVES, L. R. B.; GIORDANO, R. L. C.; GIORDANO, R. C. Effects of diffusion on the kinetics of maltose hydrolysis using glucoamylase immobilized on macroporous silica. **Brazilian Journal of Chemical Engineering**, v. 14, p. 341–346, 1997.

GUO, Z.; XU, X. Lipase-catalyzed glycerolysis of fats and oils in ionic liquids: A further study on the reaction system. **Green Chemistry**, v. 8, n. 1, p. 54–62, 2006.

HAN, P.; ZHOU, X.; YOU, C. Efficient Multi-Enzymes Immobilized on Porous Microspheres for Producing Inositol From Starch. **Frontiers in bioengineering and biotechnology**, v. 8, n. May, p. 1–9, 2020.

HWANG, E. T.; LEE, S. Multienzymatic Cascade Reactions via Enzyme Complex by Immobilization. **ACS Catalysis**, v. 9, n. 5, p. 4402–4425, 2019.

KADNIKOVA, E. N.; KOSTIĆ, N. M. Oxidation of ABTS by hydrogen peroxide catalyzed by horseradish peroxidase encapsulated into sol-gel glass. Effects of glass matrix on reactivity. **Journal of Molecular Catalysis B: Enzymatic**, v. 18, n. 1–3, p. 39–48, 2002.

KHOABI, M. *et al.* Synthesis of polyethyleneimine (PEI) and  $\beta$ -cyclodextrin grafted PEI nanocomposites with magnetic cores for lipase immobilization and esterification. **Journal of Chemical Technology and Biotechnology**, v. 91, n. 2, p. 375–384, 2016.

LAEMMLI, U. K. Cleavage of Structural Proteins during the Assembly of the Head of Bacteriophage T4. **Nature**, v. 227, p. 680–685, 1970.

LOKHA, Y. *et al.* Modulating the properties of the lipase from *Thermomyces lanuginosus* immobilized on octyl agarose beads by altering the immobilization conditions. **Enzyme and Microbial Technology**, v. 133, n. October 2019, p. 109461, 2020.

MIGNEAULT, I. *et al.* Glutaraldehyde: Behavior in aqueous solution, reaction with proteins, and application to enzyme crosslinking. **BioTechniques**, v. 37, p. 790–802, 2004.

- OLIVEIRA, U. M. F. DE *et al.* Effect of the presence of surfactants and immobilization conditions on catalysts' properties of *Rhizomucor miehei* lipase onto chitosan. **Applied Biochemistry and Biotechnology**, v. 184, n. 4, p. 1263–1285, 2017.
- ONDA, M.; ARIGA, K.; KUNITAKE, T. Activity and stability of glucose oxidase in molecular films assembled alternately with polyions. **Journal of Bioscience and Bioengineering**, v. 87, n. 1, p. 69–75, 1999.
- OTHMAN, A. M.; CORREA-DUARTE, M.; MOLDES, D. Immobilization of laccase on functionalized multiwalled carbon nanotube membranes and application for dye decolorization. **RSC Advances**, v. 6, p. 114690–114697, 2016.
- PATEL, S. K. S. *et al.* Immobilization of laccase on SiO<sub>2</sub> nanocarriers improves its stability and reusability. **Journal of Microbiology and Biotechnology**, v. 24, n. 5, p. 639–647, 2014.
- PEIRCE, S. *et al.* Development of simple protocols to solve the problems of enzyme coimmobilization. **RSC Advances**, v. 6, n. 66, p. 61707–61715, 2016.
- REKUĆ, A. *et al.* Laccase immobilization on mesostructured cellular foams affords preparations with ultra high activity. **Process Biochemistry**, v. 44, n. 2, p. 191–198, 2009.
- REN, S. *et al.* Recent progress in multienzymes co-immobilization and multienzyme system applications. **Chemical Engineering Journal**, v. 373, n. February, p. 1254–1278, 2019.
- RIOS, N. S. *et al.* Biotechnological potential of lipases from *Pseudomonas*: Sources, properties and applications. **Process Biochemistry**, v. 75, n. August, p. 99–120, 2018.
- RIOS, N. S.; ARANA-PEÑA, S.; *et al.* Reuse of Lipase from *Pseudomonas fluorescens* via Its Step-by-Step Coimmobilization on Glyoxyl-Octyl Agarose Beads with Least Stable Lipases. **Catalysts**, v. 9, n. 5, p. 487, 2019.
- RIOS, N. S.; ARANA-PEÑA, S.; *et al.* Increasing the enzyme loading capacity of porous supports by a layer-by-layer immobilization strategy using PEI as glue. **Catalysts**, v. 9, n. 7, p. 576, 2019.
- RODRÍGUEZ, M. C.; RIVAS, G. A. Assembly of glucose oxidase and different polyelectrolytes by means of electrostatic layer-by-layer adsorption on thiolated gold surface. **Electroanalysis**, v. 16, n. 20, p. 1717–1722, 2004.
- SANKAR, K. *et al.* A novel method for improving laccase activity by immobilization onto copper ferrite nanoparticles for lignin degradation. **International Journal of Biological Macromolecules**, v. 152, p. 1098–1107, 2020.
- SANTOS, J. C. S. *et al.* Bovine trypsin immobilization on agarose activated with divinylsulfone: Improved activity and stability via multipoint covalent attachment. **Journal of Molecular Catalysis B: Enzymatic**, v. 117, p. 38–44, 2015.
- SCHEIBEL, D. M.; GITSOV, I. Unprecedented Enzymatic Synthesis of Perfectly Structured Alternating Copolymers via “green” Reaction Cocatalyzed by Laccase and Lipase Compartmentalized within Supramolecular Complexes. **Biomacromolecules**, v. 20, n. 2, p. 927–936, 2019.
- SIAR, E. H. *et al.* Immobilization/stabilization of ficin extract on glutaraldehyde-activated

agarose beads. Variables that control the final stability and activity in protein hydrolyses. **Catalysts**, v. 8, n. 4, p. 149, 2018.

SILVA, J. A. *et al.* Immobilization of *Candida antarctica* lipase B by covalent attachment on chitosan-based hydrogels using different support activation strategies. **Biochemical Engineering Journal**, v. 60, p. 16–24, 2012.

SOUZA, L. T. DE A. *et al.* Immobilization of *Moniliella spathulata* R25L270 lipase on ionic, hydrophobic and covalent supports: Functional properties and hydrolysis of sardine oil. **Molecules**, v. 22, n. 10, p. 1508, 2017.

SULMAN, E. M.; MATVEEVA, V. G.; BRONSTEIN, L. M. Design of biocatalysts for efficient catalytic processes. **Current Opinion in Chemical Engineering**, v. 26, p. 1–8, 2019.

VALENCIA, P.; PINTO, M.; ALMONACID, S. Identification of the key mechanisms involved in the hydrolysis of fish protein by Alcalase. **Process Biochemistry**, v. 49, n. 2, p. 258–264, 2014.

VAZQUEZ-ORTEGA, P. G. *et al.* Stabilization of dimeric  $\beta$ -glucosidase from *Aspergillus niger* via glutaraldehyde immobilization under different conditions. **Enzyme and Microbial Technology**, v. 110, n. August 2017, p. 38–45, 2018.

VERA, M. Multienzymatic immobilization of laccases on polymeric microspheres : A strategy to expand the maximum catalytic efficiency. **Journal of Applied Polymer Science**, v. 137, n. 47, p. 49562, 2020.

VIRGEN-ORTÍZ, J. J. *et al.* Polyethylenimine: A very useful ionic polymer in the design of immobilized enzyme biocatalysts. **Journal of Materials Chemistry B**, v. 5, n. 36, p. 7461–7490, 2017.

WANG, S. *et al.* Selenium ( VI ) and copper ( II ) adsorption using polyethyleneimine-based resins : E f f e c t of glutaraldehyde crosslinking and storage condition. **Journal of Hazardous Materials**, v. 386, n. September 2019, p. 121637, 2020.

WILKE, C. R.; CHANG, P. Correlation of diffusion coefficients in dilute solutions. **AIChE Journal**, v. 1, n. 2, p. 264–270, 1955.

YAN, J. *et al.* Kinetic and thermodynamic parameters of  $\beta$ -glucosidase immobilized on various colloidal particles from a paddy soil. **Colloids and Surfaces B: Biointerfaces**, v. 79, n. 1, p. 298–303, 2010.

YU, X. *et al.* Co-immobilization of multi-enzyme on reversibly soluble polymers in cascade catalysis for the one-pot conversion of gluconic acid from corn straw. **Bioresource Technology**, v. 321, n. October 2020, p. 124509, 2021.

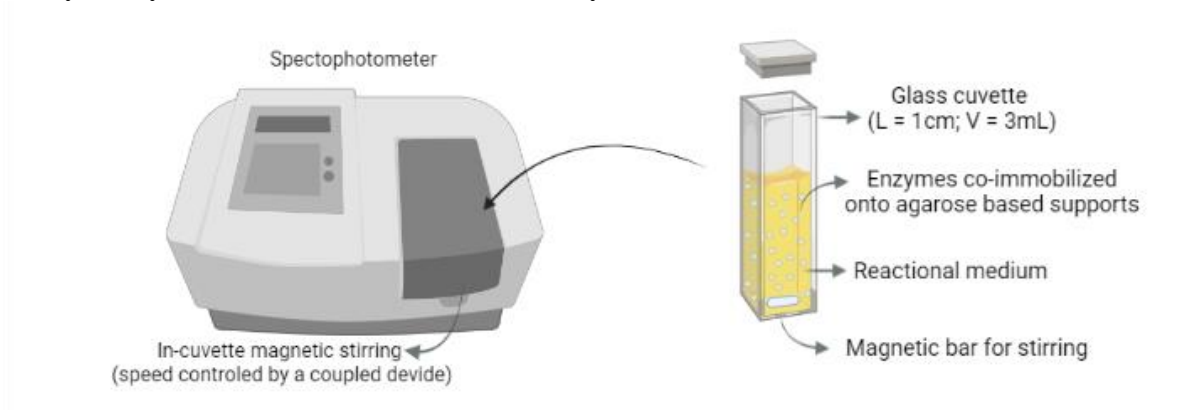
ZHANG, X. *et al.* Ionic Polymer-Coated Laccase with High Activity and Enhanced Stability: Application in the Decolourisation of Water Containing AO7. p. 1–9, 2015.

ZHANG, Y. *et al.* Synthesis of mitomycin analogs catalyzed by coupling of laccase with lipase and the kinetic model. **Journal of Chemical Technology and Biotechnology**, v. 95, n. 5, p. 1421–1430, 2020.

ZUCCA, P.; FERNANDEZ-LAFUENTE, R.; SANJUST, E. Agarose and its derivatives as supports for enzyme immobilization. **Molecules**, v. 21, n. 11, p. 1577, 2016.

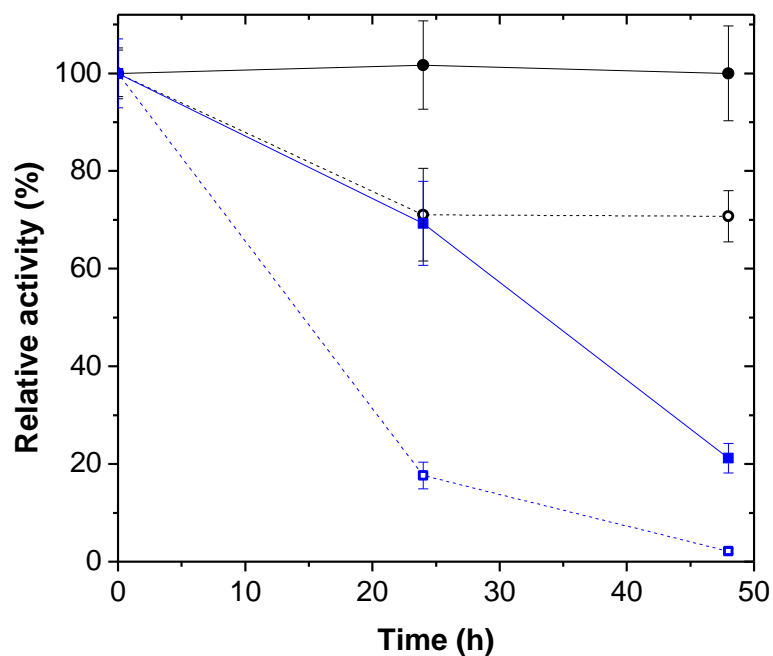
### 3.8 Supplementary Material

**Figure S3.1-** Stirred tank reactor used for monitoring initial rates (enzyme activity assay) catalyzed by the soluble and immobilized enzymes



Source: Elaborated by the author.

**Figure S3.2-** Inactivation profiles of soluble (dashed lines) and co-immobilized (solid lines) PFL (black) and laccase (blue) incubated at 50 °C (pH7) during 48 hours.



Source: Elaborated by the author.

# Chapter 4

**Chemical modifications in cellulose nanocrystalline for its application as support for lipase and laccase layer-by-layer co-immobilization**

#### 4.1 Abstract

Industrial processes usually require the use of multi-enzymatic systems to accomplish the different catalytic reactions that are a part of them. Besides the easy recovery for reutilization and higher stability, the use of co-immobilized enzymes in such multi-enzymatic processes can offer advantages in cascade reaction, decreasing the lag time of reagent diffusion between the active site of different enzymes. Frequently, the development of co-immobilized enzymes can present some drawbacks, such as limited capacity of enzyme loading and difference in the support-enzymes interactions under co-immobilization conditions, which can be overcome by using some well-ordered strategies. In this work, a layer-by-layer approach was used to co-immobilize Lipase from *Pseudomonas fluorescens* (PFL) and laccase from *Trametes versicolor* onto cellulose nanocrystalline (CNC). Firstly, PFL was adsorbed onto CNC through ionic and hydrophobic interactions. Aiming a higher PFL stabilization, CNC was functionalized with aldehyde groups through periodate oxidation or glutaraldehyde activation. FTIR analysis testified the intended chemical modifications and SEM analysis showed some morphological changes as well. After CNC functionalization, thermal stability (60 °C, pH 7) remarkably increased, from  $t_{1/2} = 0.55$  h ( $\pm 0.05$ ) to  $t_{1/2} = 9.86$ h ( $\pm 1.94$ ). Among the functionalized CNCs, CNC<sub>ox</sub> (oxidized CNC) showed the best capacity to retain higher PFL loads, and then it was chosen to proceed with the co-immobilization. For that, PFL-CNC<sub>ox</sub> was covered with polyethyleneimine (PEI), then laccase was co-immobilized, and so a final crosslinking step using glutaraldehyde was performed to covalently attach the enzymes to the support. Co-immobilized enzymes presented higher thermal stability (50 °C) than soluble ones; immobilized laccase retained 61.05% of its activity after 24 hours and PFL about 90% after 48 hours of deactivation. In the operational stability assays, the heterogeneous biocatalysts maintained more than 45% of their activities after 5 cycles. These co-immobilized enzymes represent a potential multi-active heterogeneous biocatalyst to be used in cascade reactions of industrial interest.

**Keywords:** PFL, laccase, chemical modifications, co-immobilization, cellulose activation.

## 4.2 Introduction

Lipases are a class of enzymes broadly employed in several bioprocesses of industrial interest and can catalyze the synthesis of products for energy, food, and pharmaceutical industries. Because of their relevant potential, they are considered some of the most popular enzymes in bioprocess (Arana-Peña, Carballares, Corberan, *et al.*, 2020; Rios, Mendez-Sanchez, *et al.*, 2019; Soni *et al.*, 2018). Laccases also have shown increasing importance because of their promising applications (Kołodziejczak-Radzimska *et al.*, 2020). They are a class of enzymes widely applied in the oxidation of some polyphenols and aromatic in several areas, such as bioremediation, food and textile industries, bioethanol productions, biosensor development, and others (Guerberoff e Camusso, 2019; Pramanik *et al.*, 2019). Literature reports the tandem use of lipase and laccase in several areas, such as the synthesis of perfectly structured copolymers and enantiomerically enriched dimers, development of biosensors, and synthesis of pharmaceuticals, among others (Gavezzotti *et al.*, 2011; Naseri *et al.*, 2018; Scheibel e Gitsov, 2019; Zhang *et al.*, 2019).

Some of the enzyme properties need to be improved to be applicable under certain process conditions. The immobilization allows the enhancement of several enzyme properties, such as stability and specificity (Santos, J. C. S. dos, Rueda, Nazzoly, *et al.*, 2015), and better preservation of the catalytic activity under harsh conditions (Elias *et al.*, 2018). As the immobilization may produce a heterogeneous biocatalyst, it allows easy separation of the enzyme from the reaction medium and, therefore, its recovery for reuse, which may decrease the process costs (Santos, J. C. S. dos, Rueda, Nazzoly, *et al.*, 2015). Indeed, enzyme immobilization is a requirement for several industrial applications. When more than one enzyme is required for a particular process — cascade reactions or transformation of different substrates, for example — such enzymes can be co-immobilized to produce a multi-active biocatalyst (Jin *et al.*, 2018). Co-immobilization processes have increasingly been the subject of research for developing new biocatalysts because of the potential use of them in reactions of industrial interest (Arana-Peña *et al.*, 2019; Jin *et al.*, 2018). The use of co-immobilized enzymes may benefit the reaction rate by decreasing the lag time in cascade reactions, protecting the main enzyme from bacteria attack, simplifying the bio-reactor design, etc. (Arana-Peña *et al.*, 2019; Torres e Batista-Viera, 2019). Literature reports the successful co-immobilization of different enzymes using a layer-by-layer strategy, where one enzyme is immobilized over another previously immobilized enzyme (Arana-Peña, Carballares, Corberan, *et al.*, 2020; Arana-Peña, Rios, *et al.*, 2020).



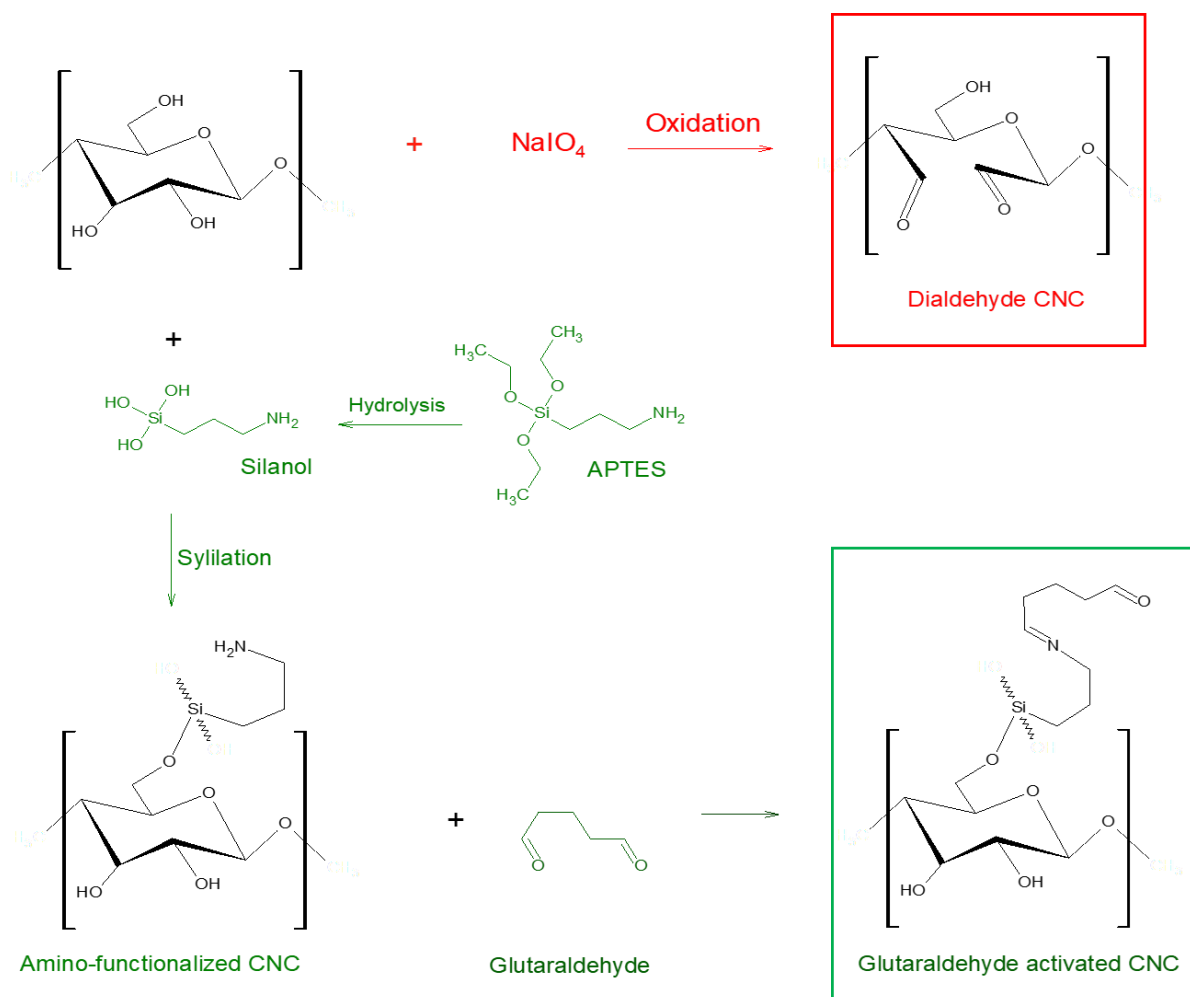
The success of an immobilization process for a particular enzyme is also closely connected to the choice of the support, modification/functionalization, and immobilization conditions. The use of nanocellulose crystalline as support for enzyme immobilization allows the production of a bioactive material with the advantageous characteristics of a resistant nanomaterial, besides properties of biocompatibility and low cytotoxicity provided by cellulose (Manan *et al.*, 2016). Enzymes can be immobilized onto CNC by physical or chemical mechanisms, depending on the interactions between the cellulose chain and the biomolecule or even on the ligand attached to the CNC and molecular forces allowing the binding formation (Uth *et al.*, 2014). CNC can be chemically modified by different processes (Habibi, 2014) or functionalized through the activation of the hydroxyl groups to further immobilize enzymes by covalent bonds (Sulaiman *et al.*, 2014). Each modification may allow a different interaction of the CNC with the enzyme putting it in a specific orientation. This way, one can produce heterogeneous biocatalysts with distinct characteristics, such as activity, specificity, and stability (Mohamad *et al.*, 2015; Siar *et al.*, 2017).

The use of aldehyde functionalized supports has been proposed as an attractive way to stabilize enzymes in immobilization processes (Cai *et al.*, 2018; Poppe *et al.*, 2013; Rodrigues *et al.*, 2008). Some modifications were explored in this work to obtain aldehyde functionalized CNCs: CNC oxidation and glutaraldehyde activation (Fig. 4.1). Sodium periodate has been widely studied as an oxidant able to selectively cleave the C<sub>2</sub>-C<sub>3</sub> bond of the cellobiose ring to form a "dialdehyde cellulose", (Liu *et al.*, 2012; Vicini *et al.*, 2004; Yang, Chen e Ven, van de, 2015). This oxidized CNC can be employed to immobilize enzymes through stronger interactions by forming covalent bonds with the amino groups of the enzyme residues (Schiff base), enabling a higher stabilization of these biomolecules (Nikolic *et al.*, 2010). Also, glutaraldehyde is an activation agent widely applied for the immobilization of several enzymes and has presented relevant results in studies involving different lipases (Ait Braham *et al.*, 2019; Barbosa *et al.*, 2012, 2014; Hrydziuszko *et al.*, 2019; Monteiro *et al.*, 2019; Zaak *et al.*, 2017). Glutaraldehyde activated supports can interact covalently with the enzymes in order to produce a more stable biocatalyst (Barbosa *et al.*, 2014). Firstly, to activate CNC with glutaraldehyde, this material is silylated, which could be reached by reacting it with APTES (3-aminopropyltriethoxysilane), for example. This modification allows the insertion of amine groups, present in the reagent containing silane, to react then with glutaraldehyde (Khanjanzadeh *et al.*, 2018).

Although periodate oxidation and glutaraldehyde activation insert aldehyde groups in cellulose, these two functionalization strategies may affect the biocatalyst differently due to

the length of space arms between the enzyme and the support. Then, immobilized enzymes may present different characteristics, depending on their length and their nature. A longer spacer arm may involve a higher area of the protein interacting with the support and can favor multi-point binding (Santos, J. C. S. Dos, Barbosa, Oveimar, *et al.*, 2015). The long spacer arm also enables the movement of the enzyme always from the support surface, reducing steric hindrances during catalysis. In general, a shorter one avoids higher mobility of the enzyme, allowing a better stabilization of the molecule under severe conditions. (Sulaiman *et al.*, 2014; Xia *et al.*, 2016). Besides being dependent on the length of the spacer arm, the properties of immobilized enzymes depend on other characteristics of it (hydrophobicity and presence of charge, for example). These characteristics of the spacer arm can make it behave as an heterofunctional carrier, establishing different kinds of interactions with the enzyme (Barbosa *et al.*, 2014; Meryam Sardar, 2015). This establishment of different types of interactions can minimize the enzyme release from the support (those only adsorbed) under some conditions in which hydrophobic or ionic interactions, for example, can be ceased. Fig. 4.1 shows that the two aldehydes functionalized CNC are very different in length and characteristics of the space arms. The one finishing with glutaraldehyde the longer and having the higher diversity of groups. Then, the enzyme immobilization using these different supports may produce insoluble biocatalyst with distinct properties.

Figure 4.1 – Aldehyde functionalization of CNC using two different chemical modifications. In red, cellulose oxidation by sodium periodate leads to the glucopyranoside ring's cleavage and the introduction of two aldehyde groups, forming a “dialdehyde cellulose” (CNCox). In green, the preparation of an aminated cellulose through the silane grafting of cellulose using 3-aminopropyltriethoxysilane (APTES) is followed by the glutaraldehyde activation of the aminated cellulose. Elaborated by the author.



Source: Elaborated by the author.

In this paper, cellulose nanocrystalline was obtained from cellulose microcrystalline and then activated by different reactions to be used as support for PFL and laccase co-immobilization. A layer-by-layer strategy was used for the co-immobilization process. This strategy proposed first the immobilization of PFL onto the support as the first step. Then, the interactions established between PFL and CNC and activated CNC were analyzed. After a trial, a functionalized CNC was chosen to proceed with the co-immobilization. Following the first step of the co-immobilization process, a PEI (polyethyleneimine) layer covering PFL immobilized allowed the immobilization of the second enzyme — laccase. The use of PEI is related in literature to the co-immobilization of several enzymes able to be attached

by ionic exchanges onto this polymer (Arana-peña, Rios, Mendez-sanchez, *et al.*, 2020; Peirce *et al.*, 2016; Rios, Arana-Peña, *et al.*, 2019). Since PEI is a polycationic polymer (Arana-Peña, Rios, *et al.*, 2020), and the isoelectric point of both enzymes are around pH 4 (Rios *et al.*, 2018; Xia *et al.*, 2016), the ionic interactions between PEI (working as a glue) and the enzymes were established at pH 7. Also, the combined use of PEI with glutaraldehyde crosslinking is reported in literature as necessary to prevent enzyme release (Arana-Peña, Carballares, Berenguer-Murcia, *et al.*, 2020; Arana-Peña, Rios, *et al.*, 2020; Rios, Arana-Peña, *et al.*, 2019). Then, the whole process was concluded with glutaraldehyde crosslinking. Applying this layer-by-layer strategy, a multi-active and thermally stable heterogeneous biocatalyst could be obtained and was used in recycles of reactions performed by the enzymes.

### **4.3 Experimental**

#### **4.3.1 Materials**

Lipase from *Pseudomonas fluorescens*, *p*-nitrophenyl butyrate (*p*-NPB), laccase from *Trametes versicolor*, 2,2'-Azino-bis (3-ethylbenzothiazoline-6-sulfonic acid) diammonium salt (ABTS), 3-aminopropyltriethoxysilane (APTES) and glutaraldehyde were purchased from Sigma-Aldrich. Cellulose microcrystalline (for thin-layer chromatography) was obtained from Vetec. All other chemicals used were of analytical grade.

#### **4.3.2 CNC preparation**

Cellulose nanocrystals (CNC) were prepared from microcrystalline cellulose (MCC) according to (Shankar e Rhim, 2016) and (Adsul *et al.*, 2012) with some modifications. First, MCC is treated with NaOH and urea according to a protocol reported in the literature for cellulose dissolution (Kamida *et al.*, 1984; Zhou e Zhang, 2000). 5 grams of MCC were added into 100mL of an aqueous solution containing NaOH 7% (w/w) and urea 12% (w/w). Initially, the mixture was stirred for 30 min at 25 °C, then kept at -16 °C for 16 h in a cooling chamber. After that, the cellulose was regenerated by adding excess (approximately 1L) of deionized water. The mixture was stirred at 7000 rpm for 5 minutes and separated by centrifugation at 4500 rpm for 10 min. This procedure of water addition, mixing, and centrifugation was repeated for the NaOH and urea removal until the pH of the mixture achieved the pH of deionized water.

Afterward, the mixture was ultrasonicated (UIP1500hdT) two times for 5 min at 75% amplitude and then centrifuged at 13000 rpm for 10 min. The prepared CNC was stored at 4 °C.

#### 4.3.3 CNC oxidation and quantification of aldehyde groups

The hydroxyl groups of CNC were oxidized to aldehyde groups, according to a protocol described in the literature (Sun *et al.*, 2015) with some modification. Concentrations of 250, 500, and 1000  $\mu\text{mol NaIO}_4/\text{g}$  of CNC were tested. In this cellulose modification, high excess of periodate should be avoided in order to prevent an undesired overoxidation (Martins De Oliveira *et al.*, 2021; Siller *et al.*, 2015). 1 gram of a previously dried (under vacuum) CNC was added to 10 mL of a sodium periodate solution, and the pH was set (3 or 5) using acetic acid 36% (v/v). The mixture was kept under agitation for 5 hours in the absence of light. After the oxidation reaction, the mixture was centrifuged and washed with abundant distilled water and dried under vacuum. The CNC activated by oxidation (CNCox) was stored at 4 °C, and the supernatant was used for the aldehyde group quantification.

The aldehyde groups generated by hydroxyl group oxidation were determined according to the literature (Guisán, 1988), with some modifications. It was carried out by analyzing the supernatant of the oxidation reaction since the aldehyde group formation is related to the periodate consumption. The periodate ( $\text{IO}_4^-$ ) that remained in the solution may react with potassium iodide to form iodine, which can be colorimetrically detected for the intensity of its color is proportional to its concentration in the medium. For that, firstly, R, a solution source of iodide (X), was prepared from the mixture (1:1) of a saturated  $\text{NaHCO}_3$  with a 10% (w/v) potassium iodide. 100  $\mu\text{L}$  of the periodate solution (before being used for the CNC oxidation) added to 3mL of solution A was used as the Standard Solution, and a wavelength ( $\lambda$ ) was selected when the absorbance of this standard solution ( $\text{Abs}_{\text{standard}}$ ) was near to 0.7. A solution containing 100  $\mu\text{L}$  of distilled water added to 3mL of solution A was used to blank the spectrophotometer. Periodically, 100  $\mu\text{L}$  of the supernatant solution of the CNC oxidation mixture were withdrawn, added to 3mL of solution A and its absorbance was detected ( $\text{Abs}_{\text{sample},t}$ ) at the wavelength previously selected. The aldehyde (CHO) quantification was calculated using the Equation 4.1, as follows:

$$C_{\text{CHO}_t} (\mu\text{mol}/\text{g}) = 2 * C_{\text{IO}_4^-} (\mu\text{mol}/\text{g}) * \left( 1 - \frac{\text{Abs}_{\text{sample},t}}{\text{Abs}_{\text{standart}}} \right) \quad (4.1)$$

Where  $C_{\text{CHO}}$  is the concentration of aldehyde groups per gram of CNC, proportional to the consumption of periodate (represented in the equation by the relative  $\text{Abs}_{\text{sample},t}$  decay), and  $C_{\text{ClO}_4^-_0}$  is the initial concentration of periodate per gram of CNC.

#### **4.3.4 CNC activation with glutaraldehyde**

According to the literature, CNC was first modified by a silylation reaction using APTES (3-aminopropyltriethoxysilane) (Khanjanzadeh *et al.*, 2018). 5 mL of APTES was added to 100mL of ultrapure water under stirring, and the solution was adjusted to pH 4 using glacial acetic acid. Then, 1 g of CNC was added to the adjusted solution, and the mixture was stirred for 2 hours, at 25 °C. After, the mixture was centrifuged (4000 rpm, 10 min) and washed 2 with ultrapure water. In order to promote the reaction, the precipitate was put in an oven at 105 °C for 15 min. After, in order to remove all remained reagents, this precipitate was washed two times (again with centrifugation) using ethanol 96% and one time with ultrapure-Q water. According to the methodology in literature (Rodrigues *et al.*, 2008), this final precipitate was activated with glutaraldehyde by modifying the amino groups inserted on the CNC chain after reaction with APTES. 1g of CNC modified with APTES was put to react with 10 mL of a 5% glutaraldehyde solution (prepared in a 100mM sodium phosphate buffer pH 7) for 1 h, at room temperature, under stirring. After, the solid was washed with abundant distilled water and dried under vacuum. Then, the glutaraldehyde-activated CNC (CNC-GA) was stored at 4 °C.

#### **4.3.5 CNC and functionalized CNC characterization**

All the samples were previously lyophilized for all characterization assays. Morphology of Cellulose microcrystalline (MCC), cellulose nanocrystalline (CNC) and activated CNCs were analyzed with micrograph images obtained via SEM (FEG Quanta 450). EDS (Energy dispersive X-Ray Spectroscopy) spectra were used to investigate compositional information (chemical elements) of the materials. CNC and activated CNC were also characterized by Fourier Transform infrared spectroscopy (FTIR) in order to analyze chemical modification caused by the different transformations studied in this work. An accessory Golden Gate Single Reflection Diamond ATR System was used, and the measurement of Transmittance was detected in the range of 4000 – 640  $\text{cm}^{-1}$ . Using the ratio of the absorbance of band at 1430  $\text{cm}^{-1}$  (known as “crystallinity band”) to the band at 893  $\text{cm}^{-1}$  (known as “amorphous band”) it

was possible to calculate the crystallinity index (CI) for unmodified CNC and functionalized CNC (Adsul *et al.*, 2012; Ciolacu *et al.*, 2011). Absorbance values were obtained according to Equation 4.2 (Jelle e Hovde, 2012):

$$A = \log_{10}\left(\frac{1}{T}\right) \quad (4.2)$$

Where A is absorbance and T is transmittance.

#### ***4.3.6 Determination of enzyme activity, protein concentration, and some immobilization parameters***

For PFL, protein concentration determination was performed using the Bradford method and bovine serum albumin as the reference standard (Bradford, 1976). To determine PFL activity, a hydrolysis reaction using p-Nitrophenyl butyrate (100mM *p*-NPB prepared in acetonitrile) as substrate was performed at 25 °C according to literature, with slight modifications (Rodrigues *et al.*, 2009). 50µL of substrate solution were added to 2.5 mL of sodium phosphate buffer pH 7 (25 mM) and 50µL of enzymatic solution. The formed product, p-nitrophenol, was quantified using a spectrophotometer at 348 nm. The activity was given in U<sub>NPB</sub>, which corresponds to the number of enzymes able to hydrolyze 1µmol of *p*-NPB per minute at 25 °C.

The determination of protein concentration for laccase was performed using the BCA (bicinchoninic acid reagent) Protein Assay kit from Thermo Fisher Scientific (Rockford, Illinois, United States). The quantification was realized in a spectrophotometer at 562 nm, using Bovine serum albumin as standard (P.K.Smith *et al.*, 1985). Laccase activity was quantified by the oxidation of 3mM 2,2'-Azino-bis (3-ethylbenzothiazoline-6-sulfonic acid diammonium salt (ABTS), according to literature (Addorisio *et al.*, 2013) with some modifications. The oxidation was quantified by using spectrophotometer at 418nm. ABTS oxidation was performed in 10 mM acetate buffer at pH 4.5 containing 1mM CuSO<sub>4</sub>·5H<sub>2</sub>O at 25 °C, and the activity was given in U<sub>ABTS</sub> (1 U<sub>ABTS</sub> = amount of enzymes able to oxidize 1µmol of ABTS per minute at 25 °C).

Immobilization yield (IY - %), theoretical activity (TA – U<sub>NPB</sub> /g) and recovered activity (RA - %) were calculated by equations 4.3, 4.4 and 4.5 (Rios, Neto, *et al.*, 2019; Silva *et al.*, 2012), respectively.

$$IY (\%) = \frac{(Actv_i - Actv_f)}{Actv_i} * 100\% \quad (4.3)$$

$$TA (U/g) = Actv_{off} * \frac{IY}{100} \quad (4.4)$$

$$RA (\%) = \frac{Atv_{biocat.}}{TA} * 100 \quad (4.5)$$

Where  $Actv_i$  and  $Actv_f$  represent the activity ( $U_{pNPB}$  /mL for PFL or  $U_{ABTS}$ /mL for laccase) of the immobilization solution before and after the immobilization. The value of  $Actv_{off}$  (activity offered to the immobilization per gram of support,  $U_{pNPB}$  /g or  $U_{ABTS}$ /g) can be obtained by multiplying the initial activity ( $Actv_i$ , in  $U_{pNPB}$  /mL or  $U_{ABTS}$ /mL) by 10 (which is the ratio between enzyme solution, in mL, and mass of support, in g).  $Atv_{biocat.}$  represents the measured activity of the heterogeneous biocatalyst obtained from the enzyme immobilization.

#### 4.3.7 PFL and laccase co-immobilization

Initially, several tests of PFL immobilization were performed before the co-immobilization of laccase. For PFL immobilization onto CNC or activated CNCs (CNCox and CNC-GA), 1 g of support was added to 10 mL of a solution containing a specific protein load.  $1.7 \text{ mg}_{\text{protein}}/\text{g}_{\text{support}}$  was used for initial immobilizations and higher amounts — 5, 10, and 20  $\text{mg}_{\text{protein}}/\text{g}_{\text{support}}$  — for the tests of protein load increase. The immobilization solutions were prepared using 5mM Sodium phosphate buffer at pH 7 (Rios, Arana-Peña, *et al.*, 2019). The immobilization tests in the presence of salt were performed by adding NaCl 200mM to the enzyme solution. For the study of the influence of the surfactant during the immobilization, 0.1% Triton-X was added to the enzyme solution. After stirring support and enzyme solutions during the desired time, the heterogeneous biocatalysts were washed with an excess of distilled water and stored at 4 °C. For the immobilization course analysis, samples of the mixture were periodically withdrawn, and after centrifugation, the activities of supernatants were determined. Thus, a decrease in the activity of supernatant represented that the enzyme molecules were getting attached to the support by different kinds of interactions, depending on the condition and support.



PFL and laccase were then co-immobilized onto CNCox-250 (CNC oxidized using 250  $\mu\text{mol NaIO}_4/\text{g}$  of CNC). The co-immobilization was carried out through 4 steps by using a layer-layer strategy. Firstly, PFL was immobilized onto CNCox-250 at pH 7 (5 mM sodium phosphate buffer) by mixing the enzyme solution with the mass of support during the desired time and then washed with abundant distilled water (using centrifugation) to obtain CNCox-250-PFL. In order to attach the second enzyme layer, this biocatalyst was covered with PEI 10% (pH 7) by mixing the mass of the biocatalyst with PEI solution at 4 °C and 70 rpm overnight (Arana-Peña, Carballares, Berenguer-Murcia, *et al.*, 2020; Arana-Peña, Rios, *et al.*, 2020; Rios, Arana-Peña, *et al.*, 2019). After this process, the mass was washed with abundant distilled water (again with centrifugation). Laccase was then co-immobilized onto this last biocatalyst (CNCox-250-PFL-PEI). Laccase immobilization was performed at pH 7 (5mM sodium phosphate buffer with 1mM  $\text{CuSO}_4 \cdot 5\text{H}_2\text{O}$ ) by mixing the mass of the previous heterogeneous biocatalyst with the enzyme solution during a particular time and after washing it with abundant distilled water (with centrifugation) (Baldrian e Gabriel, 2002; Sankar *et al.*, 2020). This last biocatalyst was called CNCox-250-PFL-PEI. As a final step, glutaraldehyde crosslinking of the co-immobilized enzymes was performed using 1% glutaraldehyde (prepared in 50mM sodium phosphate pH 7) (Arana-Peña, Rios, *et al.*, 2020). This last biocatalyst (CNCox-250-PFL-PEI-Lac-GA) was then washed and stored at 4 °C.

#### **4.3.8 Desorption**

Desorption assays were performed by putting the heterogeneous biocatalysts obtained from immobilization (24 hours) of PFL onto different supports in contact with specific solutions for analyzing the desorption of the enzyme molecules. For desorption in NaCl, a solution containing 1M of NaCl was prepared in a 5mM sodium phosphate buffer and adjusted to pH 7. For desorption in the presence of detergent, a solution containing 1% Triton-X was prepared with the same buffer and adjusted to pH 7. A control assay was also performed where the solution was constituted only by the 5mM sodium phosphate buffer at pH 7. The ratio between the heterogeneous biocatalyst and solution was 1:10 (g/mL) for all the desorption tests. After 2 hours at 25 °C under stirring, the mixture was centrifuged, and the supernatant and heterogeneous biocatalyst activity was determined.

#### **4.3.9 Thermal Stability**

The thermal stability of PFL immobilized onto the studied supports was performed at 60 °C in a 50 mM Tris-HCl buffer pH 7. For that, samples were periodically withdrawn, and the activity of the heterogeneous biocatalyst was determined. For the calculation of relative activity (%), the activity of the heterogeneous biocatalyst at the beginning of the assay was considered 100%.

#### ***4.3.10 Operational stability of the co-immobilized enzymes***

Repeated batches of pNPB hydrolysis and ABTS oxidation were performed using PFL and laccase co-immobilized onto oxidized CNC (CNCox-250) in order to analyze the operational stability of the multi-active heterogeneous biocatalysts. For that, a mass of the produced biocatalyst was put to catalyze 5 consecutive cycles of the specific reaction. To analyze the operational stability of co-immobilized PFL, a mass of biocatalyst was placed to react under the same conditions already described for pNPB hydrolysis. After each cycle, the biocatalyst was washed 3 times (using centrifugation) and used again to catalyze pNPB hydrolysis using a new substrate preparation. For co-immobilized laccase, the conditions used were the same ones described for ABTS oxidation. Also, after each cycle, the biocatalyst was washed (3 times, with centrifugation) and put to work with a new substrate preparation.

#### ***4.3.11 Statistical analysis***

One-way analysis of variance (ANOVA) test was used to detect significant differences. ANOVA test was performed by using Origin and  $P < 0.05$  was accepted as a significant difference.

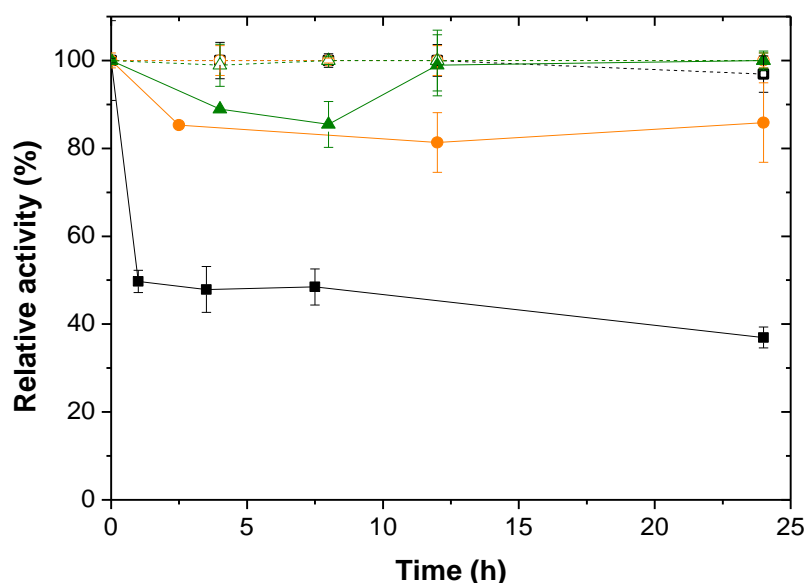
### **4.4 Results and Discussion**

The general purpose of this work was to use a nanocrystalline cellulose-based material as support for lipase and laccase co-immobilization through a layer-by-layer strategy. In this strategy, the first immobilization was conducted using lipase, followed by a PEI layer to allow the laccase immobilization, and the final step of glutaraldehyde crosslinking. For that, it was necessary to understand the interactions that could be established between the cellulose and the first enzyme layer (lipase from *Pseudomonas fluorescens*, PFL)

#### 4.4.1 PFL immobilization onto unmodified CNC

Initially, PFL was immobilized onto unmodified CNC at pH 7 using 1.7 mg<sub>protein</sub>/g<sub>support</sub> of protein load. The immobilization was expected to be only by adsorption since the support was not yet activated to form covalent bonds. Because different physical interactions could allow this adsorption, the nature of the adsorption could be analyzed by changing the environment of the immobilization process (Barbosa *et al.*, 2015). For that, immobilization courses in three different conditions were monitored, by measuring the activity of the supernatant during immobilization, for 24 hours, as shown in Fig 4.2. Firstly, a PFL immobilization using only a 5mM sodium phosphate buffer was conducted, in which different interactions could cause the PFL adsorption. Secondly a PFL immobilization was performed in the presence of salt by adding 200 mM NaCl to the 5mM sodium phosphate buffer to avoid ionic interactions between the support and the enzyme (Ait Braham *et al.*, 2019). Finally, immobilization was conducted in the presence of a surfactant by adding 1% Triton-X to the 5mM sodium phosphate buffer (with no addition of 200 mM NaCl). The use of a surfactant should avoid hydrophobic interactions between PFL and the support by the well-known phenomena of lipase interfacial activation (Barbosa *et al.*, 2013).

Figure 4.2 - Immobilization course of PFL onto CNC conducted at pH 7 (1.7 mg<sub>protein</sub>/g<sub>support</sub> Of protein load). A solution containing soluble PFL at the pH of immobilization (7) was used as reference (dashed lines); solid lines represent the supernatant of PFL immobilization onto CNC at different conditions: using only a 5mM sodium phosphate buffer (■), with the addition of NaCl 200mM (●) or with the addition of 1% Triton-X (▲).

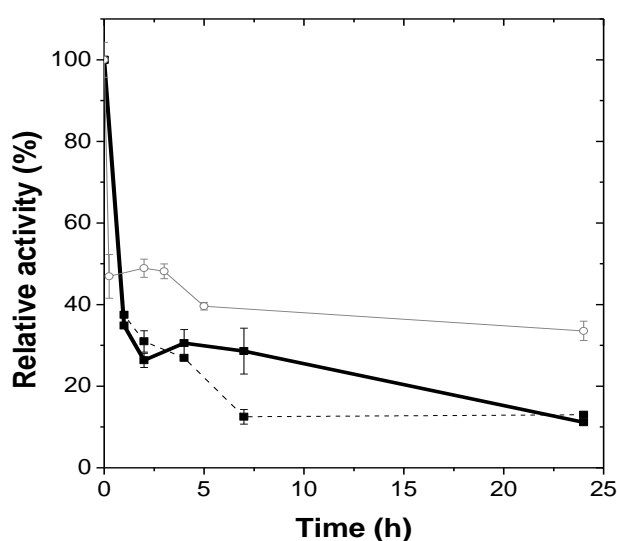


Source: Elaborated by the author.

When the PFL immobilization was performed with no additives, about 50% of the enzyme was immobilized after the 1 hour, and after 24h, the immobilization yield reached nearly 60%. With the addition of a concentrated salt in the immobilization solution (NaCl 200 mM), more enzyme molecules remained in the supernatant, and the immobilization yield was around 15% in 24 hours. The addition of a surfactant (1% Triton-X) promoted a similar behavior, and most enzyme molecules remained in the solution. In the points  $t = 12\text{h}$  and  $t = 24\text{h}$ , ANOVA tests showed no significant difference between the immobilization course in the presence of NaCl and Triton. This difference in the immobilization course caused by the addition of the salt (NaCl) or the surfactant (Triton) indicates that both ionic and hydrophobic interactions contributed to the first immobilization (in the presence of buffer only), that is to say, enzyme adsorption on unmodified CNC.

Knowing that the thermal stability is an essential characteristic of a biocatalyst for its industrial application, a thermal deactivation ( $60\text{ }^{\circ}\text{C}$  and  $\text{pH } 7$ ) of the biocatalyst produced from the PFL immobilization onto CNC with no additives was performed. Two biocatalysts were tested, the first one obtained after 2 hours of immobilization (activity of  $6.98\text{ U}_{\text{pNPB}}/\text{g}_{\text{biocatalyst}} \pm 0.77$ ) and the second one obtained after 7 hours of immobilization (activity of  $7.95\text{ U}_{\text{pNPB}}/\text{g}_{\text{biocatalyst}} \pm 0.79$ ). The results of the thermal stability analysis during 24 hours are shown in Fig. 4.3. The inactivation of soluble PFL under the same conditions was also analyzed for comparison purposes.

Figure 4.3 – Stability at  $60\text{ }^{\circ}\text{C}$  and  $\text{pH } 7$  (50mM Tris-HCl buffer) of soluble PFL ( $\circ$ ) and PFL immobilized onto unmodified CNC ( $\blacksquare$ ). Heterogeneous biocatalysts were obtained after 2 hours of immobilization (solid black line) and 7 hours of immobilization (dashed black line).



Source: Elaborated by the author.

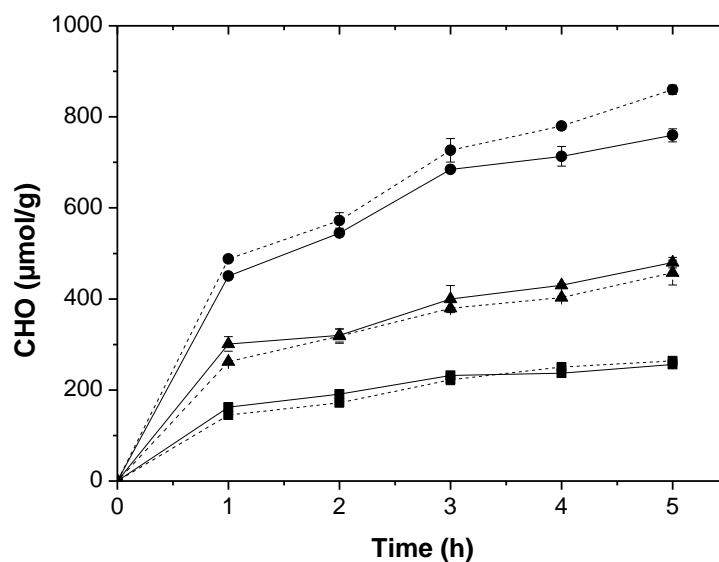
A rapid inactivation of the enzymes immobilized onto CNC with both immobilization times was observed. Half-lives of both biocatalysts were smaller than 1 hour —  $t_{1/2} = 0.55$  h ( $\pm 0.05$ ) for 2 h and  $t_{1/2} = 0.75$  h ( $\pm 0.06$ ) for 7 h of immobilization, which are not significantly different according to statistical tests. ANOVA tests also showed no significant difference in the deactivation profiles of both heterogeneous biocatalysts. Therefore, one can consider that this immobilization time increase has no influence in the enzyme stability. This result may be attributed to the type of interactions established between the support and the enzyme, which were unable to stabilize and keep the active form of the immobilized molecules of PFL (Jesionowski, Zdarta e Krajewska, 2014). Comparing the heterogeneous biocatalysts with the soluble PFL, it was observed that the immobilization of this lipase onto unmodified CNC decreased its thermal stability. Literature reports that some enzymes may present groups that are crucial for some characteristics of this protein, such as activity, selectivity and also stability (Rueda *et al.*, 2016). Because of the interactions between enzyme and support, immobilization can affect some of these key groups (that can be part of the active site, for example), exposing them to the medium, which can decrease the enzyme stability (Rodrigues, Berenguer-Murcia e Fernandez-Lafuente, 2011; Siar *et al.*, 2017). In order to obtain insoluble biocatalyst with higher stabilities, different interactions between enzyme and support should be enabled, which could be reached by changing the nature of the support. Then, some chemical modifications of CNC were searched to introduce groups able to establish covalent bonds between the PFL and support.

#### ***4.4.2 CNC functionalization with aldehyde groups and characterization***

Some chemical treatments were tested to modify CNC in order to introduce aldehyde groups on its surface, able to interact with PFL. These groups were introduced by two protocols: periodate oxidation and silylation followed by glutaraldehyde activation.

In the first protocol, sodium periodate was used to oxidize the hydroxyl groups of CNC and form aldehyde groups that could react covalently with the enzyme (Nikolic *et al.*, 2010). Different concentrations of sodium periodate were tested — 250, 500, and 1000 ( $\mu\text{mol NaIO}_4/\text{g}$  of CNC) — and the reactions were performed at pH 3 and 5, at room temperature. In this reaction, usually conducted under acidic conditions, each mole of  $\text{NaIO}_4$  consumed generates 2 moles of aldehyde group (Chemin *et al.*, 2016). Fig. 4.4 shows the influence of the initial periodate concentration and pH on the generation of aldehyde groups along the 5 hours of reaction.

Figure 4.4 - Influence of the initial  $\text{NaIO}_4$  concentration on the aldehyde content in the oxidized CNC, expressed in  $\mu\text{mol}$  of CHO per gram of CNC. Tested concentrations: 250 ( $\blacksquare$ ), 500 ( $\blacktriangle$ ), and 1000( $\bullet$ )  $\mu\text{mol NaIO}_4/\text{g}$  of CNC at pH 3 (solid lines) and pH 5 (dashed lines). The proportion of  $1\text{g}_{\text{CNC}}/10\text{mL}_{\text{NaIO}_4}$  solution was used.



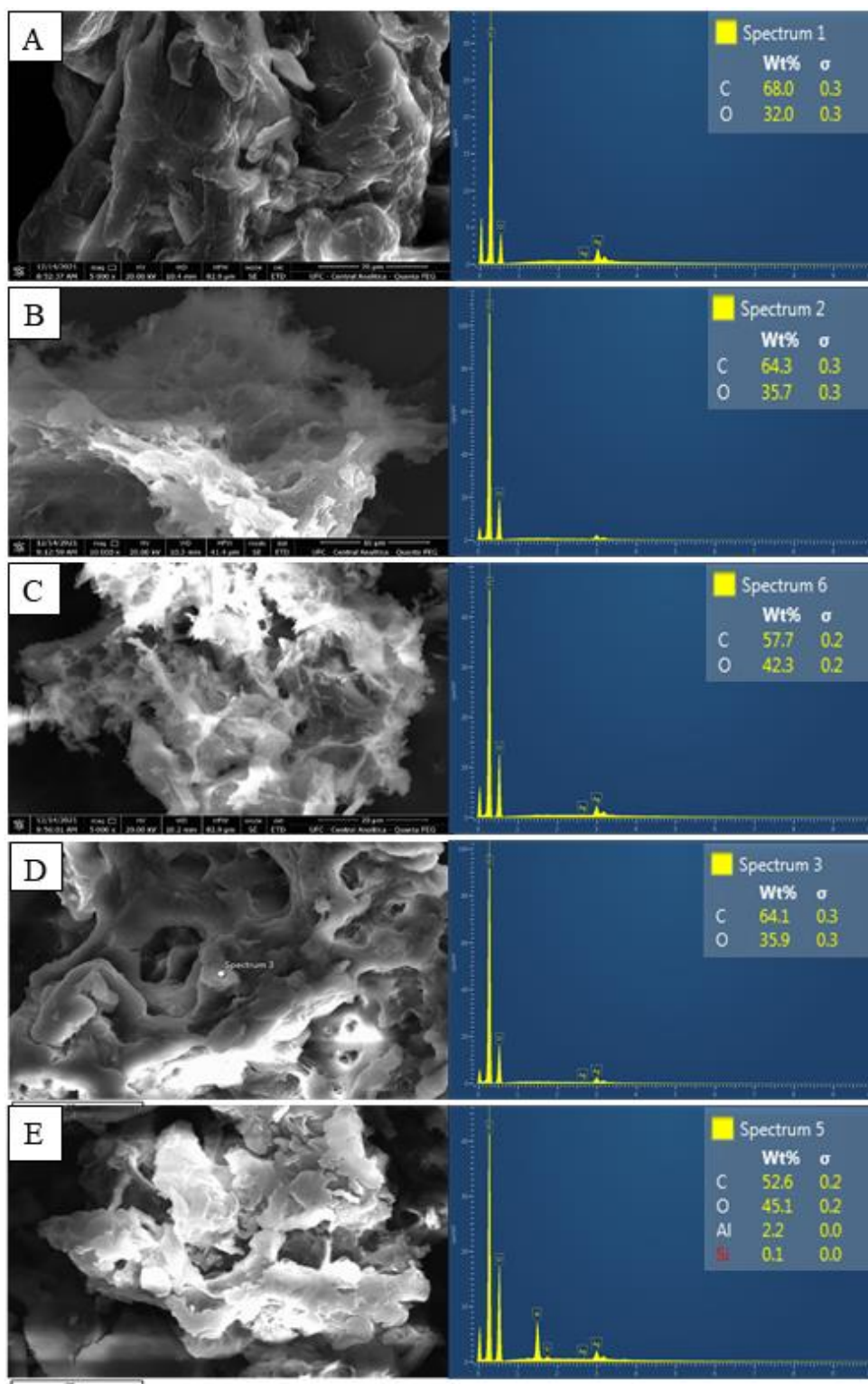
Source: Elaborated by the author.

The  $\text{NaIO}_4$  concentration has an expressive effect on the aldehyde content since it could be increased from 457.9 to 859.8  $\mu\text{mol CHO/g}$  of oxidized CNC when the initial concentration rose from 500 to 1000  $\mu\text{mol NaIO}_4/\text{g}$  of CNC with 5 hours of oxidation, at pH 5. The oxidation rate is also affected by the oxidant concentration, the aldehyde content (CHO) increases with the increase in  $\text{NaIO}_4$  concentration. After 3-4 hours, the oxidation rate shows a relevant deceleration (more expressive using 1000  $\mu\text{mol NaIO}_4/\text{g}$  of CNC), which is also reported in the literature to other cellulosic materials, and the aldehyde content become almost constant in some cases (Nikolic *et al.*, 2010). Overall, the effect of the pH was not relevant concerning the aldehyde content since ANOVA tests showed no significant difference between pHs in most of the points shown in the curves of Fig. 4.4. Then, the oxidized supports obtained at pH 5 (the mildest one) was chosen for the next experiments. The oxidized CNC was named as CNCox.

The second CNC activation studied was using glutaraldehyde. Firstly, a chemical modification of CNC was performed by silylation using APTES (3-aminopropyltriethoxysilane). Then, this support was activated by glutaraldehyde to produce CNC-GA.

All the functionalized supports, as well as MCC and CNC, were characterized to analyse possible changes on the morphology or composition of the materials. SEM images and EDS spectra are shown in Fig. 4.5 for the commercial MCC, the obtained CNC and functionalized CNC (CNCox using 250  $\mu\text{mol NaIO}_4/\text{g}$  of CNC and CNC-GA). SEM images show that all the materials present a rough surface and an heterogeneous morphology. Comparing MCC and CNC, this later present a spongy surface, with a higher porosity appearance and consequently a greater area available for enzyme immobilization. This is an advantageous aspect since the surface area is crucial for the capacity of enzyme loading and can greatly influence the catalytic performance (Xiao *et al.*, 2019). After periodate oxidation using the lower concentration of periodate (CNCox-1000) the material did not present remarkable changes on its morphology and the support remained spongy as well. The oxidized support with a higher aldehyde content (CNCox-1000) showed a smoother surface than CNCox-250. Regarding to CNC-GA, literature reports that silylation of CNC did not affect greatly its morphology (Khanjanzadeh *et al.*, 2018), however after glutaraldehyde activation the surface of silylated CNC became smoother, decreasing its porous aspect. This slight change in morphology can be attributed to the fact that glutaraldehyde has a crosslinking action which causes a “polymer tightening” effect on the surface (Voicu *et al.*, 2016). EDS spectra showed the presence of silicon element (Si) in CNC-GA as a result of the insertion of silane groups (step before glutaraldehyde activation) through the reaction using APTES.

Figure 4.5 – SEM images and EDS spectra of MCC (A), CNC (B), CNCox-250 (obtained at pH 5) (C), CNCox-1000 (obtained at pH 5) (D) and CNC-GA (D). The samples of the materials were previously lyophilized.

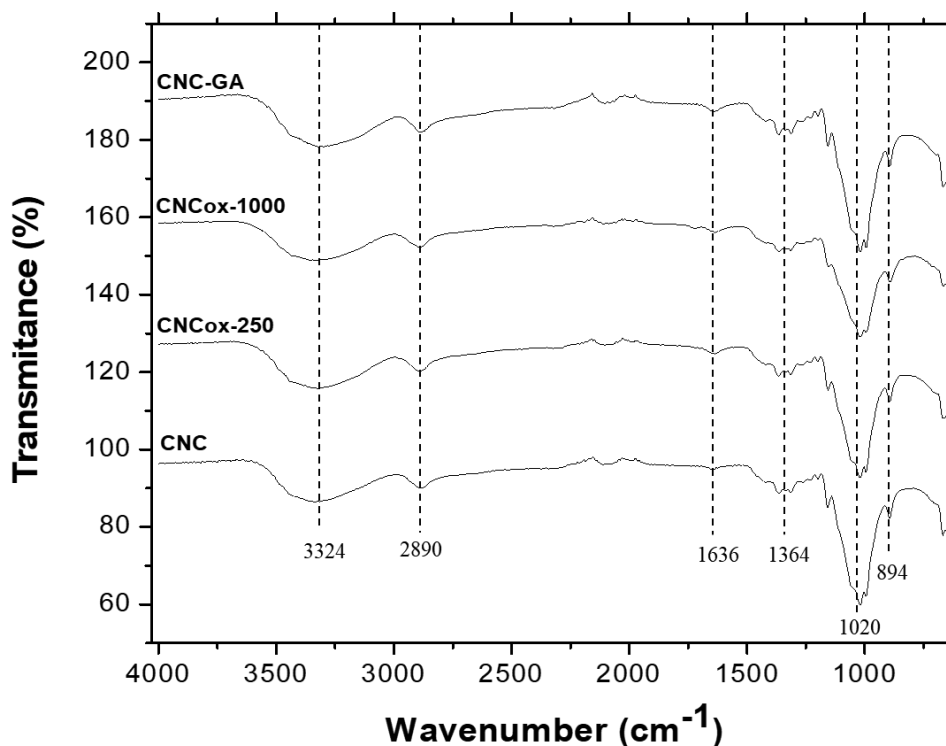


Source: Elaborated by the author.



FTIR analyses were performed to verify the presence of aldehyde groups in CNC after the modifications, and the results are presented in Fig. 4.6. The obtained spectra are very similar to each other. The similar peaks obtained at  $3324\text{ cm}^{-1}$  are due to the stretching of -OH groups. The peaks at  $2890\text{ cm}^{-1}$  correspond to C-H stretching of  $-\text{CH}_2$  and C-H groups, and the peaks at  $1364$  to C-H bending vibration. The peaks obtained at  $1020$  and  $894\text{ cm}^{-1}$  are due to C-O-C (ring deformation vibration) and  $\beta$ -glycosidic binding between the sugar units in the cellulose chain, respectively. Compared to CNC, the CNCox-250, CNCox-1000 and CNC-GA peaks at  $1636\text{ cm}^{-1}$  refers to the characteristic absorption to C=O, which indicates the introduction of aldehyde groups by periodate oxidation and glutaraldehyde activation (Liu *et al.*, 2012; Sun *et al.*, 2015; Yang, Chen e Ven, van de, 2015). Crystallinity index (CI) was calculated for MCC (microcrystalline cellulose) and CNC (cellulose nanocrystalline) and the values obtained were 1.041 and 1.025, respectively, showing that no significant changes in crystallinity occurred in the cellulose structure. CI for CNCox-250, CNCox-1000 and CNC-GA were also calculated and the values were 1.032, 1.026 and 1.033, respectively. Again, these values evidence no great changes in crystallinity of CNC after the chemical modifications.

Figure 4.6 - FTIR spectra of CNC, CNCox-250, CNCox-1000, and CNC-GA.

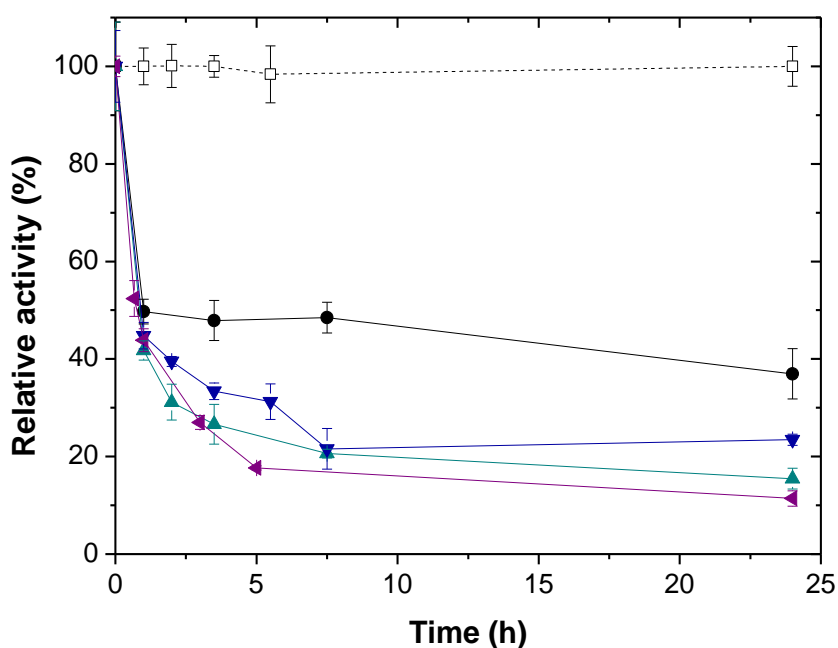


Source: Elaborated by the author.

#### 4.4.3 Immobilization of PFL using different activated CNCs

PFL was immobilized at pH 7 using differently activated CNCs as supports — two different CNCox and the CNC-GA — and the immobilization courses along 24 hours are shown in Fig. 4.7. The two CNCox chosen for this analysis were: one CNC with high content of aldehyde groups (using 1000  $\mu\text{mol NaIO}_4/\text{g}$  of CNC — CNCox-1000) and the other one with the smallest content (using 250  $\mu\text{mol NaIO}_4/\text{g}$  of CNC — CNCox-250). Both were obtained after 4 hours of oxidation at pH 5, the mildest pH among that one studied. Then, Fig. 4.7 presents PFL immobilization courses onto the 4 supports: CNC (for comparison), CNCox-250, CNCox-1000, and CNC-GA.

Figure 4.7 – Immobilization course of PFL onto CNC and modified CNCs at pH 7 (1.7  $\text{mg}_{\text{protein}}/\text{g}_{\text{support}}$  of protein load). A solution containing soluble PFL at the pH of immobilization (7) was used as reference ( $\square$ ); Solid lines represent the supernatant of PFL immobilization using the following supports: CNC ( $\bullet$ ), CNCox-250 ( $\blacktriangle$ ), CNCox-1000 ( $\blacktriangledown$ ), and CNC-GA ( $\blacktriangleleft$ ).



Source: Elaborated by the author.

Compared to native CNC, all the modified CNCs enabled higher immobilization yields after 24 h. The immobilization course obtained for both oxidized CNC were very similar along the time, which means that the difference in the aldehyde content in CNCox had no great influence on the enzyme retention capacity by the support in this case. However, for 24 hours of immobilization, ANOVA tests showed that the difference in the immobilization yields using

both oxidized CNC was significant. Then, using the CNC with CHO smaller content (CNCox-250) allowed the immobilization of a greater amount of enzymes when a higher contact time was provided. Using the support activated with glutaraldehyde (CNC-GA), a similar behavior of the immobilization course was also observed. Indeed, for 24 hours of immobilization, ANOVA testes showed no significant difference between CNCox-250 and CNC-GA.

A desorption essay for each heterogeneous biocatalyst obtained after 24 hours of immobilization was conducted in the presence of NaCl 1M and Triton 1%, separately, for 2 hours. An assay using only the buffer used for the preparation of NaCl and Triton solutions (5mM sodium phosphate, pH 7) was also performed. Table 4.1 shows the results of the heterogeneous biocatalyst before ( $t = 0$ ) and after the desorption assay for each condition. These assays were performed with biocatalyst from PFL immobilization onto unmodified CNC for its analysis and comparison.

Table 4.1 – Activities of the heterogeneous biocatalysts before ( $t = 0$ ) and after 2 h of desorption in the presence of 5mM sodium phosphate buffer, NaCl 1M or Triton-X 1% (the last two prepared in 5 mM sodium phosphate buffer), performed at pH 7 and 25 °C. Each biocatalyst was obtained from PFL immobilization during 24 hours, using 5mM sodium phosphate buffer and 1.7 mg/g of protein load.

<b>Support used for PFL immobilization</b>	<b>Heterogeneous biocatalyst activity (U/g)</b>			
	<b>Control (t = 0h)</b>	<b>Only buffer (t = 2h)</b>	<b>NaCl 1M (t = 2h)</b>	<b>Triton 1% (t = 2h)</b>
<b>CNC</b>	10.7 ± 0.2	10.1 ± 0.5	5.3 ± 0.5	3.2 ± 0.2
<b>CNCox-250</b>	16.01 ± 1.05	19.1 ± 0.4	12.11 ± 0.5	4.5 ± 0.2
<b>CNCox-1000</b>	9.0 ± 0.4	10.4 ± 1.0	9.02 ± 0.2	7.2 ± 0.2
<b>CNC-GA</b>	6.2 ± 0.3	6.2 ± 0.4	4.3 ± 0.03	3.7 ± 0.2

Source: Elaborated by the author.

The first column (Control,  $t = 0$ ) shows the activity of each biocatalyst obtained from PFL immobilization onto differently activated CNC. Using CNCox-250 for immobilization, which was the support with a lower oxidation level, the heterogeneous biocatalyst activity obtained was greater than using CNCox-1000. As reported before, statistical test showed a significant difference in the immobilization yield (%) after 24 hours of contact for these two supports ( $84.53 \pm 2.13$  for CNCox-250 and  $76.56 \pm 1.17$  for CNCox-1000).

However, the difference in the activity (U/g) of these two heterogeneous biocatalysts ( $16.01 \pm 1.05$  for CNCox-250 and  $9.0 \pm 0.4$  for CNCox-1000) is remarkably greater than the difference in the immobilization yield reported. It indicates that the amount of enzyme molecules immobilized on CNCox-250 in active form is somehow higher than the amount of those ones immobilized on CNCox-1000. The oxidation of CNC (producing CNCox-250 and CNCox-1000) probably was not complete, and some regions remained unmodified. So, these CNCox supports present a mix of closed glucopyranose rings containing hydroxyl groups ( $-\text{OH}$ ) and opened glucopyranose rings containing aldehyde groups ( $=\text{O}$ ). The results show that the support presenting lower aldehyde group content provided a more advantageous interaction between the PFL and the support in terms of biocatalyst activity. The kind of interaction between the enzyme and  $-\text{OH}$  or  $=\text{O}$  is very different, being with the first one adsorption and the second one covalent. The interactions by adsorption typically do not change tertiary enzyme structure, preserving its activity (Jesionowski, Zdarta e Krajewska, 2014). On the other hand, covalent immobilization can result in a distortion on the enzyme structure altering its activity. Besides, the rigidification provided by the covalent binding results in a minimization of the conformational dynamics and so the restriction of the motion required for the catalytic function, which lead to a decrease in activity (Manzo *et al.*, 2015; Miletić, Nastasović e Loos, 2012; Souza *et al.*, 2017; Weltz *et al.*, 2020). Thus, the support providing more covalent attachments — CNCox with higher aldehyde content — affected more strongly its activity. Besides, it was observed during the experiments that the heterogeneous biocatalyst from immobilization onto CNCox-1000 formed agglomerates that were very difficult to be dispersed. Regarding CNC-GA support, a biocatalyst with low activity was achieved by the immobilization onto it, compared to the others, although the immobilization yield at 24 hours was not significantly different (ANOVA) from the immobilization yield for CNCox-250. At low ionic strength, generally, first enzyme adsorption onto glutaraldehyde-activated support is assumed to occur, and later the covalent bonding takes place to attach the enzymes irreversibly to the support (Andrades, de *et al.*, 2019; Barbosa *et al.*, 2012; Siar *et al.*, 2018). Thereby, again the distortion or rigidification caused by the formed covalent bonds may have decreased the activity of the enzyme immobilized onto glutaraldehyde-activated support.

The analysis of the results of the biocatalysts activities after desorption assays gives a better understanding of the kinds of interactions established between the lipase and each support analyzed. PFL immobilized onto CNC presented a decrease in activity after desorption in the presence of both NaCl and Triton, however, this decrease was greater with the surfactant (ANOVA tests showed significant difference). It means that the nature of adsorption

interactions established between PFL and the unmodified CNC is predominantly hydrophobic. The aldehyde functionalization performed on CNC was made in order to enable the formation of covalent bonds between the aldehyde groups on CNC and the enzyme. Then, if a portion of the enzymes immobilized on each functionalized support (CNCox and CNC-GA) were covalently attached to it, a higher amount of enzyme was expected to remain on the support after the desorption assay. For CNC-GA, a decrease in the biocatalyst activity (probably because of enzyme desorption) after both desorption assays was observed (ANOVA tests showed no significant difference between NaCl and Triton desorptions in this case). However, a considered portion of the enzymes remained on the support, probably linked by covalent bonds. Glutaraldehyde-activated supports are considered heterofunctional. The literature reports that first enzyme adsorption followed by covalent binding occurs when glutaraldehyde-activated supports are used (Barbosa *et al.*, 2014). Besides, glutaraldehyde functionalized supports are assumed to interact by both hydrophobic and ionic exchange interactions (Santos, J. C. S. Dos, Barbosa, Oveimar, *et al.*, 2015).

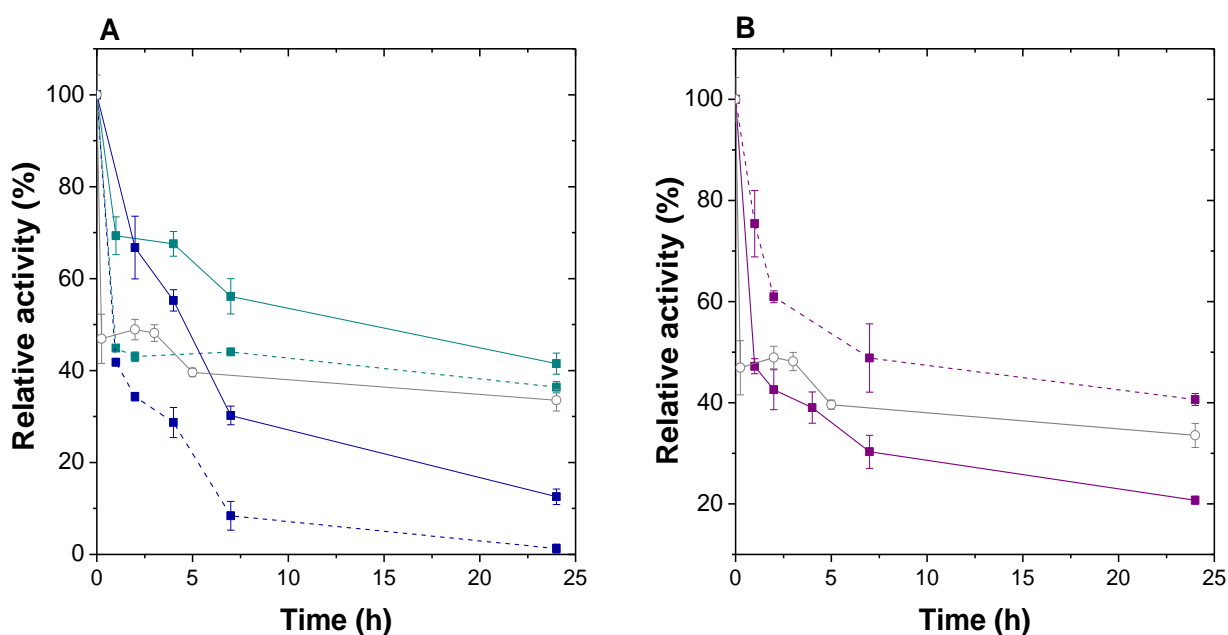
Concerning the oxidized supports, CNCox-250 and CNCox-1000, remarkable differences between the biocatalysts were observed after desorption assays. CNCox-250 presented a relevant decrease in activity after contact with Triton, whereas with NaCl, the reduction was smaller. It shows that a considerable amount of enzyme is just adsorbed by hydrophobic interactions on this support. When desorption in the presence of Triton was performed with the biocatalyst using CNCox-1000 as support, the decrease (probably related to enzyme release) in activity was smaller than with CNCox-250. ANOVA tests showed no significant difference in the activity of the heterogeneous biocatalyst before and after desorption in the presence of NaCl, which means that no enzymes must have been immobilized onto CNCox-1000 by ionic interactions. The higher level of aldehyde content on this support may have led to a higher amount of covalent bonds established between the enzyme and the support, which prevents the enzyme release (Weltz *et al.*, 2020).

#### ***4.4.4 Thermal stability of PFL immobilized onto CNC-based supports***

The thermal stabilities at 60 °C and pH 7 of the heterogeneous biocatalysts obtained from the immobilization of PFL using CNCs as supports were studied. Biocatalysts obtained after different times of immobilization were analyzed. The deactivation profiles are shown in Fig. 4.8, and the half-life obtained from these deactivation assays is shown in Table 4.2. Half-life times were calculated by Sadana & Hanley equation related in literature (Sadana e Henley,

1987). The results obtained for deactivation of soluble PFL and PFL immobilized onto unmodified CNC were also included here for comparison purposes.

Figure 4.8 – Stability at 60 °C and pH 7 (50mM Tris-HCl buffer) of soluble PFL (□) and PFL immobilized onto different aldehyde functionalized supports — CNCox (A) and CNC-GA (B). Supports: CNCox-250 (■), CNCox-1000 (■), and CNC-GA (■). The heterogeneous biocatalysts were obtained after different times of immobilization (pH 7): 2 hours for CNCox and 5 hours for CNC-GA (solid lines); 7 hours for CNCox and 24 hours for CNC-GA (dashed lines).



Source: Elaborated by the author.

Table 4.2 – Values of half-life and initial activity ( $t = 0$ ) obtained from the deactivation assays at 60 °C and pH 7 (50mM Tris-HCl buffer) of soluble PFL and PFL immobilized onto CNC and modified CNC during different immobilization times. All the half-life values were obtained from Sadana & Henley equation, except for CNCox-250 2 hours and CNC-GA 24 hours.

Samples	Immobilization time (h)	Initial activity	
		(U/mL – Soluble PFL)	(U/g – Immobilized PFL)
<b>Soluble PFL</b>	-	$0.99 \pm 0.04$	$2.24 \pm 0.19$
<b>CNC</b>	2	$6.98 \pm 0.77$	$0.55 \pm 0.05$
	7	$7.95 \pm 0.79$	$0.75 \pm 0.06$
<b>CNCox-250</b>	2	$7.21 \pm 0.32$	$9.86 \pm 1.94$
	7	$10.07 \pm 0.51$	$0.71 \pm 0.07$
<b>CNCox-1000</b>	2	$4.73 \pm 0.43$	$4.13 \pm 0.43$
	7	$6.02 \pm 0.45$	$0.79 \pm 0.09$
<b>CNC-GA</b>	5	$6.35 \pm 0.34$	$1.06 \pm 0.07$
	24	$4.52 \pm 0.66$	$3.98 \pm 0.13$

Source: Elaborated by the author.

The different aldehyde functionalization performed on CNC allowed to obtain biocatalysts with higher thermal stability than the soluble enzyme. Comparing the two oxidized supports — CNCox-250 and CNCox-1000 — a higher stabilization was achieved on the support with a lower aldehyde content level. These oxidized supports contain different combinations of aldehyde and remaining hydroxyl groups, which should interact differently with the enzyme. Immobilization of an enzyme onto a support is hardly achieved randomly. As a consequence, there is a primary orientation in which the enzymes are attached to the support, which is determined by the first bond established between them (Hernandez e Fernandez-Lafuente, 2011). Here, the difference found on the surface of each oxidized support may result in different orientations of the immobilized enzymes. Moreover, different orientations of an immobilized enzyme may result in different stabilities of this immobilized biocatalyst (Andrades, de *et al.*, 2019; Barbosa *et al.*, 2014). For both oxidized CNC, the increase in immobilization time caused a decrease in the half-life time. As seen in Fig. 4.1, a quite small spacer arm on CNC surface is achieved by the periodate oxidation. This fact, together with the increase in immobilization time (which allows the formation of more bonds), reduces the mobility of the immobilized enzyme resulting in a more rigid enzymatic structure (Rodrigues *et al.*, 2008; Santos, J. C. S.

Dos, Barbosa, Oveimar, *et al.*, 2015). The literature also reports that some structural tensions in the enzyme or excess of its rigidity can destabilize the immobilized biocatalyst (Balcão e Vila, 2015; Torres e Batista-Viera, 2019).

Using CNC-GA as support for PFL immobilization, a different influence of the immobilization time increase on the stability was observed. As previously pointed out, using glutaraldehyde-activated support, a first adsorption may occur during the first moments of immobilization, and over time covalent bonds can be established (Ait Braham *et al.*, 2019; Andrades, de *et al.*, 2019). Here, the increase of the immobilization time from 5 to 24 hours clearly improves the enzyme's thermal stability. With a longer time, the enzymes had enough time to react with the support chemically and then established covalent bond. Besides, a higher immobilization time supplies more possibilities for multi-point bonds to be formed, which provides a better stabilization for this biocatalyst (Rodrigues *et al.*, 2008).

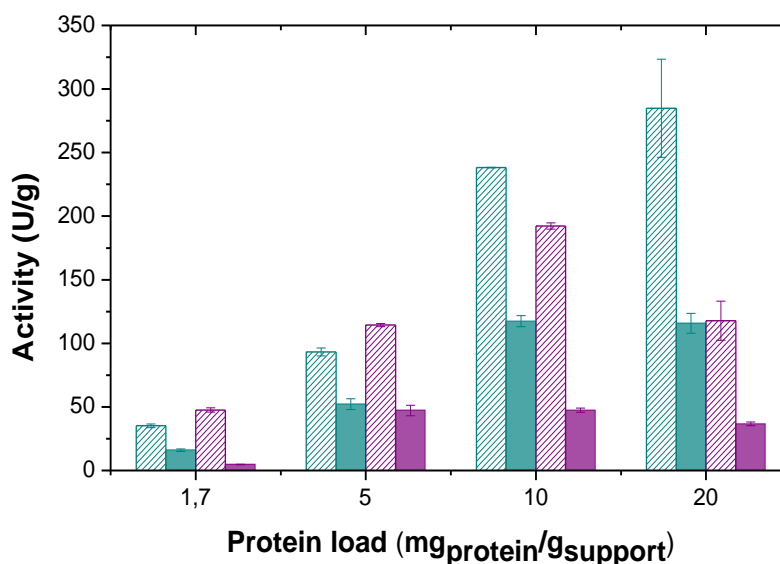
All the supports allowed the production of heterogeneous biocatalysts with half-life time higher than the soluble enzyme. Notably, PFL immobilized on CNCox-250 (2 hours of immobilization) showed the best thermal stability. ANOVA tests showed no significant difference in half-life time for CNCox-1000 (2 hours of immobilization) and CNC-GA (24 hours of immobilization). To investigate the effect of the protein load on the immobilization using differently activated materials, CNCox-250 and CNC-GA were chosen as supports.

#### ***4.4.5 Effect of the enzyme loading on PFL immobilization***

Aiming to produce heterogeneous biocatalysts with high activities using the CNCox-250 and CNC-GA as supports, the enzyme load (given in protein load –  $\text{mg}_{\text{protein}}/\text{g}_{\text{support}}$ ) used for immobilization was increased. Furthermore, incubation was carried out for 24 hours to provide enough time for the bonds between the enzyme molecules and the support to be established. Fig. 4.9 show the results of theoretical and observed activity for the biocatalyst obtained using the different initial protein loads.



Figure 4.9 – Theoretical activity (textured columns) and observed activity (solid columns) of the heterogeneous biocatalysts from the immobilization of PFL onto CNCox-250 (■) or CNC-GA (■) for 24 hours, at pH 7 (5mM sodium phosphate buffer) and 25 °C, using different protein loads at the beginning of immobilization.



Source: Elaborated by the author.

With every protein load tested, the highest theoretical activities were obtained when CNCox-250 was used, which can indicate the great capacity of this support in retaining higher amounts of PFL molecules. When 10 mg/g of protein load or more was offered for this support, it was observed more accentuated differences between theoretical and observed activity. For both theoretical and observed activities obtained for CNCox-250, ANOVA tests showed no significant difference between the values obtained for 10 and 20 mg/g. It reveals that from 10 mg/g onwards, the increase in the number of enzyme molecules immobilized does not represent a significant increase in activity of the biocatalyst. The blocking of active sites or diffusion effects caused by the enzyme loading increase on the support may have decreased the observed activity of the heterogeneous biocatalyst (Arana-peña, Rios, Carballares, *et al.*, 2020; Siar *et al.*, 2018).

A lower capacity for retaining higher amount of enzymes was observed for the immobilization using CNC-GA as support. As seen in Fig. 4.5 (SEM images) the porous appearance of CNC-GA compared with CNCox is lower, and consequently its area available to immobilize the proteins is smaller. Besides, CNC-GA presents a longer spacer arm than CNCox

(Fig. 4.1), which can greatly influence on the capacity of enzyme immobilization. Longer space arms are able to reach a higher area of the enzyme (Santos, J. C. S. Dos, Barbosa, Oveimar, *et al.*, 2015). This can result in the same enzyme being reached, in different regions, by several spacer arms present in the support. Then, with different spacer arms (and consequently the functional groups) engaged with a single enzyme, there will be a lower amount of enzyme molecules immobilized on the support. As overall consequence, this support presents a lower capacity of retaining higher amount of enzymes. ANOVA tests showed no significant difference between the observed activities obtained when 5 and 10 mg/g of protein was used for CNC-GA. Besides, the statistical test revealed that the difference (decrease) in observed activity when the protein load was increased to 20 mg/g is significant. It means that the observed activity of PFL-CNC-GA presented an increase only up to the point of 5mg/g, and showed even a decrease when the highest protein load was used. The blocking of active sites or diffusion problems greatly affects the observed activity of the heterogeneous biocatalyst obtained with CNC-GA. Then, CNCox-250 was the support that showed the higher capacity to retain PFL and, therefore, it was chosen for the following co-immobilization process.

#### ***4.4.6 Co-immobilization of lipase and laccase onto CNCox-250 support***

After all the analyses between different CNC-based supports and PFL (the first enzyme layer of the co-immobilization strategy), lipase and laccase enzymes were co-immobilized through a layer-by-layer process using CNCox-250 as support. The protein load used for each enzyme immobilization was 10 mg<sub>protein</sub>/g<sub>support</sub>. The biocatalyst activities after each co-immobilization step, the immobilization yields and recovered activities after the immobilization of each enzyme were presented in Table 4.3. Each enzyme immobilization was performed at pH 7 during 24 hours.

Table 4.3 – Catalytic activity for immobilized lipase and laccase after each stage of the 4-steps co-immobilization process using CNCox-250 as support. Immobilizations were performed using  $10 \text{ mg}_{\text{protein}}/\text{g}_{\text{support}}$  of initial protein loading for each enzyme. In the immobilization solutions, activity of soluble PFL was  $40.58 \pm 1.39 \text{ U}_{\text{PNPB}}/\text{mL}$  and of soluble laccase was  $20.92 \pm 1.05 \text{ U}_{\text{ABTS}}/\text{mL}$

	<b>PFL</b>	<b>Lac</b>
<b>Immobilization yield (%)</b>	$58.71 \pm 0.05$	$87.17 \pm 0.78$
<b>Recovered activity (%)</b>	$49.3 \pm 1.86$	$67.24 \pm 0.01$
<b>Biocatalysts</b>	<b>PFL activity (<math>\text{U}_{\text{PNPB}}/\text{g}</math>)</b>	<b>Lac activity (<math>\text{U}_{\text{ABTS}}/\text{g}</math>)</b>
CNCox-250-PFL	$117.44 \pm 4.43$	-
CNCox-250-PFL-PEI	$62.49 \pm 6.24$	-
CNCox-250-PFL-PEI-Lac	$33.67 \pm 1.22$	$122.63 \pm 0.02$
CNCox-250-PFL-PEI-Lac-GA	$34.76 \pm 3.41$	$121.01 \pm 8.86$

Source: Elaborated by the author.

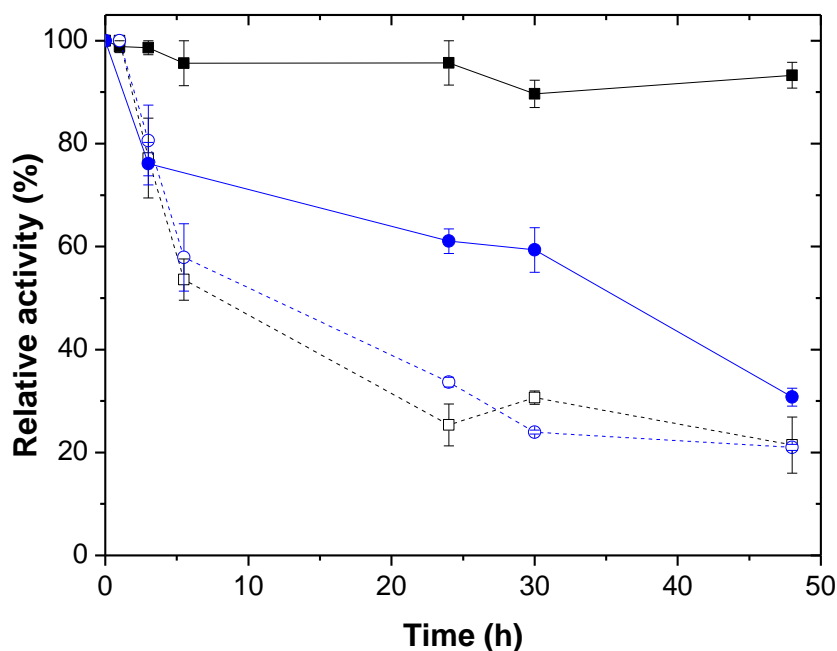
Firstly, PFL was immobilized during 24 hours onto CNCox-250, in which about 50% of the activity of the immobilized PFL was recovered. Then, this heterogeneous biocatalyst (CNCox-250-PFL) was covered with 10% PEI (pH 7) overnight. After that step, an expressive loss of activity (approximately 47 %) was observed (CNCox-250-PEI-PFL in Table 4.3). It is probably due to some competition between PEI in solution and CNCox-250 for the interaction of PFL. This competition resulted in the release of enzyme molecules and, consequently, loss in the heterogeneous biocatalyst activity. This release was confirmed by the activity found in supernatant (not quantified because of PEI interference in the activity measurement). Some authors also observed such desorption when putting some layers of lipase using PEI as a glue between each layer, which could be assigned to this competition between PEI in solution and the layer of PEI previously fixed on the support (Arana-peña, Rios, Mendez-sanchez, *et al.*, 2020). Also, diffusion effects due to this layer insertion may have made it difficult for the substrate to reach the enzyme active site, decreasing its observed activity (Wang *et al.*, 2019). These restrictions may yet be increased by the fact that the immobilized PFL became rigid and its mobility is reduced making the substrate diffusion even more difficult (Rios, Arana-Peña, *et al.*, 2019).

After, laccase was co-immobilized at pH 7 onto this CNCox-250-PFL-PEI for 24 hours. The activity of co-immobilized laccase is showed in Table 4.3. Again, a loss in PFL activity was observed after another layer (laccase) has been inserted on the support. The final step was the crosslinking of the co-immobilized enzymes (CNCox-250-PFL-PEI-Lac) using glutaraldehyde, which did not cause great changes in activity of both enzymes.

#### ***4.4.7 Thermal stability of enzymes co-immobilized onto CNCox-250***

Thermal inactivation of the final biocatalyst (CNCox-250-PFL-PEI-Lac-GA) containing both co-immobilized enzymes was performed for thermal stability analysis. For PFL singly immobilized on CNC and functionalized CNC the temperature of 60 °C was used for the inactivation assays. However, literature relates that, in general, lipases are more robust as enzyme than laccases (Naseri *et al.*, 2018). Then, thermal stability of laccase could be expected to be lower than lipase. Besides, literature reports a very low thermal stability of soluble laccase from *Trametes versicolor* at 60 °C, for it loss its almost total activity after 6 hours of incubation at this temperature (Noreen *et al.*, 2016). Thus, in order to analyze the thermal inactivation of both enzymes, at both soluble and co-immobilized forms, during a reasonable long period (48 hours), the assays of thermal stability for the co-immobilized enzymes were performed at a lower temperature, 50 °C this time. The thermal incubation was performed at pH 7. The profiles obtained for both co-immobilized enzymes are shown in Fig. 4.10. Also, the inactivation profile for both soluble enzymes was performed for comparison purposes.

Figure 4.10 – Thermal stability at 50 °C and pH 7 (50mM Tris-HCl buffer) of soluble (dashed lines) and co-immobilized (solid lines) PFL (black) and laccase (blue) using CNCox-250 as support.



Source: Elaborated by the author.

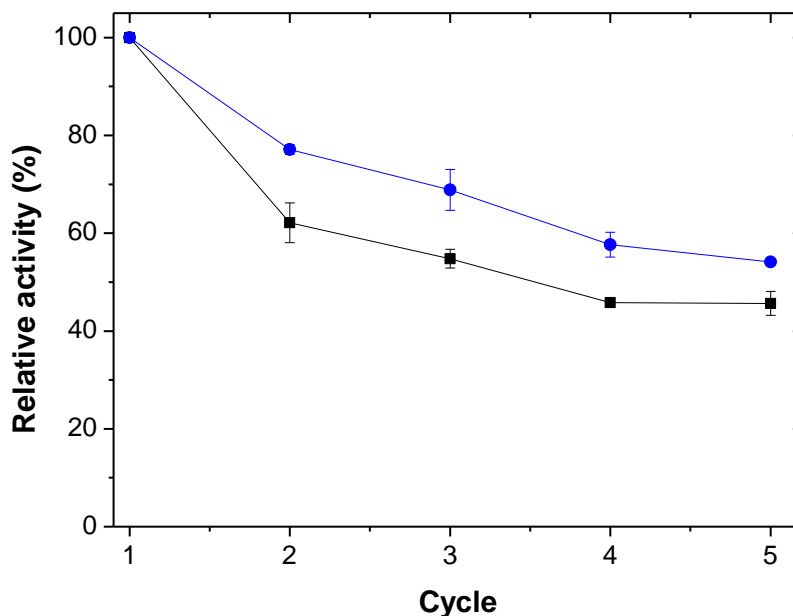
Soluble enzymes presented very similar inactivation profiles when incubated at 50 °C, keeping about 20% of their initial activities after 48 hours of thermal inactivation. As seen in the obtained results, co-immobilized enzymes showed a deactivation profile much slower than soluble enzymes. In fact, it is important to note that both co-immobilized enzymes presented a half-life time higher than 24 hours. Performing a chemical crosslinking, in this case using glutaraldehyde over the multilayer biocatalyst, is an strategy broadly reported in literature for enzyme stability improvement (Barbosa *et al.*, 2014). Co-immobilized laccase kept about 60% of its activity even after 30 hours of incubation. Literature reports a laccase from *Trametes versicolor* immobilized onto aldehyde supports keeping about 40% of its activity when incubated at 55 °C (pH 7) or 50 °C (pH 7) for 30 hours (Addorisio *et al.*, 2013). Co-immobilized PFL showed the highest thermal stability, keeping more than 90% of its initial activity after 48 hours of inactivation at 50 °C. This thermal stability advantage of co-immobilized PFL is an important characteristic of the obtained multi-active biocatalyst, especially when one takes into account the difference in activity of PFL and laccase observed in CNCox-250-PFL-PEI-Lac-GA (Table 4.3). Thus, the low lipase activity found in the produced biocatalyst is offset by its

higher stability, since its almost total activity could be maintained much longer than co-immobilized laccase.

#### ***4.4.8 Reuse of co-immobilized enzymes***

Reusability of immobilized enzymes is an important parameter to consider them as potential biocatalysts for industrial application (Khoobi *et al.*, 2015). CNCox-250-PFL-PEI-Lac-GA was used to catalyze consecutive cycles of reaction to analyze the operational stability of the co-immobilized enzymes. For PFL analysis, the reaction was the hydrolysis of pNPB performed under the previously described conditions. For laccase, the oxidation of ABTS under the previously described conditions was performed. After each cycle, the mass of the heterogeneous biocatalyst was washed and reintroduced in a new reactional medium. The initial activity of both co-immobilized enzymes was considered 100%. The results of relative activities of each co-immobilized enzyme obtained for 5 sequential cycles are presented in Fig. 4.11. The co-immobilized enzymes presented not greatly different behaviors along 5 cycles between them both, with PFL keeping about 45% of the initial activity after 5 cycles, while laccase kept about 55%. Studying co-immobilized enzymes aiming application in multi-enzyme reactions, it is interesting to analyze also the influence of the performance of one enzyme on the activity of the other one. Then, another analysis was performed (results not shown) in which the same mass of biocatalyst (CNCox-250-PFL-PEI-Lac-GA) was put to react with pNPB (PFL substrate), after with ABTS (laccase substrate substrate), and then with pNPB again. The inverse was performed as well. In both cases, this heterogeneous biocatalyst showed no evidence of significant activity loss of one enzyme after the biocatalyst reacts with the substrate of the other one. Such results can be considered as an indications of the ability of the co-immobilized enzymes to perform their reactions without significant negative interference on the performance of the other enzyme. This whole set of results serves as a basis for future research using this obtained biocatalyst in the accomplishment of cascade reactions of industrial interest in a continuous way or even as sequential batches.

Figure 4.11 – Operational stability of co-immobilized PFL and laccase. CNCox-250-PFL-PEI-Lac-GA was used as biocatalyst in the recycles of pNPB hydrolysis (black line) and ABTS oxidation (blue line) for PFL and laccase analysis, respectively.



Source: Elaborated by the author.

## 4.5 Conclusions

Different aldehyde functionalizations were performed in CNC surface — through sodium periodate oxidation and glutaraldehyde activation — and the chemical changes were confirmed by FTIR. These materials allowed the establishment of different kinds of interactions with the first enzyme layer (PFL), and greater activities and thermal stabilities could be obtained after that CNC activation. CNC oxidized using 250  $\mu\text{mol NaIO}_4/\text{g}$  of CNC showed to be the most advantageous support in terms of activity, stability and capacity to retain a higher amount of PFL. With this material, the co-immobilization of lipase and laccase proceeded by applying the layer-by-layer strategy proposed. As intended, the biocatalyst obtained showed higher thermal stability than soluble enzymes. Besides, it could be used in consecutive batches of reaction catalyzed by both enzymes, which kept more than 45% of their activities after 5 sequential batch cycles. In conclusion, the layer-by-layer lipase and laccase co-immobilization onto functionalized CNC generated a multi-active and stable insoluble biocatalyst with great potential to be used in cascade or other multi-enzymes reactions demanding both lipase and laccase activities.

## 4.6 Acknowledgements

The authors would like to thank the financial support and scholarships from the Brazilian agencies CNPq (Conselho Nacional de Desenvolvimento Científico e Tecnológico), CAPES (Coordenação de Aperfeiçoamento de Pessoal de Nível Superior) and Funcap (Fundação Cearense de Apoio ao Desenvolvimento Científico e Tecnológico). In addition, the authors thanks Embrapa Agroindústria Tropical for the support in some analysis.

## 4.7 References

- ADDORISIO, V. *et al.* Oxidation of phenyl compounds using strongly stable immobilized-stabilized laccase from *Trametes versicolor*. **Process Biochemistry**, v. 48, n. 8, p. 1174–1180, 2013.
- ADSUL, M. *et al.* Facile approach for the dispersion of regenerated cellulose in aqueous system in the form of nanoparticles. **Biomacromolecules**, v. 13, n. 9, p. 2890–2895, 2012.
- AIT BRAHAM, S. *et al.* Cooperativity of covalent attachment and ion exchange on alcalase immobilization using glutaraldehyde chemistry: Enzyme stabilization and improved proteolytic activity. **Biotechnology Progress**, v. 35, n. 2, p. 1–4, 2019.
- ANDRADES, D. DE *et al.* Immobilization and stabilization of different  $\beta$ -glucosidases using the glutaraldehyde chemistry: Optimal protocol depends on the enzyme. **International Journal of Biological Macromolecules**, v. 129, p. 672–678, 2019.
- ARANA-PEÑA, S. *et al.* New applications of glyoxyl-octyl agarose in lipases co-immobilization: Strategies to reuse the most stable lipase. **International Journal of Biological Macromolecules**, v. 131, p. 989–997, 2019.
- ARANA-PEÑA, S.; CARBALLARES, D.; CORBERAN, V. C.; *et al.* Multi-combibilipases: Co-immobilizing lipases with very different stabilities combining immobilization via interfacial activation and ion exchange. The reuse of the most stable co-immobilized enzymes after inactivation of the least stable ones. **Catalysts**, v. 10, n. 10, p. 1–23, 2020.
- ARANA-PEÑA, S.; RIOS, N. S.; *et al.* Coimmobilization of different lipases: Simple layer by layer enzyme spatial ordering. **International Journal of Biological Macromolecules**, v. 145, p. 856–864, 2020.
- ARANA-PEÑA, S.; RIOS, N. S.; MENDEZ-SANCHEZ, C.; *et al.* Use of polyethylenimine to produce immobilized lipase multilayers biocatalysts with very high volumetric activity using octyl-agarose beads : Avoiding enzyme release during multilayer production. **Enzyme and Microbial Technology**, v. 137, n. October 2019, p. 109535, 2020.
- ARANA-PEÑA, S.; CARBALLARES, D.; BERENQUER-MURCIA, Á.; *et al.* One pot use of combibilipases for full modification of oils and fats: Multifunctional and heterogeneous substrates. **Catalysts**, v. 10, n. 6, p. 605, 2020.
- ARANA-PEÑA, S.; RIOS, N. S.; CARBALLARES, D.; *et al.* Effects of Enzyme Loading



and Immobilization Conditions on the Catalytic Features of Lipase From *Pseudomonas fluorescens* Immobilized on Octyl-Agarose Beads. v. 8, n. February, p. 1–13, 2020.

BALCÃO, V. M.; VILA, M. M. D. C. Structural and functional stabilization of protein entities: State-of-the-art. **Advanced Drug Delivery Reviews**, v. 93, p. 25–41, 2015.

BALDRIAN, P.; GABRIEL, J. Copper and cadmium increase laccase activity in *Pleurotus ostreatus*. **FEMS Microbiology Letters**, v. 206, p. 69–74, 2002.

BARBOSA, O. *et al.* Versatility of glutaraldehyde to immobilize lipases: Effect of the immobilization protocol on the properties of lipase B from *Candida antarctica*. **Process Biochemistry**, v. 47, n. 8, p. 1220–1227, 2012.

BARBOSA, O.; TORRES, R.; ORTIZ, C. *et al.* Heterofunctional supports in enzyme immobilization: From traditional immobilization protocols to opportunities in tuning enzyme properties. **Biomacromolecules**, v. 14, n. 8, p. 2433–2462, 2013.

BARBOSA, O.; ORTIZ, C.; BERENQUER-MURCIA, Á. *et al.* Glutaraldehyde in biocatalysts design: A useful crosslinker and a versatile tool in enzyme immobilization. **RSC Advances**, v. 4, n. 4, p. 1583–1600, dez. 2014.

BARBOSA, O.; ORTIZ, C.; BERENQUER-MURCIA, Á. *et al.* Strategies for the one-step immobilization-purification of enzymes as industrial biocatalysts. **Biotechnology Advances**, v. 33, n. 5, p. 435–456, 2015.

BRADFORD, M. M. A Rapid and Sensitive Method for the Quantitation of Microgram Quantities of Protein Utilizing the Principle of Protein-Dye Binding. **Analytical Biochemistry**, v. 72, p. 248–254, 1976.

CAI, Q. *et al.* Enhanced activity and stability of industrial lipases immobilized onto spherelike bacterial cellulose. **International Journal of Biological Macromolecules**, v. 109, p. 1174–1181, 2018.

CHEMIN, M. *et al.* Periodate oxidation of 4-O-methylglucuronoxylans: Influence of the reaction conditions. **Carbohydrate Polymers**, v. 142, p. 45–50, 2016.

CIOLACU, D. *et al.* Amorphous Cellulose structure and Characterization Related papers amorphous cellulose-structure and Valent in I Popa Studies concerning the accessibility of different allomorphic forms of cellulose. **Cellulose Chem. Technol**, v. 45, n. 2, p. 13–21, 2011.

ELIAS, N. *et al.* Characterization, optimization and stability studies on *Candida rugosa* lipase supported on nanocellulose reinforced chitosan prepared from oil palm biomass. **International Journal of Biological Macromolecules**, v. 114, p. 306–316, 2018.

GAVEZZOTTI, P. *et al.* Synthesis of enantiomerically enriched dimers of vinylphenols by tandem action of laccases and lipases. **Advanced Synthesis and Catalysis**, v. 353, n. 13, p. 2421–2430, 2011.

GUERBEROFF, G. K.; CAMUSSO, C. C. Effect of laccase from *Trametes versicolor* on the oxidative stability of edible vegetable oils. **Food Science and Human Wellness**, v. 8, n. 4, p. 356–361, 2019.

GUISÁN, J. Aldehyde-agarose gels as activated supports for immobilization-stabilization of enzymes. **Enzyme and Microbial Technology**, v. 10, n. 6, p. 375–382, jun. 1988.

HABIBI, Y. Key advances in the chemical modification of nanocelluloses. **Chem Soc Rev**,

p. 1519–1542, 2014.

HERNANDEZ, K.; FERNANDEZ-LAFUENTE, R. Control of protein immobilization: Coupling immobilization and site-directed mutagenesis to improve biocatalyst or biosensor performance. **Enzyme and Microbial Technology**, v. 48, n. 2, p. 107–122, 2011.

HRYDZIUSZKO, Z. *et al.* *Burkholderia cepacia* lipase immobilization for hydrolytic reactions and the kinetic resolution of the non-equimolar mixtures of isomeric alcohols. **Bioorganic Chemistry**, v. 93, n. November 2018, p. 102745, 2019.

JELLE, B. P.; HOVDE, P. J. Fourier transform infrared radiation spectroscopy applied for wood rot decay and mould fungi growth detection. **Advances in Materials Science and Engineering**, v. 2012, p. 1–7, 2012.

JESIONOWSKI, T.; ZDARTA, J.; KRAJEWSKA, B. Enzyme immobilization by adsorption: A review. **Adsorption**, v. 20, n. 5–6, p. 801–821, 2014.

JIN, X. *et al.* A robust and stable nano-biocatalyst by co-immobilization of chloroperoxidase and horseradish peroxidase for the decolorization of azo dyes. **Journal of Chemical Technology and Biotechnology**, v. 93, n. 2, p. 489–497, 2018.

KAMIDA, K. *et al.* Study on the solubility of cellulose in aqueous alkali solution by deuteration IR and <sup>13</sup>C NMR. **Polymer Journal**, v. 16, n. 12, p. 857–866, 1984.

KHANJANZADEH, H. *et al.* Surface chemical functionalization of cellulose nanocrystals by 3-aminopropyltriethoxysilane. **International Journal of Biological Macromolecules**, v. 106, p. 1288–1296, 2018.

KHOABI, M. *et al.* Polyethyleneimine-modified superparamagnetic Fe<sub>3</sub>O<sub>4</sub> nanoparticles for lipase immobilization: Characterization and application. **Materials Chemistry and Physics**, v. 149, p. 77–86, 2015.

KOŁODZIEJCZAK-RADZIMSKA, A. *et al.* Laccase from *Trametes versicolor* supported onto mesoporous Al<sub>2</sub>O<sub>3</sub>: Stability tests and evaluations of catalytic activity. **Process Biochemistry**, v. 95, n. May, p. 71–80, 2020.

LIU, X. *et al.* A kinetic model for oxidative degradation of bagasse pulp fiber by sodium periodate. **Carbohydrate Polymers**, v. 90, n. 1, p. 218–223, 2012.

MANAN, F. A. A. *et al.* Immobilization of Tyrosinase in nanocrystalline cellulose / chitosan composite film for amperometric detection of phenol. **Malaysian Journal of Analytical Sciences**, v. 20, n. 5, p. 978–985, 2016.

MANZO, R. M. *et al.* Chemical improvement of chitosan-modified beads for the immobilization of *Enterococcus faecium* DBFIQ E36 l-arabinose isomerase through multipoint covalent attachment approach. **Journal of Industrial Microbiology and Biotechnology**, v. 42, n. 10, p. 1325–1340, 2015.

MARTINS DE OLIVEIRA, S. *et al.* Functionalization of Porous Cellulose with Glyoxyl Groups as a Carrier for Enzyme Immobilization and Stabilization. **Biomacromolecules**, v. 22, n. 2, p. 927–937, 2021.

MERYAM SARDAR, R. A. Enzyme Immobilization: An Overview on Nanoparticles as Immobilization Matrix. **Biochemistry & Analytical Biochemistry**, v. 04, n. 02, 2015.

MILETIĆ, N.; NASTASOVIĆ, A.; LOOS, K. Immobilization of biocatalysts for enzymatic polymerizations: Possibilities, advantages, applications. **Bioresource Technology**, v. 115, p.

126–135, 2012.

MOHAMAD, N. R. *et al.* An overview of technologies for immobilization of enzymes and surface analysis techniques for immobilized enzymes. **Biotechnology and Biotechnological Equipment**, v. 29, n. 2, p. 205–220, 2015.

MONTEIRO, R. R. C. *et al.* Immobilization of Lipase A from *Candida antarctica* onto Chitosan-Coated Magnetic Nanoparticles. **International Journal of Molecular Sciences**, v. 20, n. 16, p. 4018, 2019.

NASERI, M. *et al.* Lipase and Laccase Encapsulated on Zeolite Imidazolate Framework: Enzyme Activity and Stability from Voltammetric Measurements. **ChemCatChem**, v. 10, n. 23, p. 5425–5433, 2018.

NIKOLIC, T. *et al.* Sodium periodate oxidized cotton yarn as carrier for immobilization of trypsin. **Carbohydrate Polymers**, v. 82, n. 3, p. 976–981, 2010.

NOREEN, S. *et al.* Performance improvement of Ca-alginate bead cross-linked laccase from *Trametes versicolor* IBL-04. **BioResources**, v. 11, n. 1, p. 558–572, 2016.

P.K.SMITH *et al.* Measurement of protein using bicinchoninic acid. **Analytical Biochemistry**, v. 150, n. 1, p. 76–85, 1985.

PEIRCE, S. *et al.* Development of simple protocols to solve the problems of enzyme coimmobilization. **RSC Advances**, v. 6, n. 66, p. 61707–61715, 2016.

POPPE, J. K. *et al.* Enzymatic Multipoint covalent immobilization of lipases on aldehyde-activated support : Characterization and application in transesterification reaction. **Journal of Molecular Catalysis B: Enzymatic**, v. 94, p. 57–62, 2013.

PRAMANIK, S. K. *et al.* Catalyzed degradation of polycyclic aromatic hydrocarbons by recoverable magnetic chitosan immobilized laccase from *Trametes versicolor*. **Chemosphere**, p. 100310, 2019.

RIOS, N. S. *et al.* Biotechnological potential of lipases from *Pseudomonas*: Sources, properties and applications. **Process Biochemistry**, v. 75, n. August, p. 99–120, 2018.

RIOS, N. S.; ARANA-PENÑA, S.; *et al.* Increasing the enzyme loading capacity of porous supports by a layer-by-layer immobilization strategy using PEI as glue. **Catalysts**, v. 9, n. 7, p. 576, 2019.

RIOS, N. S.; NETO, D. M. A.; *et al.* Comparison of the immobilization of lipase from *Pseudomonas fluorescens* on divinylsulfone or p-benzoquinone activated support. **International Journal of Biological Macromolecules**, v. 134, p. 936–945, 2019.

RIOS, N. S.; MENDEZ-SANCHEZ, C.; *et al.* Immobilization of lipase from *Pseudomonas fluorescens* on glyoxyl-octyl-agarose beads: Improved stability and reusability. **Biochimica et Biophysica Acta (BBA) - Proteins and Proteomics**, v. 1867, n. 9, p. 741–747, set. 2019.

RODRIGUES, D. S. *et al.* Multipoint covalent immobilization of microbial lipase on chitosan and agarose activated by different methods. **Journal of Molecular Catalysis B: Enzymatic**, v. 51, n. 3–4, p. 100–109, 2008.

RODRIGUES, R. C. *et al.* Immobilization-stabilization of the lipase from *Thermomyces lanuginosus*: Critical role of chemical amination. **Process Biochemistry**, v. 44, n. 9, p. 963–968, 2009.

- RODRIGUES, R. C.; BERENQUER-MURCIA, Á.; FERNANDEZ-LAFUENTE, R. Coupling Chemical Modification and Immobilization to Improve the Catalytic Performance of Enzymes. **Advanced Synthesis & Catalysis**, v. 353, n. 13, p. 2216–2238, set. 2011.
- RUEDA, N. *et al.* Chemical Modification in the Design of Immobilized Enzyme Biocatalysts: Drawbacks and Opportunities. **Chemical Record**, v. 16, n. 3, p. 1436–1455, 2016.
- SADANA, A.; HENLEY, J. P. Single-Step Unimolecular Non-First-Order Enzyme Deactivation Kinetics. **Biotechnology and bioengineering**, v. 30, n. 6, p. 717–723, 1987.
- SANKAR, K. *et al.* A novel method for improving laccase activity by immobilization onto copper ferrite nanoparticles for lignin degradation. **International Journal of Biological Macromolecules**, v. 152, p. 1098–1107, 2020.
- SANTOS, J. C. S. DOS; RUEDA, NAZZOLY; *et al.* Evaluation of divinylsulfone activated agarose to immobilize lipases and to tune their catalytic properties. **Process Biochemistry**, v. 50, p. 918–927, 2015.
- SANTOS, J. C. S. DOS; RUEDA, NAZZOLY;; *et al.* Tuning the catalytic properties of lipases immobilized on divinylsulfone activated agarose by altering its nanoenvironment. **Enzyme and Microbial Technology**, v. 77, p. 1–7, 2015.
- SANTOS, J. C. S. DOS; BARBOSA, OVEIMAR; *et al.* Importance of the Support Properties for Immobilization or Purification of Enzymes. **CHEM CAT CHEM**, v. 7, n. 16, p. 2413–2432, 2015.
- SCHEIBEL, D. M.; GITSOV, I. Unprecedented Enzymatic Synthesis of Perfectly Structured Alternating Copolymers via “green” Reaction Cocatalyzed by Laccase and Lipase Compartmentalized within Supramolecular Complexes. **Biomacromolecules**, v. 20, n. 2, p. 927–936, 2019.
- SHANKAR, S.; RHIM, J. W. Preparation of nanocellulose from micro-crystalline cellulose: The effect on the performance and properties of agar-based composite films. **Carbohydrate Polymers**, v. 135, p. 18–26, 2016.
- SIAR, E.-H. *et al.* Stabilization of ficin extract by immobilization on glyoxyl agarose. Preliminary characterization of the biocatalyst performance in hydrolysis of proteins. **Process Biochemistry**, v. 58, n. April, p. 98–104, jul. 2017.
- SIAR, E. H. *et al.* Immobilization/stabilization of ficin extract on glutaraldehyde-activated agarose beads. Variables that control the final stability and activity in protein hydrolyses. **Catalysts**, v. 8, n. 4, p. 149, 2018.
- SILLER, M. *et al.* Effects of periodate oxidation on cellulose polymorphs. **Cellulose**, v. 22, n. 4, p. 2245–2261, 2015.
- SILVA, J. A. *et al.* Immobilization of *Candida antarctica* lipase B by covalent attachment on chitosan-based hydrogels using different support activation strategies. **Biochemical Engineering Journal**, v. 60, p. 16–24, 2012.
- SONI, S. *et al.* Exploration of the expeditious potential of *Pseudomonas fluorescens* lipase in the kinetic resolution of racemic intermediates and its validation through molecular docking. **CHIRALITY**, v. 30, p. 85–94, 2018.
- SOUZA, L. T. DE A. *et al.* Immobilization of *Moniliella spathulata* R25L270 lipase on ionic, hydrophobic and covalent supports: Functional properties and hydrolysis of sardine oil.

**Molecules**, v. 22, n. 10, p. 1508, 2017.

SULAIMAN, S. *et al.* A Review: Potential Usage of Cellulose Nanofibers (CNF) for Enzyme Immobilization via Covalent Interactions. **Applied Biochemistry and Biotechnology**, v. 175, n. 4, p. 1817–1842, 2014.

SUN, B. *et al.* Sodium periodate oxidation of cellulose nanocrystal and its application as a paper wet strength additive. **Cellulose**, v. 22, n. 2, p. 1135–1146, 2015.

TORRES, P.; BATISTA-VIERA, F. Production of D-tagatose and D-fructose from whey by co-immobilized enzymatic system. **Molecular Catalysis**, v. 463, n. July 2018, p. 99–109, 2019.

UTH, C. *et al.* A Chemoenzymatic Approach to Protein Immobilization onto Crystalline Cellulose Nanoscaffolds. v. 53, n. 46, p. 12618–12623, 2014.

VICINI, S. *et al.* Thermal analysis and characterisation of cellulose oxidised with sodium methaperiodate. **Thermochemica Acta**, v. 418, n. 1–2, p. 123–130, 2004.

VOICU, S. I. *et al.* Sericin Covalent Immobilization onto Cellulose Acetate Membrane for Biomedical Applications Sericin Covalent Immobilization onto Cellulose Acetate Membrane for Biomedical Applications. **ACS Sustainable Chemistry & Engineering**, v. 4, n. 3, p. 1765–1774, 2016.

WANG, Y. *et al.* Layered Co-Immobilization of  $\beta$ -Glucosidase and Cellulase on Polymer Film by Visible-Light-Induced Graft Polymerization. **ACS Applied Materials and Interfaces**, v. 11, n. 47, p. 44913–44921, 2019.

WELTZ, J. S. *et al.* Reduced Enzyme Dynamics upon Multipoint Covalent Immobilization Leads to Stability-Activity Trade-off. **Journal of the American Chemical Society**, v. 142, n. 7, p. 3463–3471, 2020.

XIA, T. T. *et al.* Improved performance of immobilized laccase on amine-functioned magnetic Fe<sub>3</sub>O<sub>4</sub> nanoparticles modified with polyethylenimine. **Chemical Engineering Journal**, v. 295, p. 201–206, 2016.

XIAO, Y. *et al.* Constructing a Continuous Flow Bioreactor Based on a Hierarchically Porous Cellulose Monolith for Ultrafast and Nonstop Enzymatic Esterification/Transesterification. **ACS Sustainable Chemistry and Engineering**, v. 7, n. 2, p. 2056–2063, 2019.

YANG, H.; CHEN, D.; VEN, T. G. M. VAN DE. Preparation and characterization of sterically stabilized nanocrystalline cellulose obtained by periodate oxidation of cellulose fibers. **Cellulose**, v. 22, n. 3, p. 1743–1752, 2015.

ZAAK, H. *et al.* Exploiting the versatility of aminated supports activated with glutaraldehyde to immobilize  $\beta$ -galactosidase from *Aspergillus oryzae*. **Catalysts**, v. 7, n. 9, 2017.

ZHANG, Y. *et al.* A one-pot process for synthesis of mitomycin analogs catalyzed by laccase/lipase optimized by response surface methodology. **Engineering in Life Sciences**, v. 19, n. 11, p. 805–814, 2019.

ZHOU, J.; ZHANG, L. Solubility of cellulose in NaOH / Urea Aqueous Solution. **Polymer Journal**, v. 32, n. 10, p. 866–870, 2000.

# Chapter 5

**Final considerations**

## 5 FINAL CONSIDERATIONS

Two agarose based supports able to interact by different ways with the studied enzymes were analyzed. For each one, a specific order was employed in the layer-by-layer strategy using PEI as intermediate, which proved to work greatly as a glue between the enzyme layers. The order used for immobilization employing octyl-agarose as support allowed better results of heterogeneous biocatalyst activity, whereas the order for using DEAE-agarose showed disadvantages probably due to partition effects caused by the PEI layer. The glutaraldehyde crosslinking as final step of the co-immobilization process showed to attach covalently the enzymes and prevent their release under drastic conditions. The layer-by-layer proposed strategy allowed the production of an insoluble biocatalyst containing both enzymes functionalities and improved thermal stability. External and internal mass transfer effects were studied as well as the kinetic for catalysis using both enzymes. These studies revealed that the produced insoluble biocatalysts containing high amount of enzymes (obtained using  $10 \text{ mg}_{\text{protein}}/\text{g}_{\text{support}}$  of each enzyme for the co-immobilization) could perform standard catalytic reactions with no diffusion limitations.

Also, CNC based supports were tested for the application of the proposed layer-by-layer strategy to co-immobilize lipase and laccase. Native CNC was able to adsorb the first enzyme layer (lipase) through both hydrophobic and ionic exchange interactions. CNC was functionalized with aldehyde groups through periodate oxidation (CNCox) or glutaraldehyde activation (CNC-GA). The performed functionalizations of CNC allowed the immobilization of lipase with better activity and stability. Besides the results of highest activity and stability, CNCox showed the best capacity of retaining a higher amount of lipase when the protein load for immobilization was increased. For that, CNCox was applied as support for the layer-by-layer co-immobilization of lipase and laccase, and again PEI was used as a glue between the enzymes. With that, an insoluble biocatalyst was produced presenting activity of both enzymes. Also, the process allowed a thermal stabilization of both enzymes. Besides, it was possible to reuse both co-immobilized enzymes in the catalysis of standard substrates, and some analysis showed no great interference of one enzyme in the functionality of the other one.

In conclusion, two insoluble biocatalysts were produced with lipase and laccase functionalities and improved stability of both enzymes. Besides, the difference in the physical characteristic of each material used as support gives the possibility of distinct

applications for each one. These produced biocatalysts present a great potential for industrial application requiring catalytic functions of lipase and laccase in cascade reactions or other chemical transformations.